Kobe University Repository : Kernel

PDF issue: 2026-11-24

Harnessing the potential of oleaginous yeast for sustainable lipid and biopolymer production from fatty acids

Noor Afiqah Binti Ahmad Zain

(Degree)
博士（学術）

(Date of Degree)
2025-03-25

(Date of Publication)
2026-03-01

(Resource Type)
doctoral thesis

(Report Number)
甲第9205号

(URL)
https://hdl.handle.net/20.500.14094/0100496486

※ 当コンテンツは神戸大学の学術成果です。無断複製・不正使用等を禁じます。著作権法で認められている範囲内で、適切にご利用ください。

Doctoral Dissertation

Harnessing the potential of oleaginous yeast for sustainable lipid and biopolymer production from fatty acids

脂肪酸からの持続可能な脂質および生分解性ポリマー生産のための油脂性酵母の可能性の活用

January 2025

Department of Chemical Science and Engineering

Graduate School of Engineering

Kobe University

NOOR AFIQAH BINTI AHMAD ZAIN

PREFACE

This thesis is submitted by the author to Kobe University in partial fulfilment of the requirements for the degree of Doctor of Philosophy in Engineering. This study was carried out between the period of 2021 and 2025 under the supervision of Professor Chiaki Ogino.

In the name of Allah, the One worshipped and sought for help. All praise is due to Allah for His blessing. The author expresses her deepest gratitude to those who have generously supported and shared their valuable knowledges throughout this journey.

First and foremost, the author extends her deepest sincere gratitude to her supervisors, Professor Chiaki Ogino, Professor Prihardi Kahar, and Professor Akihiko Kondo for their unwavering support, guidance and encouragement throughout the research. Their invaluable advices, constructive feedbacks and expertise have significantly shaped the direction of this work.

To her labmates, she offers heartfelt thanks for their consistent guidance, motivation and the cherished moments shared together. Gratitude is also extended to The Ministry of Education, Culture, Sports, Science and Technology (MEXT) for providing the financial support that made this study possible.

The author is deeply grateful to her husband, Emier, for his unwavering support, patience, and understanding, and for making countless sacrifices to help her pursue her dreams. To her son, Amir Elham, born in the midst of this research journey, she expresses heartfelt gratitude for the love and laughter he has brought into her life, making each day brighter with his joyful presence.

Heartfelt thank also extended to her family for their unconditional love, prayers, and support who have been a source of encouragement throughout her academic journey. Finally, the author thanks everyone who has been a part of this journey. Each individual has contributed to her success in meaningful ways, and for that, she is forever grateful.

NOOR AFIQAH BINTI AHMAD ZAIN
November 18th, 2024

TABLE OF CONTENTS

PREFACE **1**

TABLE OF CONTENTS **3**

LIST OF TABLES **5**

LIST OF FIGURES **6**

SYNOPSIS **10**

CHAPTER 1 Introduction **13**

1.1 Oleaginous yeast 13

1.2 Carbon source 15

1.3 Microbial lipid 19

1.4 Polyhydroxyalkanoate 22

1.5 Current challenge 27

CHAPTER 2 Production of single cell oil by *Meyerozyma guilliermondii* from waste plant oil generated by the palm oil mill industry **28**

2.1 Introduction 28

2.2 Materials and methods 32

2.3 Results and discussion 36

2.4 Conclusion 60

CHAPTER 3 Dimorphism of oleaginous yeast *Meyerozyma guilliermondii* during production of single-cell oil under decanoic acid stress **61**

3.1 Introduction 61

3.2 Materials and methods 63

3.3 Results and discussion 67

3.4 Conclusion 94

CHAPTER 4 Metabolic engineering of oleaginous yeast *Meyerozyma guilliermondii* for production of biodegradable polyhydroxyalkanoate (PHA) **95**

4.1 Introduction 95
4.2 Materials and methods 97
4.3 Results and discussion 101
4.4 Conclusion 108
CHAPTER 5 General conclusion and future direction 109
REFERENCES 111

LIST OF TABLES

Table 1 Various substrates assimilated by *M. guilliermondii*. 14

Table 2 Fatty acids composition in PAO. 18

Table 3 Fatty acids profile of lipids produced from *M. guilliermondii* strains. 21

Table 4 Fatty acids profile of common vegetable oils. 21

Table 5 Several type of PHA monomers based on the length of carbon. 23

Table 6 Comparison of cell growth, lipid production and FAME profile of *M. guilliermondii* cultured with additional carbon sources 40

Table 7 Biomass and lipid production of *M. guilliermondii* grown on either YPD50 or YP media supplemented with different type of FAs. 46

Table 8 FAME profile of *M. guilliermondii* grown on either YPD50 or YP media supplemented with different type of FAs. 48

Table 9 Biomass, lipid content and FAME profile of *M. guilliermondii* grown on mix FAs. 51

Table 10 Effect of surfactant on cell biomass and lipid accumulation. 53

Table 11 Cell biomass, lipid content and FAME profile of *M. guilliermondii* grown on -NMM. 56

Table 12 Cell biomass, lipid content and FAME profile of *M. guilliermondii* grown on -NMM. 59

Table 13 Biomass and lipid production of *M. guilliermondii* grown on YPD50 supplemented with C10. 80

Table 14 List of *M. guilliermondii* strains. 98

LIST OF FIGURES

Figure 1 Waste generated from palm oil industry. 16

Figure 2 Kennedy pathway in oleaginous yeast. 20

Figure 3 Chemical structures of polyhydroxyalkanoates (PHA) (39). 22

Figure 4 PHA biosynthesis pathways. 24

Figure 5 Time course analysis of glucose consumption and cell growth of *M. guilliermondii*. (A) *M. guilliermondii* grown in YPD50/YP only as control group, (B) YPD50/YP supplemented with PAO, and (C) YPD50/YP with CPKO. The closed square represents glucose consumption in YPD50. The closed circle represents the DCW of *M. guilliermondii* grown on YPD50. The open circle represents the DCW of *M. guilliermondii* grown on YP. The error bars indicate the standard deviation from three independent experiments. 38

Figure 6 Lipase activity towards pNPB as the substrate from the cell-free culture supernatant. The error bars indicate the standard deviation from three independent experiments. 42

Figure 7 Time course analysis of glucose consumption and cell growth of *M. guilliermondii*. *M. guilliermondii* grown in (A) YPD50/YP only as control group, (B) YPD50/YP + C12:0, (C) YPD50/YP + C16:0 and (D) YPD50/YP + C18:1. The closed square represents glucose consumption in YPD50. The open square represents the DCW of *M. guilliermondii* grown on YPD50. The open circle represents the DCW of *M. guilliermondii* grown on YP. The error bars indicate the standard deviation from three independent experiments. 44

Figure 8 Lipid accumulated in the cells of *M. guilliermondii* cultured in media supplemented with respective FA at 120 h. Bars: 10 µm. 47

Figure 9 Time course for glucose consumption and cell growth of *M. guilliermondii* grown in YPD50 and YP supplemented with mix FA mimicking the composition of FFA in PAO. The closed square represents glucose consumption in YPD50. The open square represents the DCW of *M. guilliermondii* grown in YPD50 + mix

FAs. The open circle represents the DCW of *M. guilliermondii* grown in YP + mix FAs. The error bars indicate the standard deviation from three independent experiments. 49

Figure 10 Time course analysis of cell growth of *M. guilliermondii* grown in -NMM medium. The open square, triangle and circle represent DCW of *M. guilliermondii* grown in -NMM supplemented with PAO emulsion, glucose and PAO as carbon source, respectively. 55

Figure 11 Lipid accumulated in the cells of *M. guilliermondii* at 120 h. (A-C) The microscopic images of *M. guilliermondii* when culturing in -NMM medium supplemented with glucose (A), PAO emulsion (B) and PAO (C). (D-F) The microscopic fluorescence images of *M. guilliermondii* stained with BODIPY (493/505). Bars: 10 µm. 57

Figure 12 Representative images of *M. guilliermondii* culture in -NMM supplemented with 40 g/L of PAO and PAO emulsion. (A) Culture with PAO at 0h. (B) Culture with PAO emulsion at 0h. (C) Culture with PAO at 120 h. (D) Culture with PAO emulsion at 120 h. 58

Figure 13 Optical density (OD_{600}) of *M. guilliermondii* grown in YPD50 supplemented with additional FA in a range of concentration from 0.5 g/L, 1 g/L, 2 g/L, 4 g/L and 8 g/L at 72 h during primary screening. The red dashed line represents the OD_{600} of *M. guilliermondii* grown in YPD50 without FA supplementation (control). 68

Figure 14 Comparison of DCW (g/L) of *M. guilliermondii* grown in YPD50 and YP supplemented with additional FA at maximum tolerance concentration cultured for 72 h in 96-deep-well plate. Maximum tolerance concentration of FA: C4 (8 g/L), C6 (4 g/L), C8 (1 g/L), C10 (0.5 g/L), C12 (1 g/L), C14 (4 g/L), C16 (4 g/L), C18:0 (2 g/L), C18:1 (2 g/L), C18:2 (2 g/L), C20 (0.5 g/L), C24 (2 g/L), C26 (2 g/L), and C30 (1 g/L). 69

Figure 15 Time course for cell growth of *M. guilliermondii* grown in YPD50 supplemented with C10. The opened square represents dry cell weight (g/L) and the closed square represents glucose consumption (g/L). [a] 0.5 g/L of C10 was added at 0 h while [b] 0.5 g/L of C10 was added at 48 h. 74

Figure 16 The morphology of *M. guilliermondii* cells at 120 h when culturing in YPD50 medium with no C10 (A), 0.25 g/L of C10 (B), 0.5 g/L of C10 at 0 h (C), 0.5 g/L of C10 at 48 h (D), 1 g/L of C10 (E) and 2 g/L of C10 (F). The microscopic fluorescence images of *M. guilliermondii* stained with BODIPY (493/505). The upper and lower panel show bright-field and fluorescence microscopy images, respectively. Bars: 10 µm. 75

Figure 17 Time course observation of morphological changes in *M. guilliermondii* cells when 0.5 g/L of C10 was added into YPD50 at 0 h. The upper panel shows bright-field microscopy images and the lower panel shows fluorescence microscopy images of the same field of view stained with BODIPY to visualize accumulated lipids (green). Bars: 10 µm. 76

Figure 18 Time course observation of morphological changes in *M. guilliermondii* cells when 0.5 g/L of C10 was added into YPD50 at 48 h. The upper panel shows bright-field microscopy images and the lower panel shows fluorescence microscopy images of the same field of view stained with BODIPY to visualize accumulated lipids (green). Bars: 10 µm. 77

Figure 19 FAME profile of *M. guilliermondii* grown on YPD50 medium supplemented with C10. (A) Major FA composition. (B) Minor FA composition less than 2%. 82

Figure 20 Reactive oxygen species (ROS) in the cells of *M. guilliermondii*. (A-B) The microscopic images of *M. guilliermondii* when culturing in YPD50 medium supplemented with 0.5 g/L of C10 (B). (C-D) The microscopic fluorescence images of *M. guilliermondii* stained with ROS Assay Kit-Highly Sensitive DCFH-DA- (Dojindo Laboratories). Bars: 10 µm. 84

Figure 21 Expression level of genes related to antioxidant. C10 (-) refers to the control condition without the addition of C10, while C10 (+) refers to the addition of 0.5 g/L of C10 at 0 h. 86

Figure 22 Expression level of genes related to autophagy. C10 (-) refers to the control condition without the addition of C10, while C10 (+) refers to the addition of 0.5 g/L of C10 at 0 h. 88

Figure 23 Effect of addition of C10 in YPD50 medium on vacuole of *M. guilliermondii*. The upper panel shows bright-field microscopy images and the lower panel shows fluorescence microscopy images of the same field of view stained with yeast vacuole membrane marker MDY-64. Bars: 10 μm. 90
Figure 24 HOG MAPK pathway. 92
Figure 25 Expression level of genes related to MAPK. C10 (-) refers to the control condition without the addition of C10, while C10 (+) refers to the addition of 0.5 g/L of C10 at 0 h. 93
Figure 26 Vector construction. 99
Figure 27 DCW of *M. guilliermondii* strains cultured in -NMM at 120 h. 103
Figure 28 Lipid accumulated in the cells of *M. guilliermondii* strains at 120 h. (A-C) The microscopic images of *M. guilliermondii* when culturing in -NMM medium. (D-F) The microscopic fluorescence images of *M. guilliermondii* stained with BODIPY (493/505). Bars: 10 μm. 104
Figure 29 Construction of vector harbouring PHA genes. 106
Figure 30 GC chromatogram of PK01-wt (pink) and PK01::phaABC (black). C8 was used as internal standard in all the sample. 107
Figure 31 GC chromatogram of PK01-wt (pink), PK01::phaABC (black) and 3HB standard (blue). 107

SYNOPSIS

Chapter 1

Meyerozyma guilliermondii formerly known as *Pichia guilliermondii* or *Candida guilliermondii*, is a versatile yeast species widely studied for its biotechnological potential. It exhibits metabolic versatility, utilizing a variety of carbon sources from sugar-based substrates to support both cellular growth and lipid biosynthesis. However, there are limited studies on its ability to grow and accumulate lipid from fatty acids substrate. This review examines the potential of *M. guilliermondii* to utilize fatty acids not only for microbial lipid biosynthesis but also a precursor for sustainable bioplastic production, highlighting its potential as a versatile for generating value-added products such as polyhydroxyalkanoate (PHA). Exploring the capacity of *M. guilliermondii* to metabolize fatty acids as a carbon source for lipids and PHA production represents a promising research direction.

Chapter 2

Only a few reports available about the assimilation of hydrophobic or oil-based feedstock as carbon sources by *Meyerozyma guilliermondii*. In this study, the ability of *M. guilliermondii* to efficiently utilize free fatty acids (FFAs) and real biomass like palm acid oil (PAO) as well as crude palm kernel oil (CPKO) for growth and lipid production was investigated. PAO, CPKO, and FFAs were evaluated as sole carbon sources or in the mixed medium containing glucose. *M. guilliermondii* was able to grow on the medium supplemented with PAO and FFAs, which contained long-chain length FAs and accumulated lipids up to 35% (w/w) of its dry cell weight (DCW). The highest lipid content and lipid concentration were achieved at 50% (w/w) and 10.1 g/L, respectively,

when *M. guilliermondii* was cultured in nitrogen-limited mineral medium (-NMM) supplemented with PAO emulsion. Hydrophobic substrate like PAO could be served as promising carbon source for *M. guilliermondii*.

Chapter 3

In this study, the ability of *M. guilliermondii* to utilize various fatty acids was evaluated, and the strain exhibited no growth in the presence of decanoic acid (C10) during the initial screening. The effects of C10 on growth, morphology, and lipid accumulation were subsequently investigated. Culturing *M. guilliermondii* in YPD50 medium supplemented with 0.5 g/L of C10 at 0 h resulted in a significantly prolonged lag phase and induced a morphological transition from yeast-like cells to pseudohyphal structures once growth resumed. Despite the growth inhibition and morphological change, lipid accumulation remained unaffected, with control and C10-exposed cells producing approximately 36 wt% lipid content. The fatty acid composition, predominantly consisting of palmitic acid (C16:0), oleic acid (C18:1), and linoleic acid (C18:2), was similar between both the control and C10-exposed cells, and C10 was not incorporated into the cellular lipids. Accumulation of reactive oxygen species (ROS) was observed in the C10-exposed cells, correlating with the upregulation of superoxide dismutase (*SOD*) genes, suggesting oxidative stress as a response to C10 exposure. Pseudohyphal cells displayed enlarged vacuoles, which may be linked to enhanced autophagy, as indicated by the upregulation of autophagy-related gene *ATG9*. YPD1 expression was also upregulated in the HOG pathway, although its interaction with oxidative stress-related transcription factors remains unclear. These findings highlight *M. guilliermondii* as a highly resilient and versatile strain, capable of adapting to environmental stress.

Chapter 4

Lipid accumulation occurs primarily in the form of TAGs. This study investigated the effect of disrupting key genes involved in TAG biosynthesis to redirect fatty acid flux towards PHA biosynthesis. Genetic disruptions of the Kennedy pathway acyltransferases, *LRO1* and *SCT1*, revealed significant differences in their roles. The ΔLRO1 mutant exhibited a 50% reduction in lipid content, whereas the ΔSCT1 mutant showed no substantial decrease. Fluorescence microscopy using BODIPY staining highlighted the diminished lipid body size in ΔLRO1 mutant. To enable PHA production, *phaA*, *phaB* and *phaC* were integrated at the *LRO1* locus. GC analysis of engineered strains confirmed the reduction in lipid synthesis evidenced by diminished fatty acid peaks and detected minimal levels of PHA in the form of P(3HB), indicating functional but low yield of PHA biosynthesis. These findings highlight the critical role of *LRO1* in TAG synthesis and established a foundation framework for further metabolic engineering to enhance PHA production in *M. guilliermondii*.

Chapter 5

This chapter presents a general conclusion on the potential of *M. guilliermondii* as a platform for PHA production, emphasizing its resilience and suitability for sustainable bioprocess. Furthermore, future directions are suggested, focusing on strain development strategies for synthesizing value-added products.

CHAPTER 1

Introduction

1.1 Oleaginous yeast

Oleaginous microorganisms, particularly yeasts, stand our as promising host for microbial lipids. These microbes are defined by their ability to store lipids as intracellular triacylglycerols (TAGs), which comprise at least 25% of their cell biomass and serve as reserves carbon and energy sources (1). Yeasts, in particular, offer advantageous over other oleaginous microorganisms due to their rapid growth rates, robust lipid accumulation, and scalability in production. Additionally, yeast can utilize various low-cost carbon sources for growth and lipid production (2). Many oleaginous yeast species have been successfully isolated and screened for lipid production, including those from the genera *Candida*, *Lipomyces*, *Rhodotorula*, *Cryptococcus*, *Yarrowia* and *Trichosporon* (2). While significant attention has been given to widely studied species like *Yarrowia lipolytica*, *Rhodosporiudium toruloides* and *Lipomyces starkeyi*, less explored yeasts also hold considerable promise for industrial applications. One such species in *Meyerozyma guilliermondii*, a yeast that combines oleaginous traits with distinct advantages.

1.1.1 Oleaginous yeast *Meyerozyma guilliermondii*

Meyerozyma guilliermondii formerly known as *Pichia guilliermondii* or *Candida guilliermondii*, is a versatile yeast species widely studied for its biotechnological potential (3). It is well known for its industrial applications, including the production of riboflavin, xylitol, bioethanol, and various industrial enzymes, making it an attractive organism for sustainable bioprocessing (4–8). It is also used for its role in bioremediation and biocontrol due to its capability to degrade various toxic compound, thus contributing to environmental sustainability (3, 9, 10) . In addition, *M.*

guilliermondii demonstrated metabolic versatility, utilizing a variety of carbon sources from sugar-based substrates, including glucose, xylose, glycerol and lignocellulosic biomass hydrolysates to support both cellular growth and to produce various chemical compound as listed in Table 1. Despite its diverse capabilities, studies on the lipid production potential of *M. guilliermondii* remain relatively limited compared to other oleaginous yeast. Certain strains of *M. guilliermondii* have demonstrated the ability to accumulate high lipid levels, making it a promising candidate for microbial lipid production. Under optimal conditions, *M. guilliermondii* has been reported to accumulate lipids up to 60.6% (w/w) of its DCW (11). The fatty acid profile of the accumulated lipids is comparable to that that of palm oil, with palmitic acid (C16:0) and oleic acid (C18:1) as the predominant fatty acids. In addition to its high potential in biotechnology, *M. guilliermondii* exhibits tolerance to inhibitory chemical compounds commonly present in industrial hydrolysates (6, 12). These attributes collectively positioning *M. guilliermondii* as a highly promising candidate for commercial lipid production.

Table 1 Various substrates assimilated by *M. guilliermondii*.

Carbon sources	Product	Reference
Glucose	Lipid, xylitol, organic acids, riboflavin	(4, 11, 13, 14)
Xylose	Ethanol, xylitol	(15, 16)
Glycerol	Lipid	(17)
Sugarcane bagasse hydrolysate	Xylitol	(18)
Sugarcane straw hydrolysate	Xylitol	(19)
Rice straw hydrolysate	Xylitol	(20)

1.2 Carbon source

Oleaginous microorganisms, including yeast are recognized for their ability to accumulate lipids through two distinct biosynthetic pathways: the *de novo* and *ex nov*o lipid synthesis pathways which are utilized depending on the carbon source provided during cultivation. Specifically, these pathways are activated when the yeasts are cultured with sugar-based and oil-based substrates, respectively. The *de novo* pathway predominantly involves the biosynthesis of lipids from simple carbon sources, such as glucose, leading to substantial lipid accumulation that primarily consists of long-chain length fatty acids, which resemble those found oils derived from agricultural crops (21). This pathway is particularly active under nitrogen-limited conditions, where excess carbon availability triggers a metabolic shift favouring lipid storage.

In contrast, the *ex novo* synthesis pathway enables oleaginous yeasts to assimilate external lipids from oil-based substrates directly into intracellular lipid stores. This pathway has the potential to alter both extracellular and intracellular lipid composition, potentially either resemble or differ from the composition of the initial substrate (21, 22). In this pathway, cells actively uptake and metabolize exogenous fatty acids, incorporating them into storage lipids without the need for complete fatty acid synthesis. This process offers significant flexibility in lipid composition, as it depends on the fatty acid profile of the provided substrate. Although most studies on lipid production have focused on sugar-based substrates, research indicates that lipid accumulation can also be achieved with oil-based substrates, including free fatty acids from animal fats (23). Additionally, fatty acid-based substrates are predicted to improve lipid yield and lower production cost compared to sugar-based substrates due to their higher carbon content per unit weight.

1.2.1 Palm acid oils

Palm oil industry has experienced tremendous growth in recent years, with Indonesia and Malaysia being the two top palm oil producers and exporters worldwide. As a result, a huge amount of palm waste was generated from palm oil mill effluent (POME) and oil palm biomass, including oil palm trunks (OPTs), oil palm fronds (OPFs), empty fruit brunches (EFBs) and palm kernel shells (PKSs) (Figure 1). As the largest fraction of waste, POME is a liquid waste obtained during the milling process and contains a high amount of biochemical oxygen demand (BOD), chemical oxygen demand (COD), oil, and grease; thus, it is suitable to be utilized for bioenergy production (24, 25). Besides being used for the production of bioenergy, volatile fatty acids (VFAs) collected from anaerobic treatment of POME can also serve as the substrate for value-added products such as polyhydroxyalkanoate (PHA) (26). Palm acid oil (PAO), a small fraction derived from palm oil mill effluent (POME), has gained attention as a cost-effective carbon source due to its high free fatty acid (FFA) content, which ranges from 27.6 to 81.2% and has limited use (27).

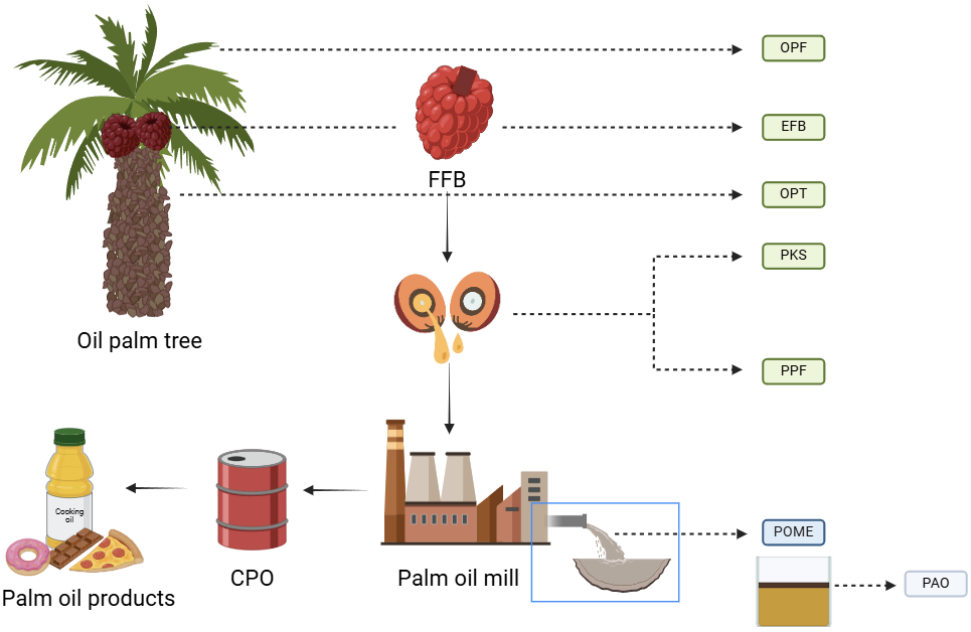

Figure 1 Waste generated from palm oil industry.

PAO is thick, brownish, greasy, non-toxic, has unpleasant odour and rapidly solidify at room temperature. Due to its high free fatty acid content, PAO serves as a rich energy source that supports microbial growth and the biosynthesis of various valuable metabolites, such as lipids, enzymes and bioactive compounds while currently being primarily utilized for the production of FAs, animal feed, low-grade laundry soap, and other products (27–29). Utilizing PAO in fermentation process not only reduces production costs and aids in waste valorization by converting an industrial byproduct into value-added products, but also adds more value to the palm oil industry and provides significant environmental benefits.

Microbial lipids have been shown to be producible from derivatives of the oleo chemical industry and animal fat, which are composed of free FA (FFAs) (23). Given that, PAO contains a high percentage of long-chain-length FFAs (Table 2), mainly palmitic acid (C16:0) and oleic acid (C18:1) (30), it has a high potential as a promising carbon source for the production of energy-dense compounds, especially lipids. In oleaginous microorganisms, PAO can be directed into lipid biosynthesis pathway, resulting in the accumulation of triacylglycerols (TAGs), which are of interest for biodiesel and other biofuel applications. Additionally, its composition which also includes medium-chain-length FFAs, is advantageous for microbes that utilize these acids as building blocks for biopolymer production, such as polyhydroxyalkanoates (PHA). Thus, using PAO in microbial fermentation represent a sustainable approach to valorize waste streams from the palm oil industry, reducing environmental impact while promoting circular bioeconomy initiatives.

Table 2 Fatty acids composition in PAO.

Fatty acid	Relative % (w/w)
Lauric (C12:0)	0.8
Myristic (C14:0)	1.1
Palmitic (C16:0)	44.7
Stearic (C18:0)	3.7
Arachidic (C20:0)	0.4
Oleic (C18:1)	40.3
Linoleic (C18:2)	9.4

1.3 Microbial lipid

Microbial lipids, also known as single-cell oils (SCOs) is accumulated as intracellular carbon storage compounds by oleaginous microorganisms. The FAs composition of the microbial lipids can vary based on the substrate supplied during the fermentation process. Due to their similarity in FA composition to oils from agricultural crops (31, 32), microbial lipid has been considered as a promising feedstocks for biodiesel production. Gowing concerns over environmental sustainability and energy security have driven interest in renewable alternatives to petroleum-based feedstock. While vegetable oils and animal fats have traditionally been used as renewable substitutes; however, their use raises concerns due to competition with food resources. In contrast, microbial lipids offer a sustainable option for biofuel production and other oleochemicals applications, including lubricants and specialty chemicals. Additionally, it also can provide an alternative source of polyunsaturated fatty acids (PUFAs), which are beneficial to human health and typically sourced from the ocean fish (31, 33). Compared to agricultural oil crops and fish oil, microbial lipid production offers several advantages including short production cycles, independence from location, season, and climate conditions, lower labor requirements, no large production land area needed, and avoidance of competition with food production.

Extensive research has been conducted on the lipid synthesis pathway in the oleaginous yeast like *L. starkeyi* (34). Lipid accumulation occurs primarily in the form of TAGs through two key pathways which are the acyl-CoA synthesis pathway and the Kennedy pathway. When glucose or other sugar-based substrates are used and nitrogen is limited, the fatty acid synthase (Fas1, Fas2) complex produces acyl-CoA using both acetyl-CoA and malonyl-CoA. This process is activated under nitrogen limitation, which redirects carbon flux from the TCA cycle to lipid synthesis. The resulting

accumulation of citrate in the mitochondria is transported to the cytosol, where cytosolic citrate is converted to oxaloacetate and acetyl-CoA. Acetyl-CoA is then further converted to malonyl-CoA, providing building blocks for fatty acid synthesis. When fatty acid-based or other hydrophobic substrates serve as carbon source, lipases hydrolyse them to release free fatty acid, which can support both cellular growth and lipid production. Free fatty acids are converted to acyl-CoA, which can either be incorporated into TAGs or degraded via *β*-oxidation pathway into acetyl-CoA and smaller acyl-CoAs. In the Kennedy pathway, there molecules of fully synthesized acyl-CoA sequentially bind to one molecule of glecerol-3-phosphate for the assembly of TAGs (Figure 2).

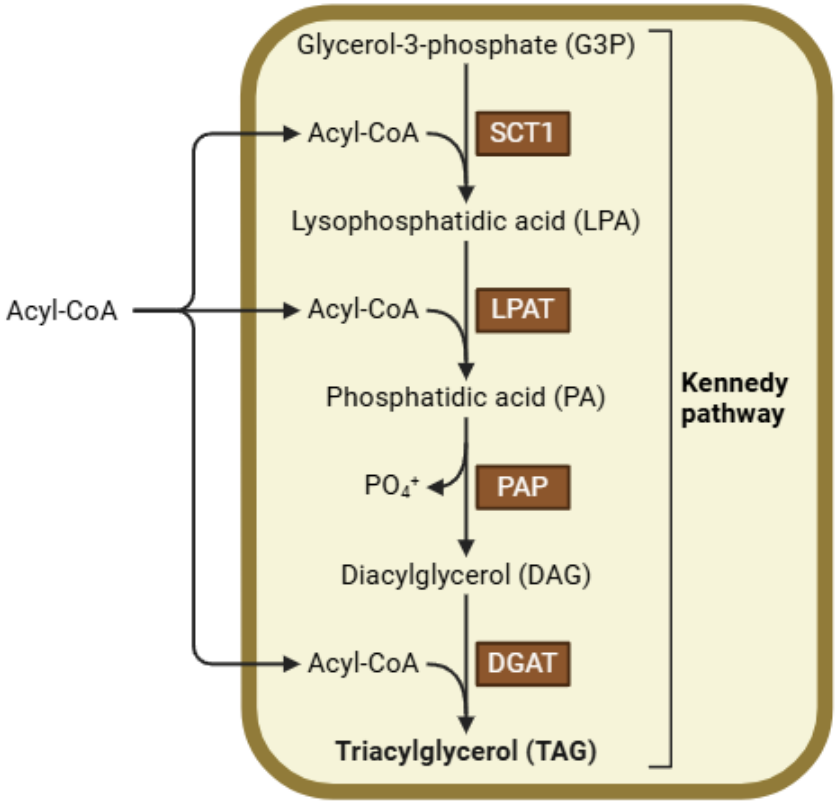

Figure 2 Kennedy pathway in oleaginous yeast.

The lipid accumulation and fatty acid composition in oleaginous yeasts are strain-dependent and can vary significantly even among strains within the same species (2). As shown in Table 3, the major fatty acids in *M. guilliermondii* are C18;1 and C16:0, regardless of strain. A comparison of the FAs profile in Table 3 and Table 4 demonstrates that *M. guilliermondii* lipids have a composition similar to common vegetable oils, supporting the potential of *M. guilliermondii* as a promising candidate for biodiesel feedstock.

Table 3 Fatty acids profile of lipids produced from *M. guilliermondii* strains.

Substrate	C16:0	C16:1	C18:0	C18:1	C18:2	Other	Reference
Inulin	21.9	12.2	5.8	57.9	1.7	0.5	(11)
Glycerol	15.2	7.4	6.4	59.8	4.7	6.4	(17)
Glucose	18.6	12.4	2.3	62.6	3.0	1.1	(35)
Mannose	20.2	13.3	2.3	60.8	1.5	1.9	(35)
Xylose	19.8	15.4	2.2	61.0	1.2	0.4	(35)

Table 4 Fatty acids profile of common vegetable oils.

Oils	C16:0	C18:0	C18:1	C18:2	C18:3	C20:0	Other [a]	Reference
Palm	35.8	4.1	43.8	14.3	0.2	0.4	1.3	(36)
Soybean	9	4	28.5	49.5	8	-	0.5	(37)
Sunflower	3.7	2	31.5	59.5	-	2.3	-	(37)

[a] Other fatty acids including C12, C14, C16:1.

1.4 Polyhydroxyalkanoate

Polyhydroxyalkanoate (PHA) is bio-based plastics that serve as sustainable alternatives to petroleum-based plastics. These biopolymers are synthesized by various microorganism as water insoluble inclusion that accumulated within the cells (38). Similar to microbial lipids, PHA function as intracellular reserves of carbon and energy, with its accumulation occurs under conditions of nutrient imbalance with excess carbon and limited nitrogen. PHA gained many interests due to its desirable features, including biocompatibility, biodegradability and negligible cytotoxicity to the cells depending on its type of monomers. Thus, it has a wide range of potential applications.

Structurally, PHA is composed of repeating monomer units, forming polymers that can be classified as either homopolymers, consisting of identical monomers, or heteropolymers, composed of different monomer units. The basic building block of PHA is the (*R*)-3-hydroxyalkanoate monomer unit (Figure 3). Depending on the number of carbon atoms in the monomeric units, PHA is categorized into two groups which is short-chain-length (scl) PHA which exhibit thermoplastics properties and medium-chain-length (mcl) PHA with elastomer-like properties (Table 5).

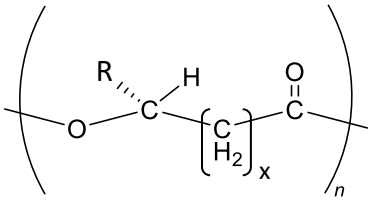

Figure 3 Chemical structures of polyhydroxyalkanoates (PHA) (39).

Table 5 Several type of PHA monomers based on the length of carbon.

Group	Number of carbons	Name of monomer
scl-PHA	4	3-hydroxybutyrate (3HB)
	4	4-hydroxybutyrate (4HB)
	5	3-hydroxyvalerate (3HV)
mcl-PHA	6	3-hydroxyhexanoate (3HHx)
	8	3-hydroxyoctanoate (3HO)
	10	3-hydroxydecanoate (3HD)
	12	3-hydroxydodecanoate (3HDD)

The biodegradation of PHA is influenced by various factors including microbial activity, moisture, temperature, and pH, as well as the molecular weight and surface area of the PHA itself. The degradation process begins with the hydrolysis of PHA into water-soluble monomers and oligomers by extracellular depolymerase (PhaZ) (40). These smaller molecules are then assimilated by the microorganisms as nutrients sources. Under aerobic conditions, PHA degradation results in the release of carbon dioxide and water, whereas anaerobic degradation produces methane as an additional byproduct (41). This production and biodegradation cycle aligns well with the carbon cycle, as the carbon dioxide generated can be recycled through photosynthesis and subsequently reincorporated into PHA.

1.4.1 PHA biosynthesis pathway

The important steps involved in PHA biosynthesis are the supply of monomer substrates from carbon sources and the polymerization of these monomers by PhaC, the

key enzyme in PHA biosynthesis pathway. The most studied pathways known to supply monomeric units for biosynthesis of PHA are summarized in Figure 4.

Among the pathways, the most common and simplest involves three series of enzymatic reactions of *phaA*, *phaB* and *phaC* (42–45). In the first step, two molecules of acetyl-CoA are condensed by enzyme *β*-ketothiolase (PhaA) to form acetoacetyl-CoA. Then, acetoacetyl-CoA is reduced to form (*R*)-hydroxybutyryl-CoA by enzyme acetoacetyl-CoA reductase (PhaB) and subsequently polymerized by PhaC into P(3HB). Another pathway involve are fatty acid *β*-oxidation pathway and fatty acid *de novo* synthesis pathway which involve in mcl-PHA production. In fatty acid *β*-oxidation pathway, acyl-CoA is converted from fatty acids and oxidized to enoyl-CoA. After that, (*R*)-specific enoyl-CoA hydratase encoded by PhaJ converts enoyl-CoA to (*R*)-3-hydroxyacyl-CoA directly (46). In fatty acid *de novo* synthesis pathway, acyl-ACP is converted to 3-hydroxyacyl-ACP through a series of enzymatic reactions, which is subsequently converted to (*R*)-3-hydroxyacyl-CoA by PhaG. (*R*)-3-hydroxyacyl-CoA then serves as a monomer for polymerization by PhaC.

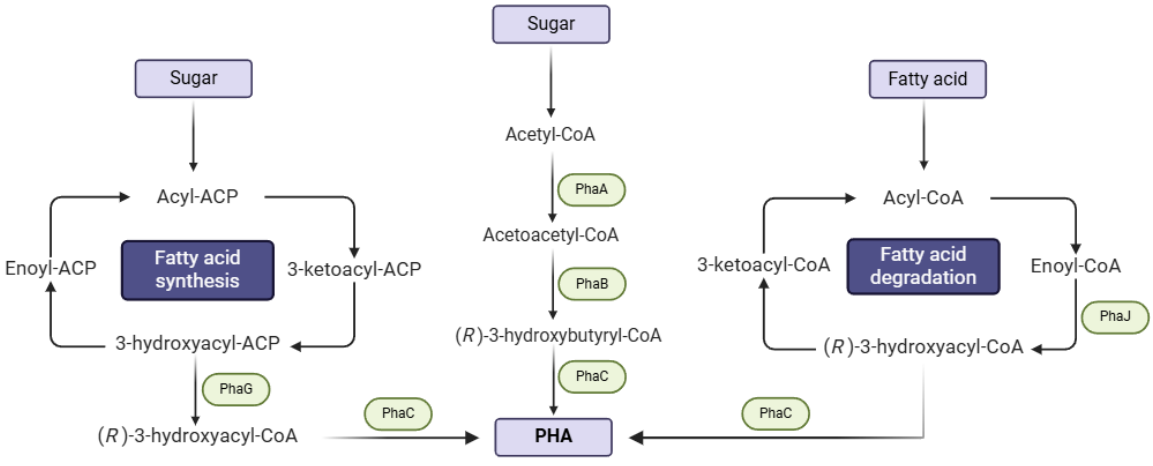

Figure 4 PHA biosynthesis pathways.

1.3.2 PHA producer

Many microorganisms either natural isolates or recombinants have been identified as PHA producers. Among these, *Cupriavidus necator* has gained the most attention and intensively investigate as the model organism for studying PHA biosynthesis due to its capability to utilize a wide range of carbon substrates and grow at high cell densities (47). Wild type strain *C. necator* H16 accumulates PHA in the form of P(3HB) in large amounts in the cell (48). Besides, a non-PHA producer such as *Escherichia coli* and yeast has been commonly employed for genetic and metabolic engineering of PHA related genes.

Yeast is a fast-growing unicellular eukaryote and could be used as a model system to study how metabolic pathways can be modified to synthesized PHA in eukaryotes. Even though it does not naturally produce PHA, as it does not harbor PhaC, several studies have employed peroxisomes of *Saccharomyces cerevisiae* (49–51), *Pichia pastoris* (52) and *Yarrowia lipolytica* (53–55) in the production of PHA. Peroxisomes of yeast are involved in *β*-oxidation of fatty acids, which supply the organelle with different length of (*R*)-3-hydroxyacyl-CoA that can be used as substrate for production of mcl-PHA. PhaCs of *Psudomonas aeruginosa* and *P. aleovorans* which are classified as Class II PhaC showing substrate preference towards mcl-PHA monomers (56) has usually been expressed in peroxisomes of yeast cells (49, 51, 53, 54). Yeast cells expressing those PhaCs were successfully accumulate PHA when fatty acids were used as carbon sources.

Yeast has also been engineered to produce scl-PHA. There were studies on expression of Class I PhaC of *C. necator* ($PhaC_{Cn}$) which actively polymerizes scl-PHA monomer (56) in recombinant yeast (49, 50). *S. cerevisiae* strain harboring a peroxisomal $PhaC_{Cn}$ was fed with an even-numbered fatty acid such as lauric acid and

oleic acid to test the effect of carbon sources supplied on the monomer composition of PHA produced. It resulted in the accumulation of copolymer PHA consisting of C_4, C_6 and C_8 monomers (49). The capabilities of PhaC$_{Cn}$ to incorporate mcl-PHA was due to additional metabolic pathways available in the host strain. It is worthwhile to express more PhaCs from different bacterial species with high enzymatic activity and broader substrate specificity in eukaryotic system to improve PHA production with novel compositions.

It thus sounds an intriguing trial to reinforce the peroxisomes through expression of suitable PhaC while at the same time giving better understanding on how enzyme can be modified to improve the productivity of PHA in recombinant yeast cell.

1.5 Current challenge

One major challenge in utilizing *Meyerozyma guilliermondii* for TAGs and PHA production is limited research available on its lipid metabolism and genetic regulation. This species has demonstrated the ability to produces lipids up to 60% of its DCW under certain conditions (11), making it a promising candidate for industrial applications. However, the information about genes and pathways involved in TAGs biosynthesis remain limited. A multi-omics analysis of lipid metabolism in a marine probiotic strain of *M. guilliermondii* identified genes involved in steroid biosynthesis and glycerolipid metabolism (57), but the study did not specifically focus on TAGs production. This knowledge gap complicated efforts to genetically engineer *M. guilliermondii* to reduce competition between TAGs and PHA production pathways, which is essential for enhancing PHA yields in yeast. Metabolic engineering is an essential tool for enhancing the capability of oleaginous yeast to produce microbial lipids or value-added chemicals. However, its application in oleaginous yeast is limited due to a lack of robust genetic tools, and transformation properties are often species-specific. These challenges highlight the need for strain-specific optimization in genetic engineering tools and a deeper understanding of lipid metabolism in *M. guilliermondii*. Such efforts will be crucial to fully exploit its potential for sustainable production of microbial lipids and other value-added bioproducts.

CHAPTER 2

Production of single cell oil by *Meyerozyma guilliermondii* from waste plant oil generated by the palm oil mill industry

2.1 Introduction

Single cell oil (SCO), also known as microbial lipid, is an intracellular carbon reserve accumulated by oleaginous microorganisms. It has a wide range of applications including biodiesel production, food, cosmetic and pharmaceuticals depending on the fatty acids (FAs) composition (31). The FA profile of microbial lipid varies based on the characteristics of the substrate used during fermentation. Microbial lipids are particularly promising as a feedstock for biodiesel production due to their FA composition being similar to that of oils derived from agricultural crops (31, 32). Additionally, microbial lipids serve as an alternative source of polyunsaturated fatty acids (PUFAs), which are known for their health benefits and are traditionally obtained from marine fish (31, 33). Compared to agricultural oil and fish oil, using microbial lipids offer significant advantages, including short production cycles, independence from geographical, seasonal, and climatic constraints, requiring less labor, minimal land use, and avoidance of competition with food production. Furthermore, oleaginous microorganisms grow rapidly, accumulate high lipid content, and are well-suited for scalable production processes. These microorganisms can utilize both sugar-based and oil-based feedstocks, synthesizing lipids through two main pathways: de novo and ex novo lipid synthesis. While de novo synthesis typically results in high lipid yields, ex novo synthesis can modify both extracellular and intracellular lipid compositions (21). For large-scale production of microbial lipids, selecting a suitable feedstock is essential. However, the cost of feedstock can largely contributed to the overall high production cost (58–60). To address this, cost-effective and renewable carbon sources are preferred.

Many studies have demonstrated the use of waste materials for lipid production from wastewater (61, 62), livestock waste (63), food waste (64–66) and waste cooking oil (67).

Palm oil industry has undergone significant growth in recent years, with Indonesia and Malaysia emerging as the leading producers and exporters globally. Consequently, substantial amount of palm waste was generated including palm oil mill effluent (POME) and oil palm biomass such as oil palm trunks (OPTs), oil palm fronds (OPFs), empty fruit brunches (EFBs) and palm kernel shells (PKSs). Among these, POME constitutes the largest fraction of waste. It is a liquid byproduct of the milling process, characterized by high levels of biochemical oxygen demand (BOD), chemical oxygen demand (COD), oil and grease, making it a suitable substrate bioenergy production (24, 25). In addition to bioenergy applications, volatile fatty acids (VFAs) collected from the anaerobic treatment of POME can serve as the substrates for the synthesis of value-added products such as polyhydroxyalkanoate (PHA) (26). A small fraction of POME known as palm acid oil (PAO) contains 27.6 to 81.2% of free fatty acids (FFAs) and has limited use (27). Currently, PAO is mainly utilized in the production of FAs, animal feed, low-grade laundry soap, and other products (27–29). Studies have demonstrated that microbial lipids can also be synthesized from derivatives of the oleochemical industry and animal fats rich in FFAs (23). As PAO contains a high percentage of long-chain-length FFA, mainly palmitic acid (C16:0) and oleic acid (C18:1) (30), it has a high potential as a carbon sources for microbial lipid production. These FFAs can either promote microbial growth or be stored as lipid droplets, leading to alteration in the lipid composition that may resemble or differ from the initial substrate, enhancing the fatty acid profile (22). In addition, FA-based

feedstocks are predicted to support better yields and lower production cost compared to sugar-based feedstock, as it contains higher carbon content per weight than sugar.

In addition, the conversion of palm oil industrial waste like PAO into microbial lipids can enhance the value of the palm oil industry while providing significant environmental benefits. Thus, this study aims to evaluate the potential of PAO as a low-cost carbon source for lipid production. Additionally, this study also evaluates the ability of *Meyerozyma guilliermondii* to utilize crude palm kernel oil (CPKO) as a potential carbon source, comparing its performance to PAO. CPKO is derived from the kernels of oil palm fruit and is primarily composed of triacylglycerides (TAGs). It contains a higher proportion of medium-chain-length saturated FA, such as lauric acid (C12:0), which makes it solid at room temperature (68, 69). Due to its carbon-rich composition, CPKO is a valuable byproduct and a suitable feedstock for microbial fermentation processes. Unlike crude palm oil (CPO), which is derived from the mesocarp of the oil palm fruit and widely used in the food industry as cooking oil, CPKO constitutes a smaller fraction of palm oil production and is mainly utilized in the oleochemical industries. Therefore, its application in microbial lipid production does not interfere with the food industry supply chain.

Efficient utilization of fatty acids (FAs) as a carbon source for growth and lipid accumulation requires the selection of microbial strains capable of growing on FAs and producing high lipid content. Currently, only a limited number of yeast strains have demonstrated the ability to grow on oil-based or hydrophobic substrates and accumulate lipids via the ex-novo lipid synthesis pathway. While much research has focused on sugar-based feedstock for microbial lipid production, studies have been shown that microbial lipids can be synthesized from oil-based feedstocks and animal fats rich in

free fatty acids (FFAs). *Yarrowia lipolytica*, as model oleaginous yeast, has benn extensively studied to elucidate the mechanisms underlying the utilization of hydrophobic substrates (1). It has been shown to grow on stearin, an industrial derivative of animal fat containing saturated FFAs, achieving a lipid accumulation of approximately 0.44 to 0.54 g of lipid per gram of biomass (23). Another strain, Cryptococcus albidus, achieved a lipid content of 27.8% (w/w) when volatile fatty acids, including acetic acid, propionic acid, and butyric acid, were used as the sole carbon source for lipid synthesis (60). Additionally, *C. curvatus* and *Rhodosporidium toruloides* successfully utilized waste cooking oil as a carbon source and produced lipids at concentrations of 13.06 g/L and 1.47 g/L, respectively (67, 70).

Another oleaginous yeast, *Meyerozyma guilliermondii* widely recognized for its diverse applications including the production of xylitol, ethanol, and enzymes, as well as its role in bioremediation (4–6, 8–10, 71). This yeast demonstrates the ability to utilize various types of carbon sources, including glucose, xylose, and lignocellulosic biomass hydrolysates (3, 13, 18, 19). Furthermore, *M. guilliermondii* is known for its adaptability to various environmental conditions and its resistance to inhibitory chemical compound typically found in industrial processes (6, 12). Despite its versatility, research on its lipid production potential remains limited. Current studies on lipid accumulation in *M. guilliermondii* have primarily focused on substrates such as glucose and glycerol (11, 17), with minimal exploration of its ability to utilize fat and oil-based feedstocks. Hence, this study investigates the capability of *M. guilliermondii* to utilize FAs from real biomass sources like PAO and CPKO through the *ex novo* lipid synthesis pathway for lipids production. To achieve this, the ability of oleaginous yeast *M. guilliermondii* to grow and accumulate lipids from PAO and CPKO was first evaluated. Additionally, lipids production was performed using single FA that represent

the major components of PAO and CPKO as carbon sources to gain deeper insights into the process. For comparative purposes, glucose was used as carbon source and served as the control.

2.2 Materials and methods

2.2.1 Yeast strain and seed preparation

Wild-type *Meyerozyma guilliermondii* from our private collection (PK01) was used in this study. The strain was routinely cultured on YPD agar (10 g/L of yeast extract, 20 g/L of peptone, and 20 g/L of D-glucose) at 30 °C with kanamycin (50 µg/mL) and ampicillin (100 µg/mL) added to prevent bacterial cross-contamination.

A seed culture was prepared by inoculating a single yeast colony in 12 mL of YPD broth containing kanamycin and ampicillin in a 100 mL Erlenmeyer flask. The flask was incubated overnight at 29 °C, 190 rpm in an orbital shaker (BioShaker BR-43FH MR, Taitec Corp., Tokyo, Japan).

2.2.2 Media preparation

For lipid production, *M. guilliermondii* was cultured in either YPD50 [10 g/L yeast extract, 20 g/L peptone, and 50 g/L D-glucose] or YP [10 g/L yeast extract and 20 g/L peptone] broth. Both media were autoclaved at 121 °C for 15 min. *M. guilliermondii* was also cultured in nitrogen-limited mineral medium (-NMM), which consisted of nitrogen sources [1.5 g/L yeast extract and 0.25 g/L $(NH_4)_2SO_4$], 1.5 g/L $MgSO_4 \cdot 7H_2O$, phosphate buffer [7 g/L KH_2PO_4 and 5 g/L $Na_2HPO_4 \cdot 7H_2O$], and a trace element solution [0.08 g/L $FeSO_4 \cdot 7H_2O$, 0.01 g/L $ZnSO_4 \cdot 7H_2O$, 0.1 g/L $CaCl_2 \cdot 7H_2O$, 0.1 g/L $MnSO_4 \cdot 4H_2O$, 0.002 g/L $CuSO_4 \cdot 5H_2O$ and 0.002 g/L $CoCl_2 \cdot 6H_2O$]. The initial pH of -NMM was adjusted to 5.5.

2.2.3 Carbon sources

The fatty acids (FAs) tested in this study, in sodium salt form, were from Tokyo Chemical Industry (Tokyo, Japan) and Sigma-Aldrich (Tokyo, Japan). Sodium laurate (C12:0) and sodium palmitate (C16:0) were dissolved in 50% ethanol and hot 50% ethanol, respectively, while sodium oleate (C18:1) and sodium linoleate (C18:2) were dissolved in 70% ethanol. All FAs were filter-sterilized using a 0.2 μm filter before use. Palm acid oil (PAO) was obtained from PT Agricinal (Bengkulu, Indonesia) and crude palm kernel oil (CPKO) was obtained from AcidChem Ltd. (Penang, Malaysia). PAO emulsion was prepared at 50 % (w/v of oil in water) by mixing 20 g of PAO with 20 mL of Milli-Q water and 1 mL of Tween 20 [5% (v/w of PAO)]. PAO, PAO emulsion and CPKO were sterilized by autoclaving at 121 °C for 15 min. The sterilized PAO emulsion was stirred at 80 °C overnight prior to usage.

2.2.4 Lipid production in shake flask

The seed culture was adjusted to an initial optical density (OD_{600}) of 14.0 – 16.0 and transferred to YPD50, YP or -NMM media with a working volume of 12 mL in 100 mL Erlenmeyer flasks. Additional carbon sources were added aseptically at 0 h. Cultures were incubated at 29 °C, 190 rpm for 120 h in an orbital shaker incubator (BioShaker BR-43FH MR, Taitec Corp., Tokyo, Japan). Samples were collected for every 24 h to measure dry cell weight (DCW). After 120 h, cultures were harvested by centrifuging at 8000 rpm for 10 min. For cultures using CPKO or PAO as the carbon source, cell pellets were washed with a 1:1 mixture of hexane and deionized water to remove residual oil, followed by two washes with deionized water and centrifuged again as described. DCW was determined after freeze-drying. Since PAO and CPKO are solid at the cultivation temperature, only the residual PAO or CPKO remaining after fermentation was measured gravimetrically. The relevant variables for yeast

concentration and lipid production were calculated as follows: DCW (g/L) was determined by dividing the cell dry weight by the volume of the medium; lipid concentration (g/L) was calculated by multiplying the lipid content (%) by the DCW; and residual biomass (g/L) was obtained by subtracting the lipid concentration from the DCW.

2.2.5 Determination of total lipid content by gravimetric analysis

Lipid production was measured gravimetrically using a modified Folch method (72). Triplicate freeze-dried cell samples (~15 mg each) were added in 2.0 mL polypropylene microvials containing 0.5 mm zirconia beads. Then, 1.5 mL of Folch solvent [2:1 of chloroform: methanol (v/v)] were added to each vial. The cells were pulverized using a Shake Master Neo ver.1.0 (BMS-M10N21, BMS, Tokyo, Japan) at 1500 rpm, 15 min. Following a 5-min centrifugation at 14000 *x*g, the supernatant was discarded, and the cell pellets were washed with 1.5 mL of deionized water, pulverized and centrifuged again. After discarding the deionized water, the cell pellets were dried at 60 °C until a constant weight was obtained. Lipid content was calculated based on the weight difference and expressed as a percent of dry cell weight.

2.2.6 Determination and quantification of total fatty acid methyl esters (FAME)

The fatty acids composition was determined by converting lipids from lyophilized cells into methyl esters using direct transesterification, following the manufacturer's protocol for the fatty acid methylation kit (Nacalai Tesque, Inc., Japan). The resulting fatty acid methyl esters (FAMEs) were extracted (light phase), transferred to a GC vial with a micro-tube glass insert, and analyzed using a gas chromatography-mass spectrometer (GC-MS) QP 2010 Ultra (Shimadzu, Kyoto, Japan). The GC-MS QP 2010 Ultra was equipped with a DB-23 capillary column (0.25 mm × 30 mm; Agilent J&W Scientific, Santa Clara, CA, USA) and used helium as the carrier gas at a

flow rate of 0.8 mL/min with a split ratio of 1:5. The injection temperature was set at 250 °C. The primary GC oven temperature was programmed at 50 °C for 1 min, increased at 25 °C/min up to 190 °C and at 5 °C/min up to 235 °C for 4 min. The temperature of ion source and interface of MS detector were set at 230 °C and 250 °C, respectively. Fatty acids were identified based on the retention time using the SUPELCO^{TM} 37 component FAME mixture (Sigma-Aldrich). Caprylic acid (C8:0) was used as an internal standard (IS) and included in all samples. The percentage of each fatty acid content was calculated as the ratio of its FAME peak area to the total peak area of all FAMEs, excluding the IS.

2.2.7 Sugar analysis

The glucose concentration was analyzed using high-performance liquid chromatography (HPLC) LC-20AB, with a refractive index detector RID-10A (Shimadzu, Kyoto, Japan) equipped with and ICSep Coregel-87H column (7.8 mm I.D × 300 mm Transgenomic) operated at a column temperature of 80 °C. The mobile phase was 5.0 mM H_2SO_4 at a rate of 0.6 mL/min. All the sample were centrifuged to remove water insoluble substances and filtered through a 0.22 μL filter before analysis.

2.2.8 BODIPY (493/503) staining

BODIPY staining was used to visualize the single-cell oil production. A BODIPY stock solution was prepared at concentration of 5 mg/mL in absolute ethanol and stored protected from light. For staining, 100 μL of culture was pelleted by centrifugation at 12000 rpm for 1 min and washed with 100 μL of phosphate saline buffer (PBS). The cells were centrifuged again at 12000 rpm for 1 min and the supernatant was discarded. After washing, the cells were resuspended in 45 μL of PBS and 5 μL of BODIPY stock solution was added and mixed well. The cells were

incubated and protected from light for at least 1 h before being visualized using a digital inverted fluorescence microscope (Keyence Biorevo BZ-9000, Keyence, Osaka, Japan).

2.2.9 Lipase activity assay

Lipase activity was determined from the cell-free culture supernatant by calculating the release of *p*-nitrophenol (pNP) from the hydrolysis of *p*-nitrophenyl butyrate (pNPB) as the substrate. The reaction mixture consisted of 0.75 mL of 0.5 mM pNPB, 0.1 mL of 40 mM phosphate buffer (pH 7.0), and 0.15 mL of sample. The mixture was incubated at 30 °C, 1500 rpm for 10 min on BioShake iQ (Qinstruments GMbh, Jena, Germany). The reaction was terminated by adding 50 µL of 5% (w/v) of trichloroacetic acid (TCA), followed by the addition of 0.1 mL of 1 M phosphate buffer (pH 7.0). The absorbance was measured at 400 nm by using PerkinElmer EnVision 2104 Multilabel Reader (PerkinElmer Plate Reader, Osaka, Japan). A calibration curve was prepared using commercial pNP as a standard. One unit lipase activity (U) was defined as the amount of enzyme required to releases 1 µmol of pNP per min, in the assay conditions described above.

2.3 Results and discussion

2.3.1 Comparison between PAO and CPKO as carbon sources for lipid production

This study evaluated the potential of palm acid oil (PAO) and crude palm kernel oil (CPKO) as carbon feedstocks for lipid production. The ability of *Meyerozyma guilliermondii* to metabolize PAO and CPKO was assessed using YPD50 and YP media, each supplemented with 10 g/L of either PAO or CPKO. Control experiments were conducted in YPD50 and YP media without PAO or CPKO supplementation. The major FA composition of PAO is C16:0 and C18:1, while CPKO contains a higher percentage of C12:0 (30, 36, 68, 69).

Glucose facilitated faster growth and lipid accumulation in *M. guilliermondii*, and supplementation with additional carbon sources such as CPKO or PAO did not enhance these processes (Figure 5). The highest dry cell weight DCW values, reaching 20.1 g/L, 19.2 g/L, and 20.5 g/L, were observed after 72 h of cultivation in YPD50, YPD50 + CPKO, and YPD50 + PAO, respectively (Figure 5) and accumulated lipid at around 32 to 35 wt% at 120 h (Table 6). Glucose was completely consumed within 24 h and these results showed that glucose was preferable as a carbon source for *M. guilliermondii*. In mixed media containing glucose with either CPKO or PAO, glucose could not be simultaneously utilized by *M. guilliermondii* as the strain showed a preference towards glucose only (Figure 5 and Table 6). The additional CPKO and PAO in the mix-medium were not utilized, as there was no increase in DCW.

Although the addition of PAO did not influence growth or lipid production, the fatty acid (FA) profile of the lipids extracted from *M. guilliermondii* cultured in YPD50 + PAO showed slight variations compared to those cultured in YPD50 and YPD50 + CPKO with 56% of C16:0 and 20% of C18:1 (Table 6). In contrast, the extracted lipid from cells cultured in YPD50 and YPD50 + CPKO contained more C18:1 (42-43%) than C16:0 (26-27%). The residual carbon concentration of PAO and CPKO at the end of fermentation of YPD50 + PAO, YPD50 + CPKO, YP + PAO, and YP + CPKO were 8.4 2.8 g/L, 6.6 2.9 g/L, 6.8 1.1 g/L, and 6.7 0.9 g/L, respectively, 2–4 g/L less than the initial concentration. This indicates that *M. guilliermondii* may not fully metabolize the breakdown products derived from these carbon sources, such as triglycerides, diglycerides, monoglycerides, free fatty acids (FFA), and oleyl esters. Consequently, the addition of PAO or CPKO likely increased the concentration of these degradation products in the culture medium. Further detailed investigations are necessary to elucidate the role of these compounds, as they appear to affect the FA composition of

biosynthesized lipids during fermentation without significantly impacting cell growth or lipid production.

M. guilliermondii exhibited slow growth and low dry cell weight (DCW) in YP medium due to the absence of an available carbon source. Furthermore, the strain demonstrated poor growth when cultivated in YP supplemented with CPKO as the sole carbon source, indicating its inability to effectively utilize carbon substrates predominantly composed of C12:0. In comparison, it was observed that PAO could still be utilized by *M. guilliermondii* to produce lipids even at a low concentration at around 2.4 g/L with major FA composition mainly consisted of C18:1 and C16:0 at 55% and 24%, respectively. The FA composition of the extracted lipid was similar to those found in extracted lipids from cells cultured in YPD50 and YPD50 + CPKO. The result shows that PAO has good potential as a carbon feedstock for *M. guilliermondii* to support growth and lipid synthesis. However, the productivity needs to be enhanced lipid productivity and achieve higher yields.

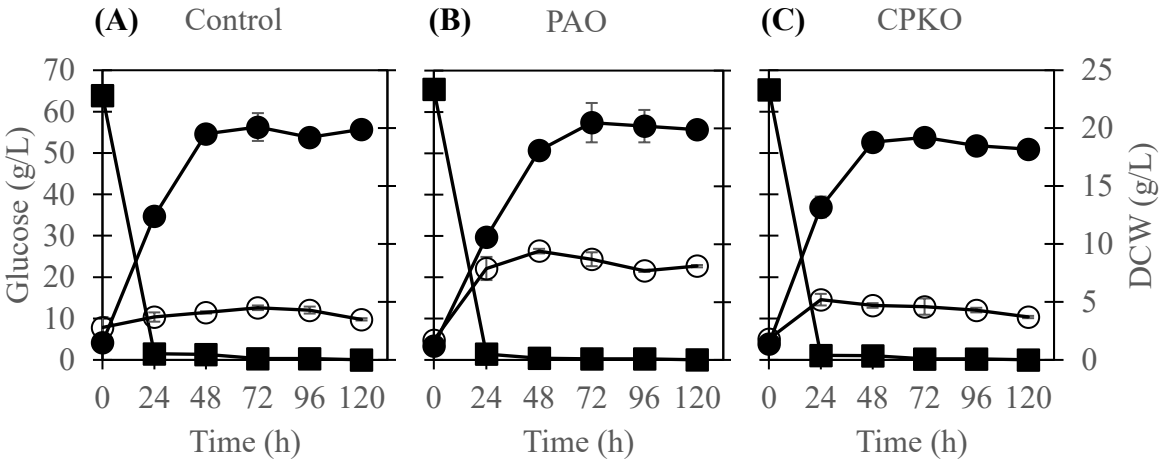

Figure 5 Time course analysis of glucose consumption and cell growth of *M. guilliermondii*. (A) *M. guilliermondii* grown in YPD50/YP only as control group, (B)

YPD50/YP supplemented with PAO, and (C) YPD50/YP with CPKO. The closed square represents glucose consumption in YPD50. The closed circle represents the DCW of *M. guilliermondii* grown on YPD50. The open circle represents the DCW of *M. guilliermondii* grown on YP. The error bars indicate the standard deviation from three independent experiments.

Table 6 Comparison of cell growth, lipid production and FAME profile of *M. guilliermondii* cultured with additional carbon sources

Media [a]	DCW (g/L) [b]	Lipid content (wt%) [c]	Lipid concentration (g/L)	FAME composition (%)						
				C16:0	C18:0	C18:1n9c	C18:1n9t	C18:2	C18:2n6t	Tr [d]
YP	3.5 ± 0.1	10 ± 7	0.4 ± 0.3	45	ND	ND	18	24	7	7
YP + CPKO	3.7 ± 0.1	14 ± 3	0.5 ± 0.1	41	5	ND	21	24	ND	9
YP + PAO	8.1 ± 0.1	29 ± 4	2.4 ± 0.3	24	ND	55	14	4	ND	3
YPD50	19.9 ± 0.2	32 ± 0	6.4 ± 0	27	6	43	ND	7	13	4
YPD50 + CPKO	18.2 ± 0.5	34 ± 3	6.2 ± 0.8	26	7	42	ND	7	12	6
YPD50 + PAO	19.9 ± 0.7	35 ± 2	6.9 ± 0.2	56	ND	20	ND	7	7	8

The values were determined in triplicate; mean values and standard deviation are provided in the table.

[a] *M. guilliermondii* was cultured in 12 mL of respective media for 5 days at 29 °C, 190 rpm.

[b] Dried cell weight (DCW) was determined after freeze-drying.

[c] Lipid content of freeze-dried cells was determined by gravimetric analysis.

[d] The total percentage of individual FAMEs below 1% categorized as trace element including C16:1, C17:0, C17:1, C18:3n6 and C24:0

ND – Not detected

The lipase activity towards pNPB as the substrate was determined from the cell-free culture supernatant of *M. guilliermondii*. The results indicated distinct lipase activities in YP and YPD50 media (Figure 6). In glucose-containing media, no significant lipase activity was detected across all samples, with no measurable increase in activity from 0 h to 120 h. In addition, the activity determined was also comparable to the control YPD50 medium without oil supplementation. Oil-based substrates are usually hydrolyzed into FFA by extracellular lipase secreted by oleaginous yeast, and these FFAs can be utilized for growth or stored as lipid droplets (21). However, previous studies have reported that glucose might inhibit the hydrolytic activities of the lipase (73). Thus, the FFAs were not available in the glucose-containing media. Nevertheless, Further investigation is necessary to confirm whether glucose suppresses the lipase activity of *M. guilliermondii*.

On the contrary, lipase activities were detected in samples from the YP medium when glucose was not present and CPKO or PAO was supplemented as sole carbon sources. The lipase activities were from 0.4 to 0.5 U/mL in YP and YP + CPKO, and from 0.2 to 0.3 U/mL in YP + PAO. Although these values were still very low compared to the extracellular lipase activity of *M. guilliermondii* cultured with olive oil mill wastewater as carbon source (74). This suggests that *M. guilliermondii* secreted insufficient extracellular lipase to effectively hydrolyze the oil-based carbon sources in the medium. Lipase activity in CPKO-containing media was higher than in PAO-containing media. However, the FFAs derived from the hydrolysis of CPKO, which predominantly contains medium-chain-length fatty acids (mcl-FAs) such as C12:0, were not utilized by *M. guilliermondii* for growth or lipid accumulation. In contrast, *M. guilliermondii* could grow on PAO as the sole carbon source.

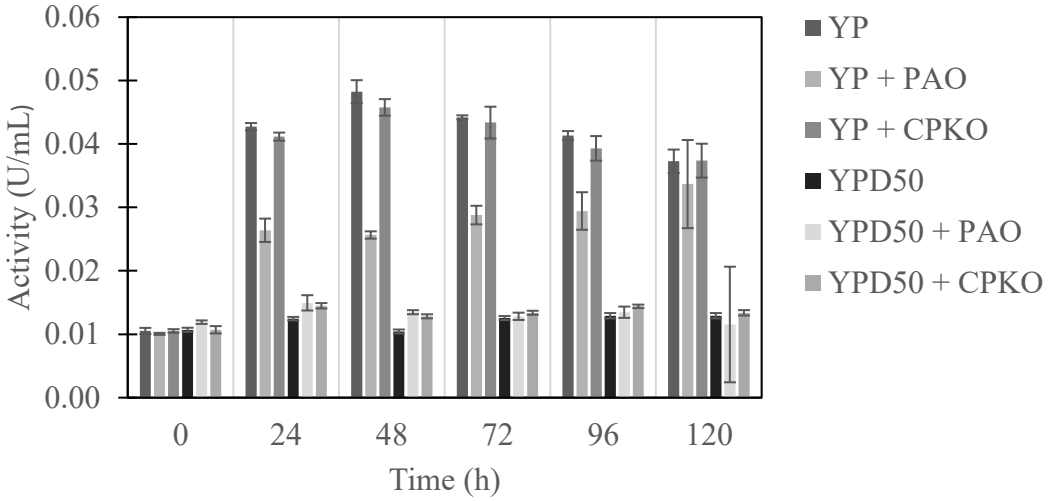

Figure 6 Lipase activity towards pNPB as the substrate from the cell-free culture supernatant. The error bars indicate the standard deviation from three independent experiments.

2.3.2 Effect of single fatty acids on cell growth and lipid accumulation

To further investigate the capacity of *Meyerozyma guilliermondii* to grow and metabolize fatty acids (FAs) present in real biomass, fermentation experiments were conducted using individual FAs as carbon sources. The strain was cultivated in media containing C12:0 (1 g/L), C16:0 (4 g/L), and C18:1 (2 g/L), corresponding to the predominant FAs in CPKO and PAO. The concentrations of the FAs were set based on the maximum tolerance levels determined during initial screening. Key parameters, including growth profile, glucose consumption, lipid accumulation, and FA composition of the extracted lipids, were assessed. *M. guilliermondii* was first cultivated in YPD50 and compared with YP medium, to evaluate its fermentation ability. For the control, the strain was also cultured in YPD50 and YP media without the addition of FAs.

Figure 7 illustrates the time course of cell growth and glucose consumption by *M. guilliermondii* cultured with fatty acids (FAs) in the presence and absence of glucose. The results demonstrate that the strain was capable of growing in YPD50 medium. When glucose was supplemented alongside additional FAs, *M. guilliermondii* exhibited higher residual biomass compared to the control YPD50 medium without FAs (Table 7), indicating that the added FAs could be utilized to support growth. n the control YPD50 medium, the strain's growth plateaued after glucose depletion at 24 h, while cultures grown in YPD50 + C16:0 and YPD50 + C18:1 continued to increase in DCW after glucose was exhausted. In contrast, the presence of C12:0 initially inhibited growth due to its toxic effects, leading to slower growth during the early incubation period. It took approximately 72 h for the strain to fully consume the glucose. After glucose depletion, rapid growth resumed, ultimately reaching a DCW comparable to that of the YPD50 control at 120 h. Despite the differences in growth dynamics, the lipid content across all conditions remained similar, ranging from 28 to 35% (w/w).

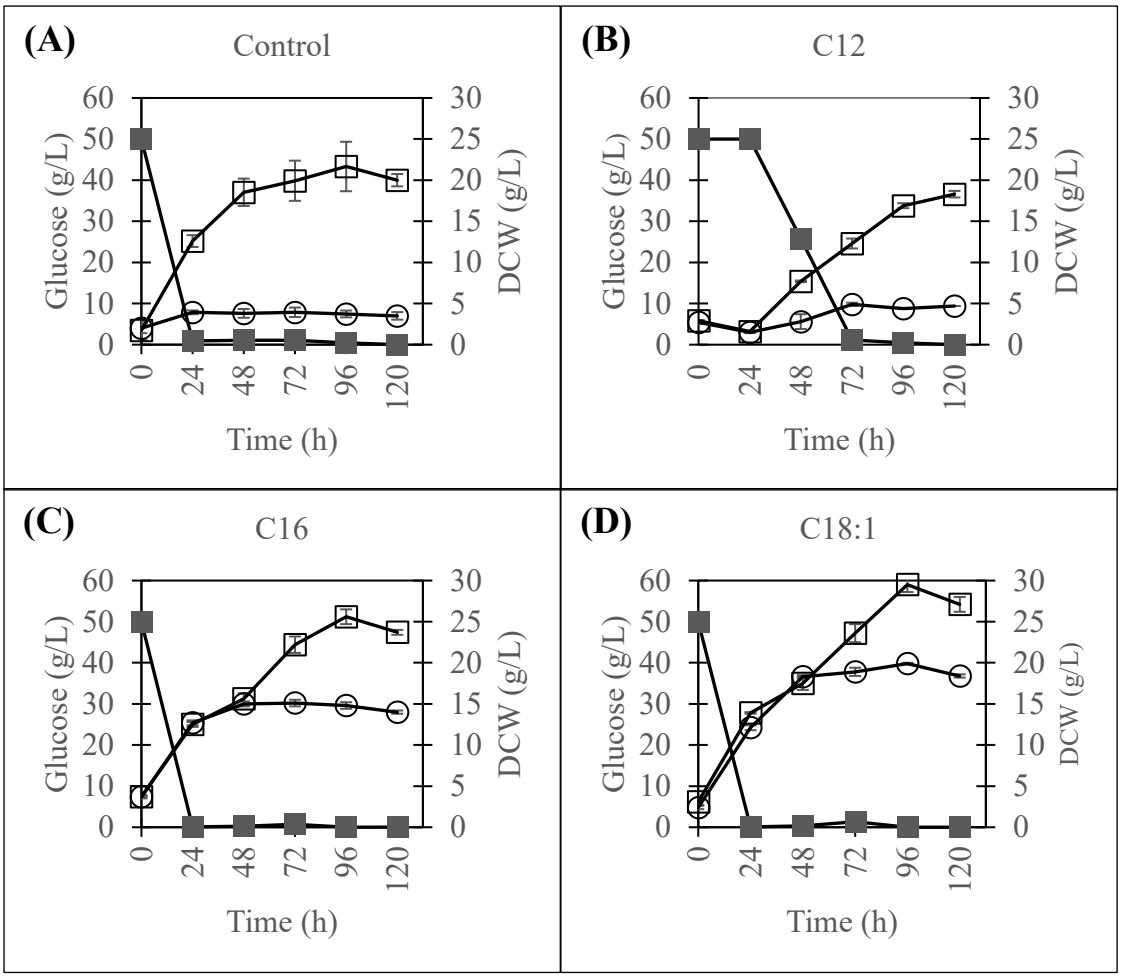

Figure 7 Time course analysis of glucose consumption and cell growth of *M. guilliermondii*. *M. guilliermondii* grown in (A) YPD50/YP only as control group, (B) YPD50/YP + C12:0, (C) YPD50/YP + C16:0 and (D) YPD50/YP + C18:1. The closed square represents glucose consumption in YPD50. The open square represents the DCW of *M. guilliermondii* grown on YPD50. The open circle represents the DCW of *M. guilliermondii* grown on YP. The error bars indicate the standard deviation from three independent experiments.

The DCW, lipid content and lipid concentration of *M. guilliermondii* grown in YP medium supplemented with C16:0 and C18:1 were higher compared to those in YP without additional FA. However, these values were still lower than those observed in YPD50 medium containing glucose (Table 7). This indicates that C16:0 and C18:1 can

serve as sole carbon sources to support both growth and lipid production in *M. guilliermondii* in the absence of glucose. In contrast, C12:0 as a sole carbon source neither support the growth nor the production of lipid in *M. guilliermondii*. Consistent with the observations in YPD50 medium, C12:0 exhibited a toxic effect as the cells of *M. guilliermondii* decreased during the initial 24 h. Growth resumed thereafter, with cells eventually reaching a DCW comparable to the YP control after 120 h. These findings highlight the potential of FAs, particularly C16:0 and C18:1, to serve as sole carbon sources for growth and lipid production in *M. guilliermondii*.

There is a very clear difference between the ability of *M. guilliermondii* to assimilate mcl-FA of C12:0 and lcl-FA. C12:0 is an uncommon saturated FA which may be more toxic than common FA like C16:0 and C18:1. This could be seen during the fermentation; C12:0 negatively affected cell growth during the first 24 h of the incubation in both YP and YPD50 media (Figure 7). As a sole carbon source, C12:0 did not support the growth, yielding only 0.8 g/L of lipid (Table 7). This outcome was consistent with observations from fermentation using CPKO as the sole carbon source (Figure 5 and Table 6), further indicating that C12:0 is unsuitable for *ex novo* lipid production by *M. guilliermondii*. Previous studies have reported that C12:0 exhibits significant cytotoxicity against *Candida* species (75). Similarly, exposure of *Saccharomyces cerevisiae* to C12:0 during ethanol production led to a substantial reduction in ethanol yield, glucose consumption, biomass, and cell viability (76). In contrast, *M. guilliermondii* demonstrated the ability to efficiently assimilate C16:0, a common saturated lcl-FA, and C18:1, a common unsaturated lcl-FA, for lipid production, even in the absence of glucose.

Table 7 Biomass and lipid production of *M. guilliermondii* grown on either YPD50 or YP media supplemented with different type of FAs.

Media [a]	Fatty acid	DCW (g/L) [b]	Lipid content (wt%) [c]	Lipid concentration (g/L)	Residual biomass (g/L)
YPD50	No FA	20.0 ± 0.8	35 ± 4	7.1 ± 0.9	12.9 ± 0.8
	C12	18.3 ± 0.4	28 ± 2	6.6 ± 0.5	17.0 ± 0.3
	C16	23.7 ± 0.3	32 ± 0	7.6 ± 0.1	16.1 ± 0.2
	C18:1	27.1 ± 0.9	31 ± 0	8.3 ± 0.4	18.8 ± 0.5
YP	No FA	3.5 ± 0.5	12 ± 1	0.4 ± 0	3.1 ± 0.5
	C12	4.7 ± 0	18 ± 3	0.8 ± 0.1	3.8 ± 0.1
	C16	14.0 ± 0.2	34 ± 2	4.8 ± 0.3	9.2 ± 0.1
	C18:1	18.4 ± 0.2	35 ± 5	6.5 ± 0.8	11.9 ± 0.9

The values were determined in triplicate; mean values and standard deviation are provided in the table.

[a] *M. guilliermondii* was cultured in 12 mL of respective media for 5 days at 29 °C, 190 rpm.

[b] Dried cell weight (DCW) was determined after freeze-drying.

[c] Lipid content of freeze-dried cells was determined by gravimetric analysis.

BODIPY staining confirmed the accumulation of intracellular lipids in *M. guilliermondii* when cultured in the presence of FA (Figure 8). The FA compositions of the lipids produced at 120 h were analyzed using GC-MS (Table 8). No major differences in FA composition were observed in the extracted lipids of *M. guilliermondii* cultured in either YPD50 or YP media. The dominant FAs were C16 and C18:1, similar to common saturated FA found in vegetable oils.

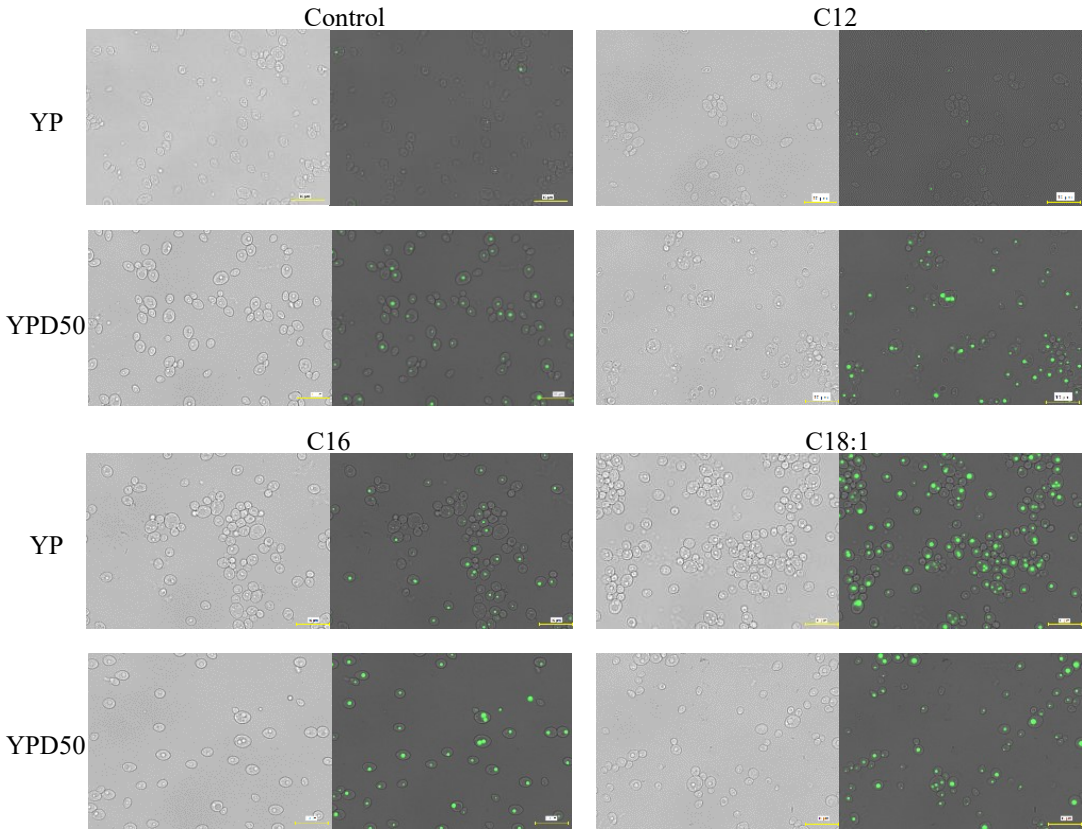

Figure 8 Lipid accumulated in the cells of *M. guilliermondii* cultured in media supplemented with respective FA at 120 h. Bars: 10 µm.

Table 8 FAME profile of *M. guilliermondii* grown on either YPD50 or YP media supplemented with different type of FAs.

Media	Fatty acid	Lipid concentration (g/L)	FAME composition (%)						
			C16:0	C18:0	C18:1n9c	C18:1n9t	C18:2	C18:2n6t	Tr [a]
YPD50	No FA	7.1 ± 0.9	33	10	32	3	5	6	11
	C12	6.6 ± 0.5	33	14	33	4	3	4	9
	C16	7.6 ± 0.1	40	12	23	3	6	10	6
	C18:1	8.3 ± 0.4	32	15	23	4	2	15	9
YP	No FA	0.4 ± 0	44	ND	17	3	28	ND	8
	C12	0.8 ± 0.1	27	10	39	3	14	ND	7
	C16	4.8 ± 0.3	32	6	37	1	7	8	9
	C18:1	6.5 ± 0.8	37	14	18	5	7	9	10

[a] The total percentage of individual FAMEs below 1% categorized as trace element including C16:1, C17:0, C17:1, C18:3n6 and C24:0

ND – Not detected

2.3.3 Evaluation of mix fatty acids

PAO contains a high percentage of free fatty acid (FFA), as previously reported, with approximately 45 % of C16:0, 40% of C18:1 and 9% of C18:2 (30, 36). To mimic the major FA composition of PAO-derived FFAs, *M. guilliermondii* was cultured in YP and YPD50 media supplemented with mixed FAs (C16:0 at 2.5 g/L, C18:1 at 2 g/L, and C18:2 at 0.5 g/L). During the initial 24 hours of fermentation, cells in both media exhibited similar growth rates (Figure 9). Following complete glucose consumption, the cells in YPD50 showed stagnant growth until 72 hours, after which growth resumed, reaching the highest DCW of 16.7 g/L at 120 h. This growth pattern aligned with previous observations during single FA fermentations using mixed carbon sources of glucose and FAs. In contrast, cells in YP medium continued to grow, reaching the highest DCW of 18.5 g/L at 96 hours.

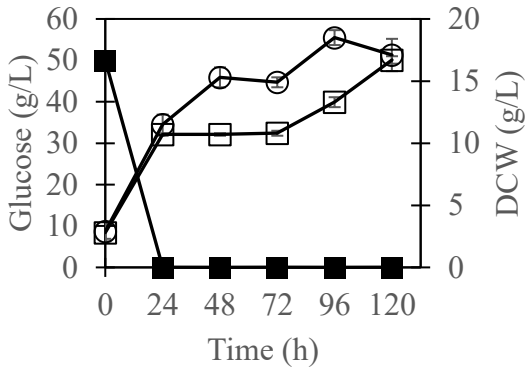

Figure 9 Time course for glucose consumption and cell growth of *M. guilliermondii* grown in YPD50 and YP supplemented with mix FA mimicking the composition of FFA in PAO. The closed square represents glucose consumption in YPD50. The open square represents the DCW of *M. guilliermondii* grown in YPD50 + mix FAs. The open circle represents the DCW of *M. guilliermondii* grown in YP + mix FAs. The error bars indicate the standard deviation from three independent experiments.

The DCW, lipid content, and lipid concentration on *M. guilliermondii* cultured in YP medium supplemented with mixed FAs were higher than those in YPD50 after 120 h of fermentation. *M. guilliermondii* accumulated lipids to a final concentration of 5.9 g/L and 4.4 g/L in YP and YPD50, respectively (Table 9). These results suggest that mixed FAs that imitate the FFAs presence in PAO could yield higher cell density and lipid concentration even without the presence of glucose. The FA compositions of the lipid produced at 120 h contained higher proportion of C18:1 compared to C16:0 in YP medium (Table 9), consistent with the extracted lipids from *M. guilliermondii* cultured in YP + PAO medium (Table 6). In contrast, the FA composition in YPD50 medium, was almost similar to that observed in single FA fermentation. The ability of *M. guilliermondii* to utilize single lcl-FAs and mixed FAs from lcl-FA showed that *ex novo* lipid synthesis is possible in *M. guilliermondii*. This supports the potential of *M. guilliermondii* to utilize real hydrophobic substrates like PAO for lipid production. However, when using real biomass as the substrate, it needs to be completely hydrolyzed into FFAs to enable efficient utilization by the strain.

Table 9 Biomass, lipid content and FAME profile of *M. guilliermondii* grown on mix FAs.

Media [a]	DCW (g/L) [b]	Lipid content (wt%) [c]	Lipid concentration (g/L)	FAME composition (%)							
				C16:0	C16:1	C18:0	C18:1n9c	C18:1n9t	C18:2	C18:2n6t	Tr [d]
YP + mix FA	17.1 ± 1.3	35 ± 2	5.9 ± 0.2	19	4	7	37	7	12	9	5
YPD50 + mix FA	16.7 ± 0.3	27 ± 1	4.4 ± 0.1	31	6	3	40	3	13	ND	4

The values were determined in triplicate; mean values and standard deviation are provided in the table.

[a] *M. guilliermondii* was cultured in 12 mL of respective media for 5 days at 29 °C, 190 rpm.

[b] Dried cell weight (DCW) was determined after freeze-drying.

[c] Lipid content of freeze-dried cells was determined by gravimetric analysis.

[d] The total percentage of individual FAMEs below 1% categorized as trace element including C14:0, C14:1 C17:0 and C18:3n6

ND – Not detected

2.3.4 Effect of surfactant on cell growth and lipid production

The ability of *M. guilliermondii* to produce lipids from hydrophobic feedstocks has been less explored. Hydrophobic substrates, like oil, are typically immiscible with water, which can hinder microbial access and utilization. For instance, PAO solidifies immediately upon addition to a liquid medium, partially limiting their consumption. Both PAO and CPKO are solid at room temperature, thus heating prior to usage was necessary. Sterile PAO and CPKO were heated to 80 °C before being added to the culture flask. In the preliminary observations, CPKO formed small droplets and maintained its liquid state, while PAO solidified instantly in the liquid medium and remained as oil clumps throughout the incubation.

To overcome this limitation, PAO was mixed with Tween 20 as a surfactant to create an emulsion. Surfactants are commonly used to ensure the homogenous dispersion of oil-based feedstocks in liquid media, improving accessibility and experimental reproducibility. The use of emulsifiers has been shown to enhance the availability of solid waste fats as carbon sources for fermentation, enabling efficient production of polyhydroxyalkanoates (77, 78). However, some studies report negative effects of emulsifiers on microbial growth and lipid production. For example, adding emulsifiers to a soybean oil-based medium during the growth of *Trichosporon dermatis* CH007 reduced lipid accumulation and altered intracellular lipid composition (79). In this study, M. guilliermondii was unable to utilize CPKO or sodium laurate, which are rich in C12:0 (Tables 6 and 7). This aligns with previous findings that C12:0, a medium-chain fatty acid, is not suitable for lipid production by M. guilliermondii, likely due to its cytotoxic effects (Table 6 and Table 7).

In this study, Tween 20 (Polysorbate 20), a derivative of C12:0 fatty acid, was used as an emulsifier to disperse PAO in water at room temperature. Tween 20 is widely

use in various applications due to its solubilizing, stabilizing and emulsifying properties especially in pharmaceuticals, food industry and biotechnology fields. A 50% (w/v) PAO emulsion solution was prepared by mixing PAO with 5% (v/w) Tween 20, followed by sterilization and stirring at 80 °C overnight. To evaluate the effect of the emulsifier, *M. guilliermondii* was cultured in YP medium supplemented with 5% Tween 20 as a control. The emulsion solution effectively dispersed PAO into small droplets within the culture medium, facilitating better access for microbial utilization. Despite this, only a small increase in DCW, lipid content and lipid concentration were observed compared to the culture without emulsification (Table 10). It was also observed that *M. guilliermondii* was unable to utilize Tween 20 as a substrate for growth, thus the DCW obtained using only Tween 20 could be negligible. Even though the fermentation with only PAO still had visible oil clumps after 120 h of cultivation, it still could be utilized as carbon source for growth and lipid production in *M. guilliermondii*.

Table 10 Effect of surfactant on cell biomass and lipid accumulation.

Media [a]	DCW (g/L) [b]	Lipid content (wt%) [c]	Lipid concentration (g/L)
YP	4.3 ± 0.1	24 ± 1	1.1 ± 0
YP + Tween 20	4.3 ± 0.1	22 ± 3	1.0 ± 0.1
YP + PAO emulsion	10.0 ± 0	32 ± 0	3.2 ± 0
YP + PAO	9.7 ± 0.1	31 ± 0	3.0 ± 0

The values were determined in triplicate; mean values and standard deviation are provided in the table.

[a] *M. guilliermondii* was cultured in 12 mL of respective media for 3 days at 29 °C, 190 rpm.

[b] Cell dry weight (CDW) was determined after freeze-drying.

[c] Lipid content of freeze-dried cells was determined by gravimetric analysis

2.3.5 Lipid production in nitrogen-limited mineral medium

Lipid accumulation in oleaginous yeasts typically occurs under nutrient imbalance with access to carbon and limited key nutrients like nitrogen (80). In the de novo lipid synthesis pathway, nitrogen limitation enhances the activity of adenosine monophosphate (AMP) deaminase, triggering a cascade of cellular processes. These processes increase citrate levels in the cytoplasm, which are subsequently channelled into lipid biosynthesis (81). Conversely, in the ex novo lipid synthesis pathway, lipid accumulation occurs concurrently with cell growth and is independent of nitrogen availability, as significant lipid production has been observed even under nitrogen-sufficient conditions (21, 82). Even so, higher lipid accumulation could still be observed in the media with low initial nitrogen concentrations (82). To further explore this phenomenon, *M. guilliermondii* was cultured in a nitrogen-limited mineral medium (-NMM) to assess its lipid accumulation and growth behaviour under nitrogen-restricted conditions.

To investigate the effect of PAO concentration on growth and lipid production, fermentation was initially conducted using varying concentrations of PAO (10, 20, 30, and 40 g/L) in nitrogen-limited mineral medium (-NMM). Sterilized PAO was heated to 80 °C before being added to the flasks. After 120 hours of incubation, the dry cell weight (DCW) and lipid content of *M. guilliermondii* were evaluated. The results revealed inconsistencies in DCW and lipid content of *M. guilliermondii* from 20, 30, and 40 g/L of PAO, with solidified PAO still remained as oil clumps in the flasks. This indicated that PAO at concentrations above 10 g/L could not be effectively utilized by the yeast in its native form. To avoid the non-reproducibility of experiments, PAO was used as an emulsion solution at higher concentrations to ensure PAO was available for the strain.

For this, *M. guilliermondii* was culture in -NMM supplemented with 40 g/L of PAO emulsion and 40 g/L of PAO. As a control group, the strain was also cultured in -NMM with 50 g/L of glucose. The fermentation was carried out for 120 hours, and the time course of cell growth was recorded (Figure 10). Among the tested carbon sources, glucose was consumed rapidly, supporting the fastest growth, with the cells reaching the highest DCW of approximately 15 g/L within 48 h of incubation. On the other hand, *M. guilliermondii* only started to grow after 24 h when cultured in -NMM containing PAO emulsion, and rapidly grew up to the highest DCW of 20.1 g/L at 120 h. The DCW obtained was almost two-fold higher than the DCW recorded when 40 g/L of PAO was used without the addition of Tween 20.

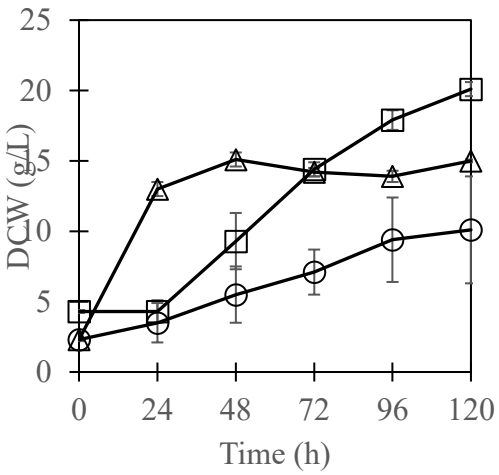

Figure 10 Time course analysis of cell growth of *M. guilliermondii* grown in -NMM medium. The open square, triangle and circle represent DCW of *M. guilliermondii* grown in -NMM supplemented with PAO emulsion, glucose and PAO as carbon source, respectively.

The effect of PAO emulsion could be seen clearly when a higher PAO concentration was used during the fermentation, which resulted in a high accumulation of lipids (Table 11). This result suggested that emulsified PAO prior to cultivation is

important to reduce its size, improving its accessibility in the culture medium. Consequently, *M. guilliermondii* was able to assimilate PAO better and produce a high amount of lipids. As mentioned earlier, fermentation using PAO resulted in high standard deviations for DCW, lipid content, and lipid concentration due to inconsistencies between replicates. the fermentation with PAO emulsion achieved the highest lipid content of 50 wt%, corresponding to a lipid concentration of 10.1 g/L. This lipid concentration was approximately four times higher than that observed when only 10 g/L of PAO was supplemented, either in YP medium (Table 6) or -NMM (data not shown), and two times higher than when 40 g/L of PAO was used without surfactant. This result showed that the addition of surfactant like Tween 20 was essential to ensure PAO was available in the culture medium for the strain and could yield high lipid concentrations.

Table 11 Cell biomass, lipid content and FAME profile of *M. guilliermondii* grown on -NMM.

Carbon source [a]	DCW (g/L) [b]	Residual carbon (g/L)	Lipid content (wt%) [c]	Lipid concentration (g/L)
Glucose	15.0 ± 0.1	6.5 ± 0	36 ± 0	5.4 ± 0.1
PAO emulsion	20.1 ± 0.5	12.3 ± 4.1	50 ± 2	10.1 ± 0.5
PAO	10.1 ± 3.8	9.3 ± 1.8	48 ± 7	5.0 ± 2.3

The values were determined in triplicate; mean values and standard deviation are provided in the table.

[a] *M. guilliermondii* was cultured in 12 mL of respective media for 5 days at 29 °C, 190 rpm.

[b] Dried cell weight (DCW) was determined after freeze-drying.

[c] Lipid content of freeze-dried cells was determined by gravimetric analysis.

Based on the BODIPY staining, the differences in the size of lipid bodies could be clearly observed (Figure 11). The lipid bodies appeared notably large, nearly encompassing the entire cell body when cultured in 40 g/L of PAO emulsion.

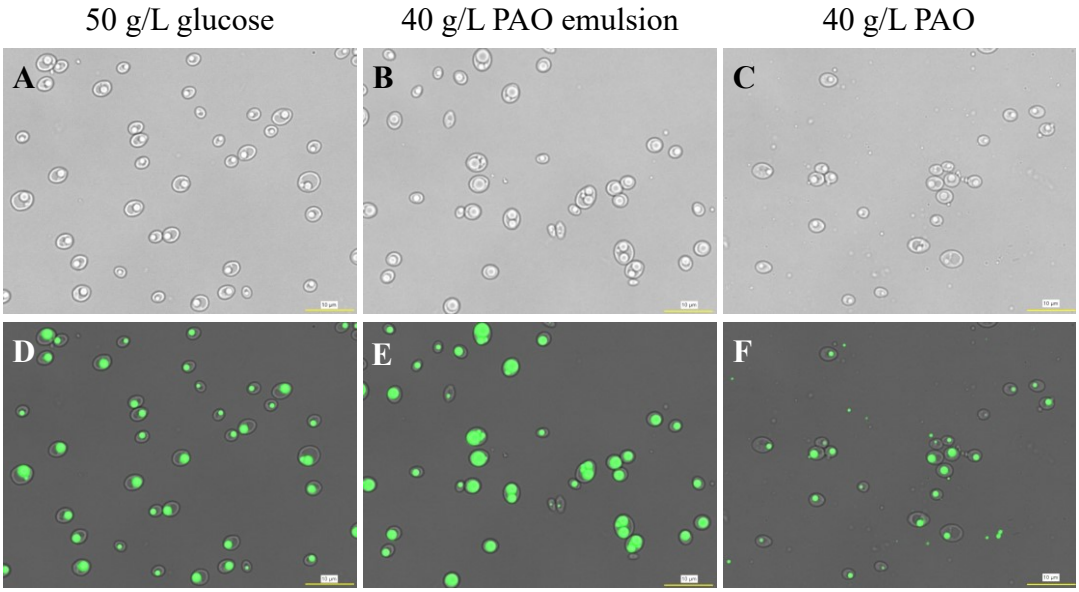

Figure 11 Lipid accumulated in the cells of *M. guilliermondii* at 120 h. (A-C) The microscopic images of *M. guilliermondii* when culturing in -NMM medium supplemented with glucose (A), PAO emulsion (B) and PAO (C). (D-F) The microscopic fluorescence images of *M. guilliermondii* stained with BODIPY (493/505). Bars: 10 μm.

However, residual PAO and PAO emulsions were still observable at the end of the experiment (Figure 12), indicating incomplete utilization of the substrate. The FA compositions of the lipid produced at 120 h showed no significant differences compared to those extracted from *M. guilliermondii* cultured in either YPD50 or YP media. The dominant FA in the accumulated lipids were C16:0 and C18:1 (Table 12).

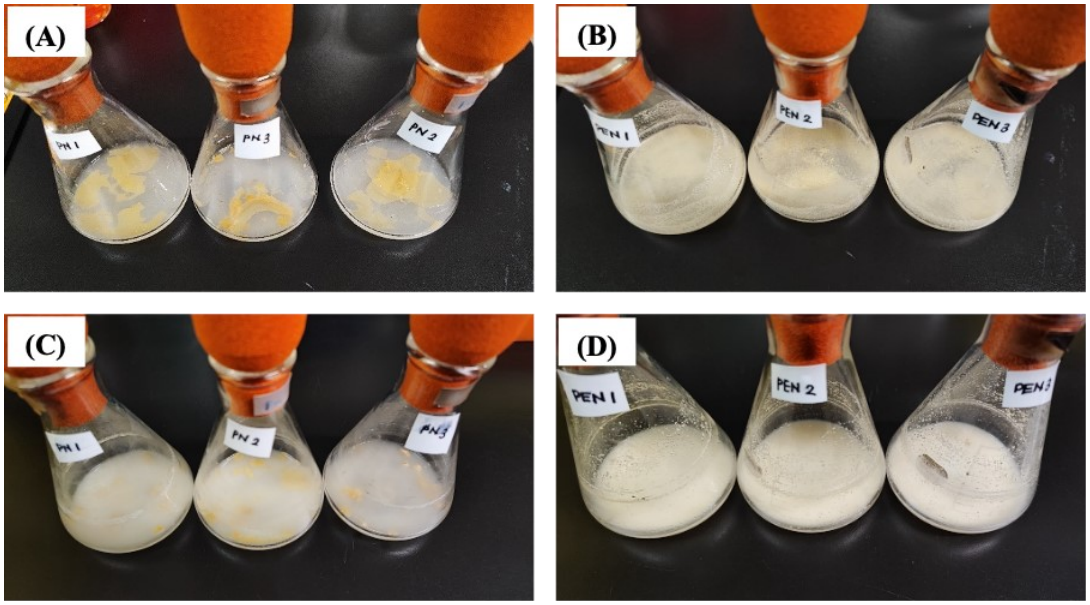

Figure 12 Representative images of *M. guilliermondii* culture in -NMM supplemented with 40 g/L of PAO and PAO emulsion. (A) Culture with PAO at 0h. (B) Culture with PAO emulsion at 0h. (C) Culture with PAO at 120 h. (D) Culture with PAO emulsion at 120 h.

Table 12 Cell biomass, lipid content and FAME profile of *M. guilliermondii* grown on -NMM.

Carbon source [a]	Lipid concentration (g/L)	FAME composition (%)							
		C16:0	C16:1	C18:0	C18:1n9c	C18:1n9t	C18:2	C18:2n6t	Tr [d]
Glucose	5.4 ± 0.1	36	17	6	19	7	4	ND	11
PAO emulsion	10.1 ± 0.5	39	9	2	20	11	ND	11	6
PAO	5.0 ± 2.3	48	5	6	17	15	3	ND	6

The values were determined in triplicate; mean values and standard deviation are provided in the table.

[a] *M. guilliermondii* was cultured in 12 mL of respective media for 5 days at 29 °C, 190 rpm.

[d] The total percentage of individual FAMEs below 1% categorized as trace element including C14:0, C15:0, C17:0, C18:3, C18:3n6 and C20:0

ND – Not detected

2.4 Conclusion

This study successfully demonstrated that *M. guilliermondii* was able to grow on PAO and efficiently accumulate lipids through the *ex novo* lipid synthesis pathway. PAO, a solid waste with limited applications, has been shown to serve as a promising carbon source by *M. guilliermondii*. In addition, this study also highlights the significance of using surfactant in emulsifying solid fat like PAO to improve its availability in liquid medium. Finally, the potential of *M. guilliermondii* to utilize waste vegetable oil generated during milling processes can be used as a source of innovation for a circular economy in the palm oil industry in the future (83).

CHAPTER 3

Dimorphism of oleaginous yeast *Meyerozyma guilliermondii* during production of single-cell oil under decanoic acid stress

3.1 Introduction

With the increasing environmental and energy concerns, lipids, including vegetable oils and animal fats, are considered renewable alternatives to petroleum feedstock. The increasing demand for lipids and the desire to avoid competition with food has led to a shift towards the utilization of microbial lipids for the sustainable production of biofuels (32, 84) and various oleochemicals including lubricants (85, 86). Producing lipids by oleaginous microbes is particularly interesting due to its high titers, production rates, and yields. In addition, microbes exhibit rapid growth, making the production process easily scalable. Oleaginous microbes are known for their ability to accumulate lipids through the *de novo* and *ex nov*o lipid synthesis pathways when fed with sugar-based and oil-based substrates, respectively. It has been reported that lipid accumulation via the *de novo* pathway typically results in significant lipid production, predominantly containing long-chain length fatty acids similar to those found in oils derived from agricultural crops (21). In contrast, both extracellular and intracellular lipid composition can be modified to potentially resemble or differ from the initial substrate through the *ex novo* pathway (21, 22).

Among various microbes, oleaginous yeasts are particularly promising due to their rapid growth and efficient accumulation of high levels of intracellular lipids (84). Most research on microbial lipids production has focused on sugar-based feedstocks. However, it has been demonstrated that microbial lipids can also be produced from oil-based feedstocks and animal fat-containing free fatty acids (23). These fatty acids can either promote microbial growth or be stored as intracellular lipids (21, 22). It has been

shown that *Yarrowia lipolytica* was able to grow on stearin, which is composed of saturated free fatty acids (23) and as a model oleaginous yeast, *Y. lipolytica* has been extensively studied to understand the mechanism underlying the utilization of oil-based feedstocks (1). In addition, there has also been research on the utilization of volatile fatty acid (VFA), including acetic acid, propionic acid, and butyric acid, for microbial lipids production (60, 87, 88). However, certain fatty acids can exhibit toxic effects depending on their structure, chain length, and degree of saturation.

Yeast can exhibit diverse morphologies ranging from single-celled or yeast-like forms to pseudohyphae or hyphae. Environmental factors such as nutrient depletion, pH, oxidative and osmotic stress play a significant role in triggering these morphological changes (89). In pathogenic *Candida albicans*, the dimorphic transition from yeast to hyphae enables it to evade macrophage phagocytosis (89, 90), and as an evolved strategy for its survival during symbiotic relationship with the hosts (91). In the brewing yeast *Saccharomyces cerevisiae*, which typically grows as single budding cells, the morphological transition has been extensively studied, revealing its ability to form pseudohyphae and exhibit filamentous growth in response to stress stimuli (92–94). In oleaginous yeasts like *Y. lipolyti*c, this morphological shift during lipid accumulation can impact the rheological behavior and viscosity of the culture medium, which in turn affects lipid production (95).

Another oleaginous yeast, *Meyerozyma guilliermondii* is a versatile yeast species widely studied for its biotechnological potential (3). It is well known for its industrial applications, including the production of riboflavin (4, 8), xylitol (14, 19, 20), and various industrial enzymes (5, 7), as well as for its role in bioremediation (9, 10). Certain strains of *M. guilliermondii* have demonstrated the ability to accumulate high lipid levels, making it a promising candidate for microbial lipid production. Under

optimal conditions, *M. guilliermondii* has been reported to accumulate lipids up to 60.6% (w/w) of its DCW (11). In addition to its high potential in biotechnology, *M. guilliermondii* exhibits tolerance to inhibitory chemical compounds (6, 12). Additionally, the species is capable of undergoing morphological transitions and forming pseudohyphae (96), although detailed reports on this phenomenon remain limited. These traits highlight their adaptability and their potential for diverse biotechnological applications.

In this study, we investigated a strain from our *M. guilliermondii* collection with high lipid production capacity. We screened for its ability to utilize various fatty acids in a medium composed of yeast extract, peptone, glucose, and additional fatty acids. Interestingly, the strain did not grow in the presence of decanoic acid (C10) during the initial screening. However, upon extended incubation, we observed growth characterized by a mixture of yeast-form cells and pseudohyphae following a prolonged lag phase. The primary focus of this study was to explore the morphological transition of *M. guilliermondii* under C10 stress and its effects on lipid production.

3.2 Materials and methods

3.2.1 Yeast strain and growth condition

Wild-type *Meyerozyma guilliermondii* from our private collection (PK01) was used in this study. Cultivation of *M. guilliermondii* strain was routinely performed on YPD agar (YPD medium containing 15 g/L of agar) at 30 °C. Kanamycin (50 µg/mL) and ampicillin (100 µg/mL) were supplemented to the media if necessary. The seed culture was prepared by inoculating a single colony of *M. guilliermondii* in 12 mL of YPD medium supplemented with kanamycin and ampicillin in a 100 mL Erlenmeyer flask and incubated overnight in an orbital shaker incubator (BioShaker BR-43FH MR, Taitec Corp., Tokyo, Japan) at 29 °C, 190 rpm. The volume of seed culture was adjusted

to an initial optical density (OD_{600}) of 1.0 or 14.0 – 16.0 before transferring to YPD50 medium for cultivation, with a working volume of 1 mL or 12 mL in a 96-deep-well plate or 100 mL Erlenmeyer flask, respectively. FAs were added aseptically at 0 h unless mentioned otherwise. The culture in a 96-deep-well plate was incubated at 29 °C, 1500 rpm for 72 h in DeepWellMaximizer (BioShaker M.BR-022UP, Taitec Corp., Tokyo, Japan) while the culture in a shake flask was incubated at 29 °C, 190 rpm for 120 h in an orbital shaker incubator. Culture samples in shake flasks were taken every 24 h for dry cell weight (DCW) and glucose consumption measurement. After the incubation, the culture was harvested by centrifugation at 8,000 rpm for 10 min and washed twice with deionized water. All culture experiments were performed in triplicate, and the results were presented as the mean ± standard deviation.

3.2.2 Media preparation

For seed culture, *M. guilliermondii* was inoculated in YPD medium [10 g/L of yeast extract, 20 g/L of peptone, and 20 g/L of D-glucose]. For lipid production, *M. guilliermondii* was cultured in YPD50 medium [10 g/L of yeast extract, 20 g/L of peptone, and 50 g/L of D-glucose]. YPD and YPD50 media were autoclaved at 121 °C for 15 min. Fatty acids in sodium salt or acid forms were from Tokyo Chemical Industry (Tokyo, Japan) and Sigma-Aldrich (Tokyo, Japan). Sodium butyrate (C4), sodium hexanoate (C6), sodium octanoate (C8), and sodium decanoate (10) were dissolved in Milli-Q water. Sodium laurate (C12) and sodium myristate (C14) were dissolved in 50 vol% ethanol. Sodium palmitate (C16) and sodium stearate (C18:0) were dissolved in 50 vol% and 70 vol% hot ethanol, respectively. Sodium oleate (C18:1) and sodium linoleate (C18:2) were dissolved in 70 vol% ethanol. Sodium arachidonate (C20), lignoceric acid (C24), cerotic acid (C26), and melissic acid (C30) were dissolved in

99.5 vol% of ethanol. FAs dissolved in Milli-Q water and 50 % ethanol were filter-sterilized through a 0.2 μm filter prior to usage.

3.2.3 Determination of total lipid content by gravimetric analysis

Gravimetric analysis was used to measure lipid production based on the modified Folch method (72). Approximately 15 mg of freeze-dried cells were added to a 2.0 mL polypropylene microvial containing 0.5 mm zirconia beads and 1.5 mL of Folch solvent [2:1 of chloroform: methanol (v/v)]. The cells were pulverized using a Shake Master Neo ver.1.0 (BMS-M10N21, BMS, Tokyo, Japan) at 1500 rpm, 15 min. After that, the cells were centrifuged at 14,000 ×g for 5 min, the supernatant was discarded, and the cell pellets were washed with 1.5 mL of deionized water. The cells were pulverized and centrifuged again; then the deionized water was discarded. The cell pellets were dried at 60 °C until a constant weight was obtained. The lipid content was determined by the difference in weight of the tube and expressed as a percent of dry cell weight.

3.2.4 Determination and quantification of total fatty acid methyl esters (FAME)

To determine the FAME composition, the lipid from the lyophilized cells was converted to methyl esters by direct transesterification according to manufacturer's protocol in the fatty acid methylation kit (Nacalai Tesque, Inc., Japan). The extracted FAME (light phase) was transferred to GC vial equipped with a micro-tube glass insert and analysed by gas chromatography-mass spectrometer (GC-MS) QP 2010 Ultra (Shimadzu, Kyoto, Japan) equipped with a DB-23 capillary column 0.25 mm × 30 mm (Agilent J&W Scientific, Santa Clara, CA, USA). Helium was used as the carrier gas at a flow rate of 0.8 mL/min with a split ratio of 1:5. The injection temperature was 250 °C. The primary GC oven temperature was programmed at 50 °C for 1 min, then increased at 25 °C/min up to 190 °C and at 5 °C/min up to 235 °C for 4 min. The

temperature of ion source and interface of MS detector were set at 230 °C and 250 °C, respectively. Fatty acids were identified based on the retention time of SUPELCO^{TM} 37 component FAME mixture (Sigma-Aldrich). Caprylic acid (C8:0) was used as internal standard (IS) and included in each sample. The percentage of total fatty acid content was calculated as the ratio of the individual FAME peak area to the sum of all FAME peak areas, excluding the IS.

3.2.5 Sugar analysis

The concentration of glucose was analyzed using high-performance liquid chromatography (HPLC) LC-20AB, refractive index detector RID-10A (Shimadzu, Kyoto, Japan) equipped with and ICSep Coregel-87H column (7.8 mm I.D × 300 mm Transgenomic) operated at a column temperature of 80 °C. The mobile phase was 5.0 mM H_2SO_4 at a rate of 0.6 mL/min. All the samples were centrifuged to remove water-insoluble substances and filtered through a 0.22 μL before subjecting to analysis.

3.2.6 Staining

BODIPY (Invitrogen) staining was employed to visualize the single-cell oil production. The vacuole membrane was stained using yeast vacuole membrane marker MDY-64 (Invitrogen), and the detection of reactive oxygen species (ROS) was performed with Dojindo's ROS Assay Kit-Highly Sensitive DCFH-DA (Dojindo Laboratories). All staining procedures were conducted according to the manufacturer's protocols. The stained cells were visualized using a digital inverted fluorescence microscope (Keyence Biorevo BZ-9000, Keyence, Osaka, Japan).

3.2.7 Quantitative PCR

Gene expression was quantified using a quantitative PCR method. RNA from frozen cells was extracted using a NucleoSpin RNA® (Macherey-Nagel, Duren, Germany),

purified with rDNase according to thr manufacturer's protocol to reduce DNA contamination and quantified using an Agilent 2100 Bioanalyzer (Mx3005P; Stratagene). Reverse transcription reactions were conducted to convert the RNAs to complementary DNAs using a ReverTra Ace® qPCR RT Master Mix with a gDNA Remover (Toyobo Co. Ltd., Osaka, Japan), which were subsequently quantified using an Agilent 2100 Bioanalyzer Mx3005P. The gene expression was quantified using KODSYBR qPCR Mix (Toyobo Co. Ltd., Osaka, Japan). Primers used for quantification were specially designed for genes of interest in *M. guilliermondii* using NCB1 Primer-BLAST Tool with the target PCR product size set at approximately 100 bp. Relative gene expression was calculated using $2^{-\Delta Ct}$ method (97), and the *TUB1* gene was used as an internal reference gene.

3.3 Results and discussion

3.3.1 Ability of *Meyerozyma guilliermondii* to grow on wide range of fatty acids

During the primary screening conducted using a 96-deep-well plate, the maximum tolerance concentration (MTC) of each fatty acid (FA) was determined based on the optical density (OD_{600}) measured at 72 h (Figure 13). The screening process was performed based on the ability of *M. guilliermondii* to grow in a YPD medium containing a mixture of 50 g/L of glucose (YPD50) and an additional FA at concentrations of 0.5 g/L, 1 g/L, 2 g/L, 4 g/L and 8 g/L as the carbon source over a 72-h cultivation period.

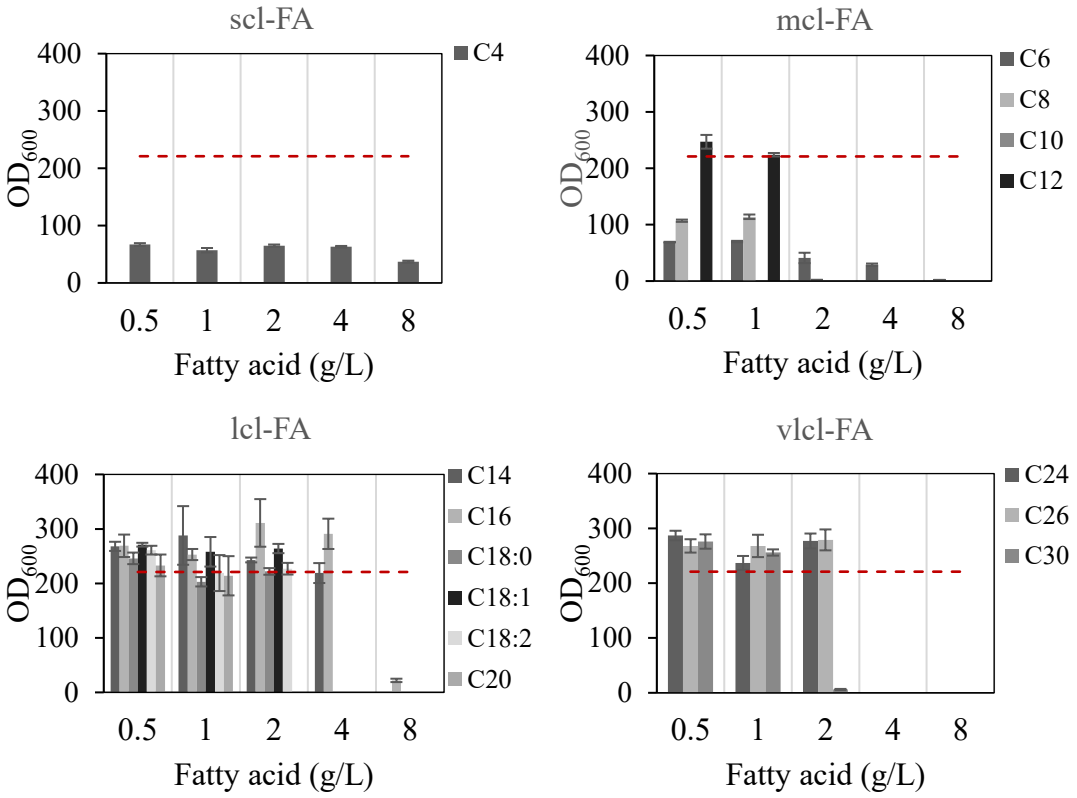

Figure 13 Optical density (OD_{600}) of *M. guilliermondii* grown in YPD50 supplemented with additional FA in a range of concentration from 0.5 g/L, 1 g/L, 2 g/L, 4 g/L and 8 g/L at 72 h during primary screening. The red dashed line represents the OD_{600} of *M. guilliermondii* grown in YPD50 without FA supplementation (control).

M. guilliermondii showed a remarkable ability to utilize a wide range of FA especially long-chain length FA (lcl-FA) and very long-chain length FA (vlcl-FA). Short-chain length FA (scl-FA) and medium-chain length FA (mcl-FA) showed toxicity effect on the growth of *M. guilliermondii* as the OD_{600} recorded for respective FA were lower compared to control (221). Despite the scl-FA being toxic, *M. guilliermondii* could tolerate up to a very high concentration of C4. It also grew on mcl-FA, mainly C12, in which the OD_{600} reading was almost similar to the control. Interestingly, the growth of *M. guilliermondii* was completely inhibited in the medium supplemented with C10, as the OD_{600} at 72 h remained unchanged from the initial value of 1, even at

the lowest concentration of 0.5 g/L. In contrast, lcl-FA and vlcl-FA exhibited no toxic effects toward *M. guilliermondii*, as the cells were able to grow at concentrations of up to 4 g/L and 2 g/L, respectively. Subsequent experiments were conducted using YP medium without glucose at the determined MTC, revealing that only lcl-FA and vlcl-FA were capable of supporting growth (Figure 14), consistent with the initial screening results in the YPD50 medium.

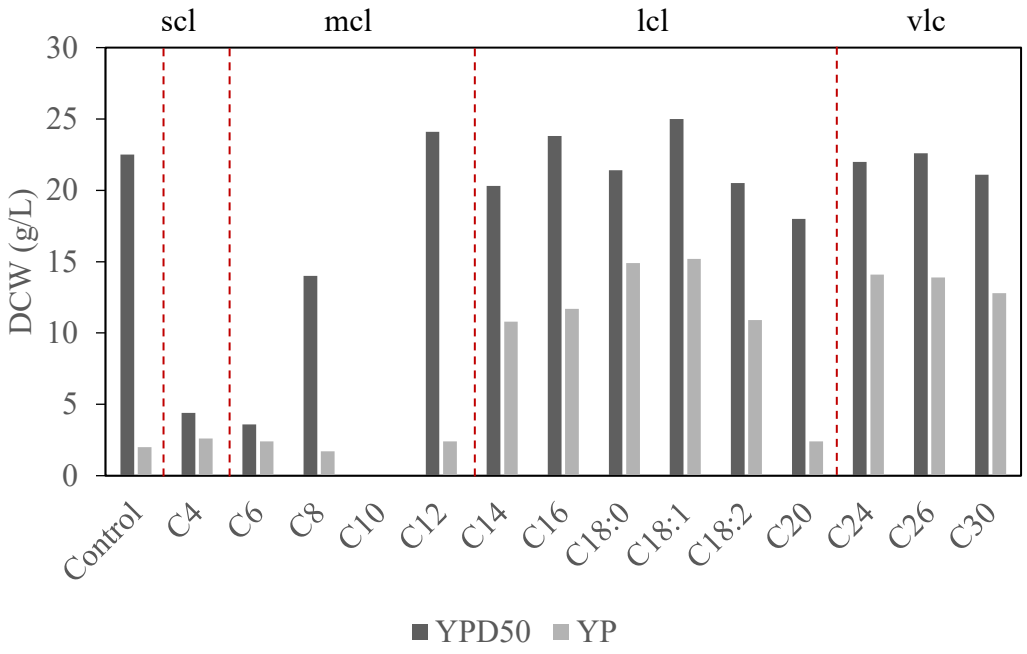

Figure 14 Comparison of DCW (g/L) of *M. guilliermondii* grown in YPD50 and YP supplemented with additional FA at maximum tolerance concentration cultured for 72 h in 96-deep-well plate. Maximum tolerance concentration of FA: C4 (8 g/L), C6 (4 g/L), C8 (1 g/L), C10 (0.5 g/L), C12 (1 g/L), C14 (4 g/L), C16 (4 g/L), C18:0 (2 g/L), C18:1 (2 g/L), C18:2 (2 g/L), C20 (0.5 g/L), C24 (2 g/L), C26 (2 g/L), and C30 (1 g/L).

3.3.2 Effect of decanoic acid on cell growth and morphology

To gain more insight into the ability of *M. guilliermondii* to grow in the presence of C10, *M. guilliermondii* was cultured in YPD50 medium supplemented with 0.25 g/L, 0.5 g/L, 1.0 g/L and 2.0 g/L of C10 under flask culture conditions. For the control experiment, *M. guilliermondii* was also cultured in a YPD50 medium without C10. Growth profile, lipid accumulation abilities, and the composition of lipids were evaluated (Figure 15).

Figure 15 shows the impact of adding different concentrations of C10 on glucose consumption and cell growth of *M. guilliermondii*. When 0.25 g/L of C10 was added to the culture medium, there was no inhibition of cell growth, and the glucose was fully consumed within 24 h, similar to the results observed in the control experiment. The highest DCW of 17.7 g/L could be observed at 48 h. With 0.5 g/L of C10, the growth of *M. guilliermondii* was inhibited for the first 72 h, consistent with the observation from the primary screening in a 96-deep-well plate, as shown in Figure 13. As the incubation was prolonged, glucose consumption began after 72 h and was completed at 96 h. Subsequently, cell growth resumed, reaching a maximum DCW of approximately 17.5 g/L, almost similar to the DCW of control (17.2 g/L) at 120 h. When C10 was supplemented at 1 g/L and 2 g/L, *M. guilliermondii* could not tolerate these higher concentrations, as no growth was observed, and no glucose was consumed, even after prolonged incubation up to 192 h. Previous research has shown that the presence of organic acids in the medium has significantly affected the growth of yeast cells on glucose, indicated by extended lag phases and decreased growth rates (98). A delay in glucose consumption might also indicate an initial stress response. Studies have shown that yeast cells experiencing decanoic acid stress exhibit increased membrane fluidity, which is accompanied by changes in membrane composition, including an elevated

proportion of oleic acid (C18:1) and a reduction in palmitoleic acid (C16:1) (99). In another study, the reduction in plasma membrane integrity may result in the leakage of intracellular materials, consequently reducing the availability of essential cofactors for biological processes (100). Those effects could possibly disrupt the normal function of membrane-bound transport proteins, potentially reducing the efficiency of glucose transport. A study reported that exposure of yeast *Saccharomyces cerevisiae* to toxic FA, especially C10, significantly altered the expression of 620 genes compared to control cells, leading to the induction of specific stress responses, including activation of transporters and several genes in the *β*-oxidation pathway and ethyl ester synthesis (101). This showed an adjustment in the metabolic activity to focus on the detoxification of C10 to mitigate its effects. This could explain why yeast growth was inhibited in our study, suggesting that the cells may redirect their resource toward managing the stress induced by C10 rather than investing in growth and proliferation. Upon the uptake and metabolization of C10, its concentration in the medium decreases, subsequently allowing for glucose consumption and the resumption of cell growth. Notably, at lower concentrations of C10, the glucose consumption rate remains unaffected, suggesting that the stress response is alleviated, enabling normal metabolic activity and growth.

To clarify further for this unusual phenomenon, the cells were observed under a fluorescence microscope. Interestingly, the addition of C10 in the YPD50 medium caused some cells to become unusually elongated, likely forming pseudohyphae (Figure 16), indicating that *M. guilliermondii* exhibited a mixture of yeast-form cells and pseudohyphae under these conditions. In contrast, no such morphological changes were observed with other FAs tested during the screening, as cells maintained a morphology similar to the control (data not shown). Pseudohyphal growth is

characterized by the formation of elongated cells that bud synchronously in a unipolar fashion without separating, resulting in chains of cells referred to as pseudohyphae (92). Pseudohyphae exhibited various degrees of elongation and have constrictions between adjacent compartments (102). It has been reported that *M. guilliermondii* is capable of forming pseudohyphae on Dalmau plate culture on morphology agar (96). However, there have been no detailed investigations of the underlying mechanisms of this phenomenon. A previous study on *Candida guilliermondii* highlighted phenotypic switching associated with pseudohyphae formation and morphological changes in response to farnesol (103, 104). The morphological transition in *M. guilliermondii* was more pronounced with supplementation of 0.5 g/L of C10 as the microscope images revealed that some elongated cells remain attached, with notable constrictions present (Figure 16). For concentrations of 1 and 2 g/L of C10, as the cells could not survive the high C10 concentration, the cells also remained in the yeast-form morphology. The response of yeast cells to C10 exhibited many similarities to oxidative stress (101), and oxidative stress plays a significant role in triggering the morphological transition from yeast-like forms to pseudohyphae or hyphae (89).

As exogenous medium chain fatty acids can be toxic to the cells at high concentrations, 0.5 g/L of C10 was added during the exponential growth phase rather than at the beginning to observe its effects. When C10 was added at 48 h of cultivation, when glucose was fully consumed, no unusual cell growth was observed except for a decrease in DCW (Figure 15 and Figure 16D). Initially, the cells exhibited a growth rate similar to that of the control. However, the DCW decreased upon adding C10, while the control cells continued to grow, reaching the highest DCW of 19.5 at 72h. The morphology of the cells exposed to C10 at 48 h remained the same as that of the control cells (Figure 16). A study demonstrated that the toxicity of linoleic acid (LA) is cell-

density dependent, with LA being toxic only to cell cultures having lower cell densities, leading to the hypothesis that cell density may regulate physiological mechanisms that influence LA uptake and metabolism (105). During the exponential phase, yeast cells are actively dividing and metabolizing. Thus, their response towards stress might differ compared to adding it at the lag phase. During this phase, cells might be more resilient to stress due to their active metabolism and division.

The cells were stained with BODIPY to visualize the lipid body accumulation (Figure 16). Stained lipid bodies were observed in control cells and cells exposed to 0.25 g/L and 0.5 g/L of C10 at 0 h, exhibiting similar fluorescence intensity. In contrast, cells exposed to 0.5 g/L of C10 at 48 h displayed smaller lipid bodies while no lipid bodies were observed in cells that did not grow when exposed to 1 and 2 g/L of C10.

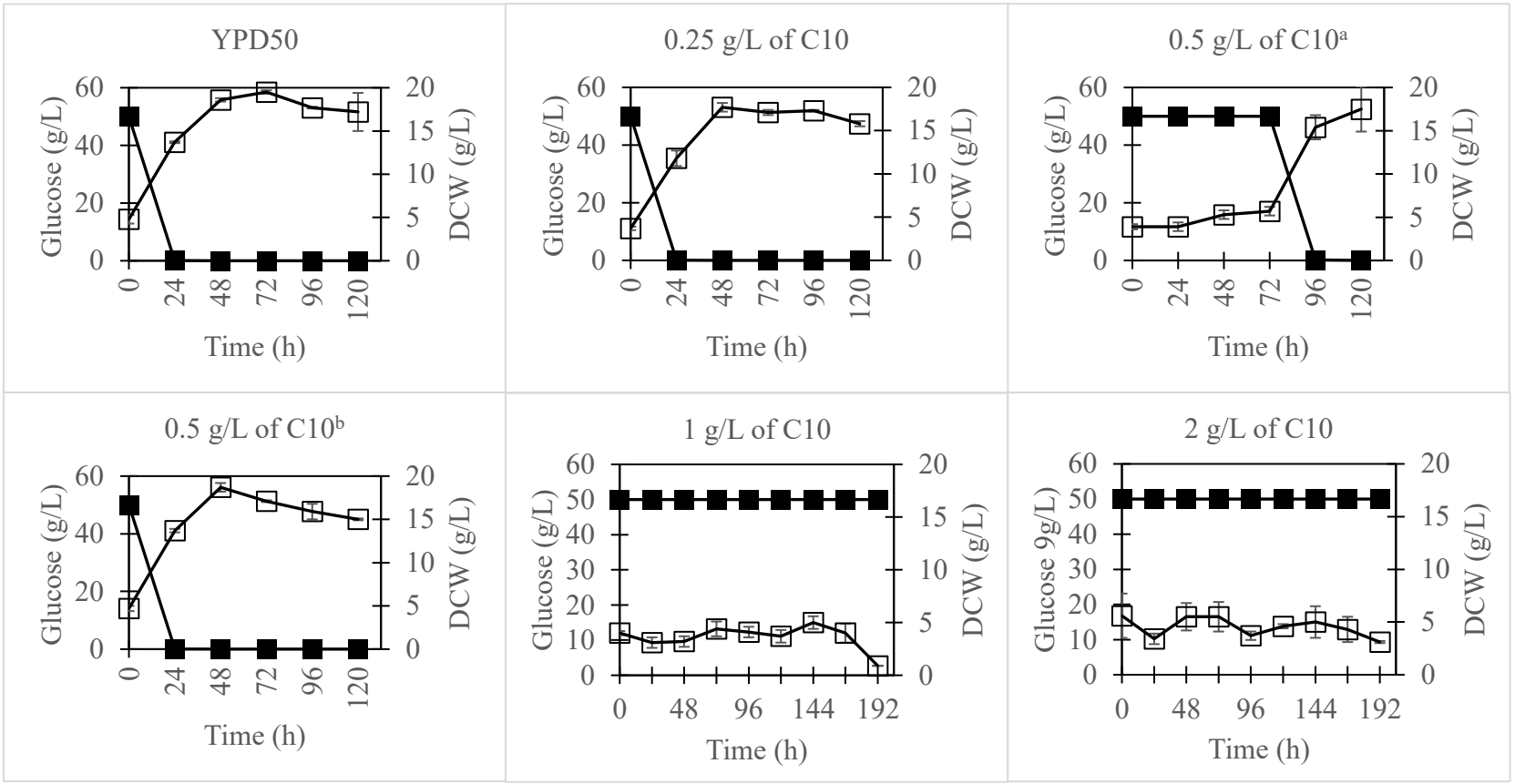

Figure 15 Time course for cell growth of *M. guilliermondii* grown in YPD50 supplemented with C10. The opened square represents dry cell weight (g/L) and the closed square represents glucose consumption (g/L). [a] 0.5 g/L of C10 was added at 0 h while [b] 0.5 g/L of C10 was added at 48 h.

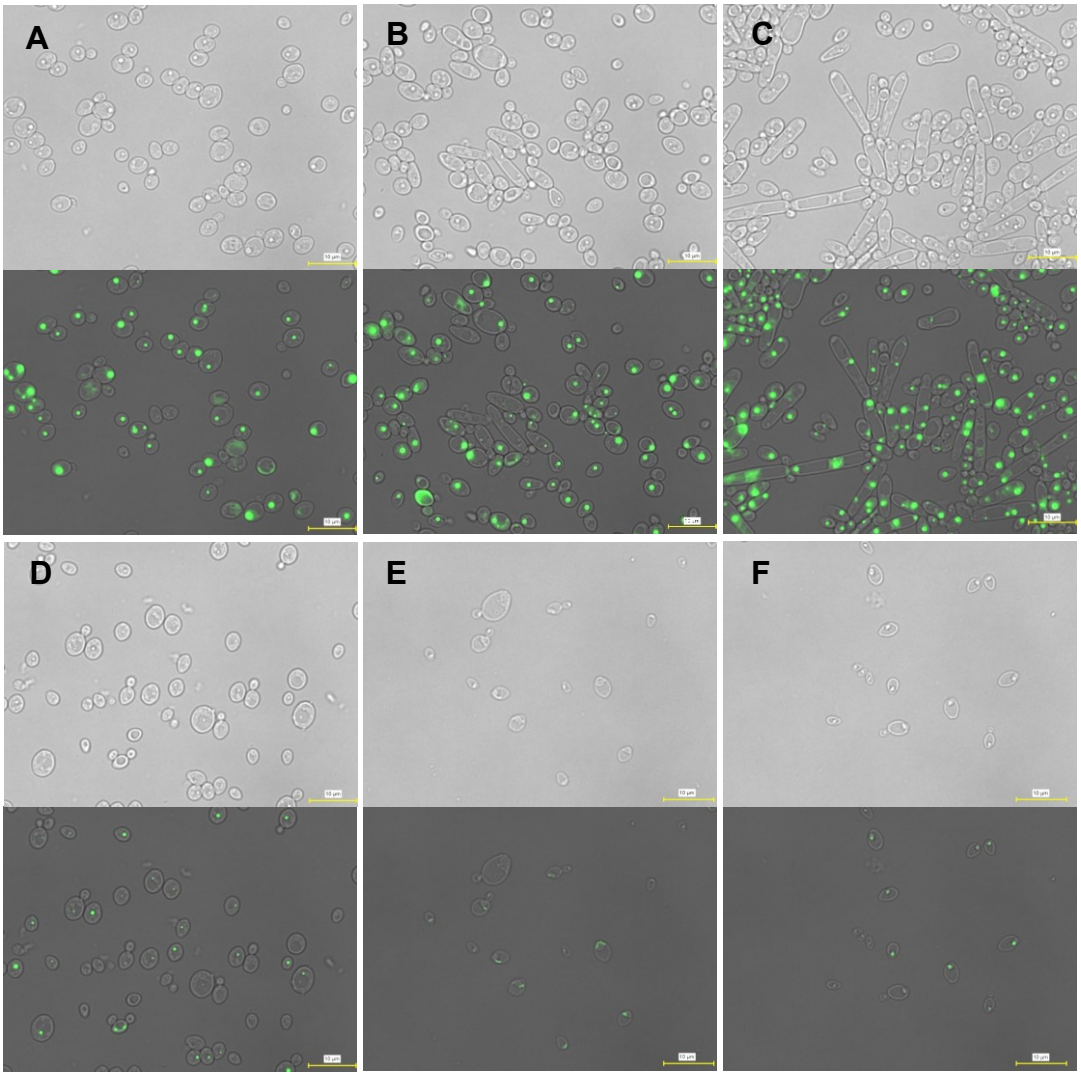

Figure 16 The morphology of *M. guilliermondii* cells at 120 h when culturing in YPD50 medium with no C10 (A), 0.25 g/L of C10 (B), 0.5 g/L of C10 at 0 h (C), 0.5 g/L of C10 at 48 h (D), 1 g/L of C10 (E) and 2 g/L of C10 (F). The microscopic fluorescence images of *M. guilliermondii* stained with BODIPY (493/505). The upper and lower panel show bright-field and fluorescence microscopy images, respectively. Bars: 10 μm.

To find more evidence for the formation of pseudohyphae in *M. guilliermondii*, its change in morphology over time was observed. For this experiment, only cells exposed to 0.5 g/L of C10 at 0 h and 48 h were observed. Samples were taken every 24 h after adding the C10, stained with BODIPY, and visualized under a fluorescence microscope. It was confirmed that when C10 was added at 0 h, some cells started to grow unusually after day 2 and had the most accumulated lipid on day 5 (Figure 17). Prolonged incubation up to 7 days maintained the unusual cell morphology of some cells, but the accumulated lipids exhibited less fluorescence intensity.

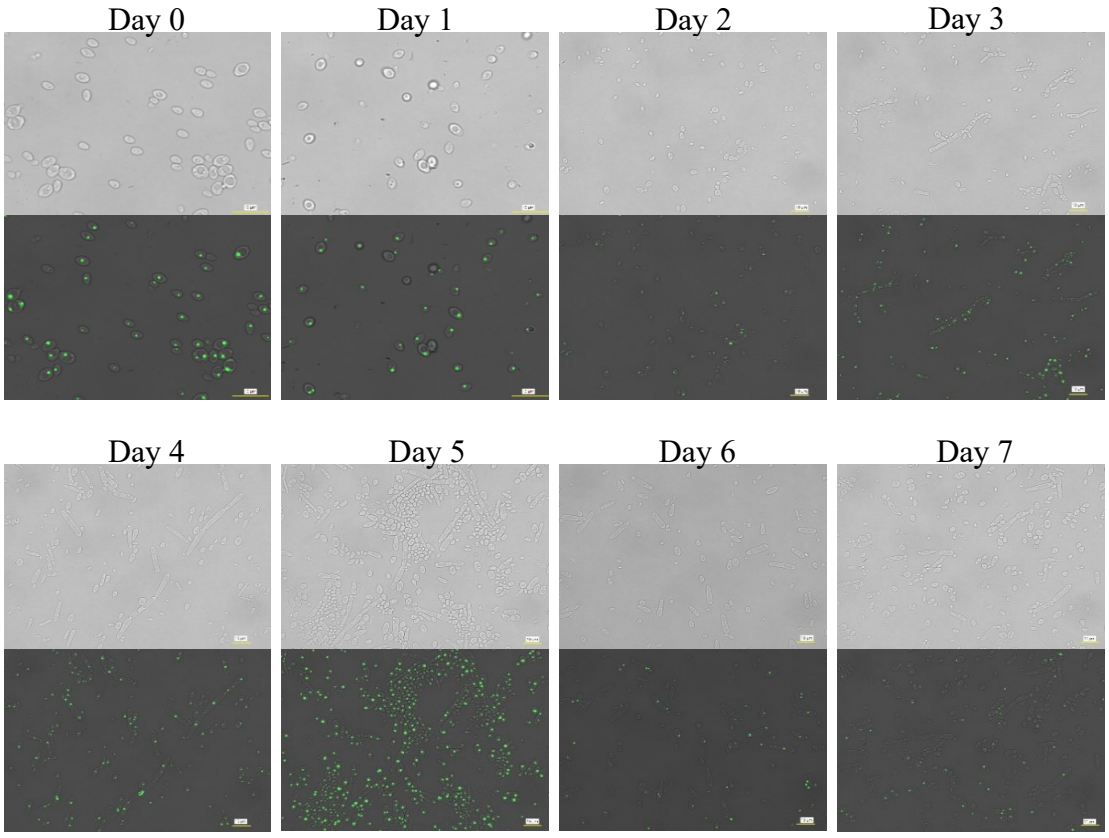

Figure 17 Time course observation of morphological changes in *M. guilliermondii* cells when 0.5 g/L of C10 was added into YPD50 at 0 h. The upper panel shows bright-field microscopy images and the lower panel shows fluorescence microscopy images of the same field of view stained with BODIPY to visualize accumulated lipids (green). Bars: 10 μm.

In contrast, no morphological transition was observed when C10 was added during the exponential phase (Figure 18). Instead, the stained lipid bodies appeared smaller over time, with fluorescence intensity becoming undetectable.

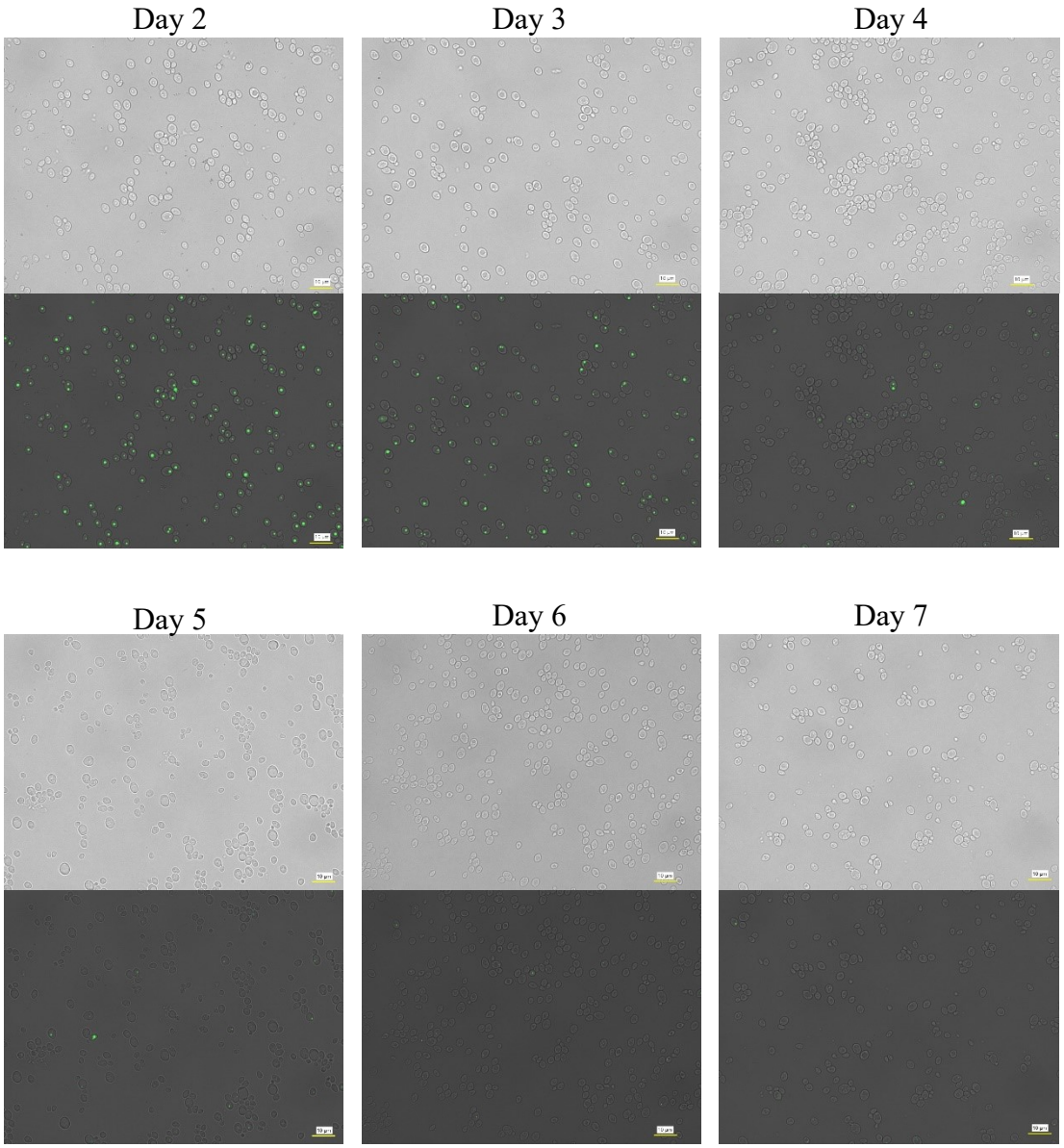

Figure 18 Time course observation of morphological changes in *M. guilliermondii* cells when 0.5 g/L of C10 was added into YPD50 at 48 h. The upper panel shows bright-field microscopy images and the lower panel shows fluorescence microscopy images of the same field of view stained with BODIPY to visualize accumulated lipids (green). Bars: 10 μm.

3.3.3 Analysis of lipids produced during decanoic acid stress

Despite the morphological shift, lipid bodies were still observed in *M. guilliermondii* when stained with BODIPY (Figure 16). Thus, the freeze-dried cells were subjected to gravimetry analysis to evaluate the production of lipids (Table 13). Overall, the lipid content at the time of harvesting remains fairly consistent across all conditions in control cells and cells exposed to 0.25 g/L or 0.5 g/L of C10 at 0 h, indicating that C10 does not significantly affect the percentage of lipids within the cells. When C10 was supplemented at 0.5 g/L at 0 h, an apparent inhibitory effect was observed on cell growth, morphology, and glucose consumption (Figure 15). Once growth resumed, the cells eventually grew similarly to control cells, and their ability to accumulate lipids was not significantly different from control, with lipid concentrations of 5.9 ± 0.9 g/L and 6.1 ± 0.8 g/L, respectively (Table 13). This suggests that while metabolic and growth rates are initially affected, the cells are capable of achieving similar overall productivity. In addition, the consistent lipid content across all conditions also suggests that while cell growth might be affected (Figure 15), the cellular machinery responsible for lipid accumulation remains relatively unaffected by the exposure of C10. A study on *Trichosporon cutaneum* demonstrated that higher nitrogen concentrations in the medium induce morphological changes, which subsequently affect growth, glucose consumption and lipid production (106). Additionally, research on oleaginous yeast *Y. lipolytica* showed that lipid production is influenced by the rheological properties and viscosity of the culture medium, which are affected by morphological changes (95). However, in this study, the morphological shift did not show a significant effect on lipid accumulation in *M. guilliermondii*.

However, when 0.5 g/L of C10 was supplemented at 48 h, the lipid content was slightly lower at 32 ± 1 wt% compared to control cells. This is also supported by the

smaller lipid size observed under this condition at 120 h (Figure 16) and by time-course observation showing that the stained lipid bodies progressively decreased in size over time, with the fluorescence intensity eventually becoming undetectable (Figure 18). As shown in Figure 15, the DCW of the cells decreased after exposure to C10 at 48 h. The decrease in DCW may be attributed to a reduction in lipid content, as the residual biomass at 120 h was not significantly different from that of the control cells (Table 13). This could suggest that the timing of C10 exposure during the exponential phase may affect the metabolic pathways involved in lipid synthesis, potentially reducing lipid accumulation rather than impacting growth and morphology, as observed when C10 was added at 0 h. Additionally, it has been reported that in *S. cerevisiae*, exposure to organic acids during the adaptation phase on glucose led to a decrease in steryl esters while triacylglycerols content increased (98). This observation further supports the hypothesis that organic acid exposure can shift lipid metabolism, potentially in a manner similar to the effect of C10 observed in this study. However, future experiments are needed to confirm the effects of C10 added during the exponential phase.

Table 13 Biomass and lipid production of *M. guilliermondii* grown on YPD50 supplemented with C10.

Media [a]	DCW (g/L) [b]	Lipid content (wt%) [c]	Lipid concentration (g/L) [d]	Residual biomass (g/L) [e]
YPD50	17.2 ± 2.2	36 ± 0	6.1 ± 0.8	11.1 ± 1.4
YPD50 + 0.25 g/L C10	15.8 ± 0.3	34 ± 1	5.3 ± 0.2	10.5 ± 0.1
YPD50 + 0.5 g/L C10[f]	17.5 ± 2.6	34 ± 2	5.9 ± 0.9	11.6 ± 1.8
YPD50 + 0.5 g/L C10[g]	15.0 ± 0.1	32 ± 1	4.8 ± 0.2	10.3 ± 0.2

The values were determined in triplicate; mean values and standard deviation are provided in the table.

[a] *M. guilliermondii* was cultured in 12 mL of respective media for 5 days at 29 °C, 190 rpm.

[b] Dried cell weight (DCW) was determined after freeze-drying.

[c] Lipid content of freeze-dried cells was determined by gravimetric analysis.

[d] Lipid concentration was determined by multiplying the lipid content (%) with the DCW (g/L)

[e] Residual biomass was determined by subtracting the lipid concentration (g/L) from the DCW (g/L)

[f] 0.5 g/L of C10 was added at 0 h

[g] 0.5 g/L of C10 was added at 48 h

The FA compositions of the lipid produced by *M. guilliermondii* at 120 h were analysed using GC-MS (Figure 19). The lipids were predominantly composed of palmitic acid (C16:0), oleic acid (C18:1), and linoleic acid (C18:2) in both the control cells and cells exposed to C10, similar to common FA found in vegetable oils (37). However, slightly differences in the percentage of each FA were observed. In both control cells and the cells exposed to 0.5 g/L of C10 at 48 h, the FA percentages were similar. However, cells exposed to 0.25 g/L and 0.5 g/L of C10 at 0 h showed notably high standard deviation especially in the percentage of C18:1, indicating substantial variability in FA composition among these samples. Despite adding C10 as a carbon source in the YPD50 medium, *M. guilliermondii* did not directly utilize C10 for FA synthesis. The free FAs incorporated into the cells may either be utilized for growth or serve as substrates for intracellular lipid synthesis via *ex novo* pathway (21). This observation is consistent with a study on *Crytococcus curvatus*, where the relative content of C10 in the lipid product was below 1% when cultured in the presence of 10 g/L of C10 (107). Similarly, in the present study, C10 was not incorporated into the lipid profile, as the FAME composition (%) of C10 was almost similar to that of the control cells. This lack of C10 incorporation suggests that the *ex novo* pathway may not be activated. Instead, previous research has shown that the exposure of yeast cells to C10 activates a gene related to the β-oxidation pathway (101), indicating that C10 may be degraded via β-oxidation pathway rather than being used for lipid synthesis.

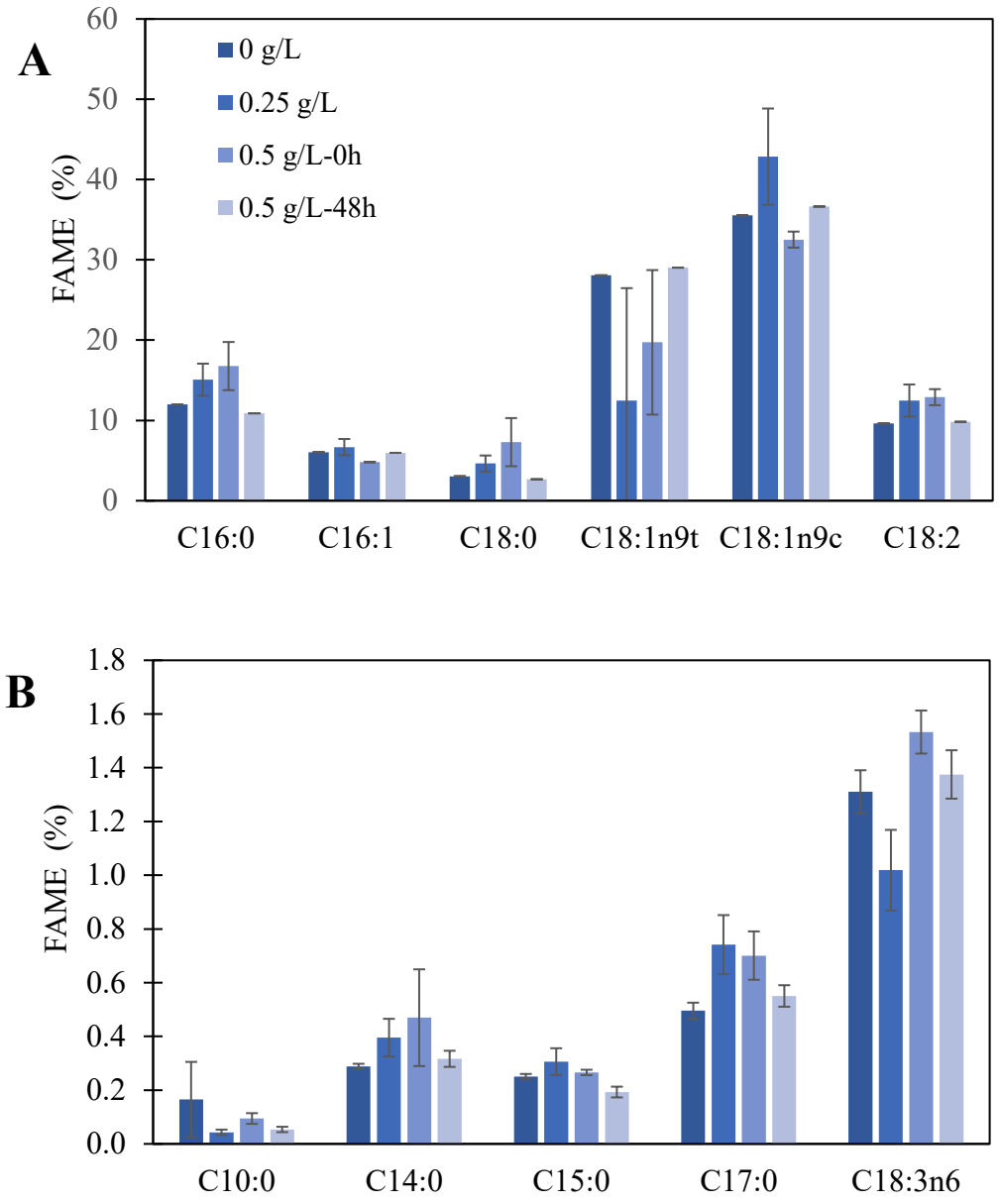

Figure 19 FAME profile of *M. guilliermondii* grown on YPD50 medium supplemented with C10. (A) Major FA composition. (B) Minor FA composition less than 2%.

3.3.4 Effect of decanoic acid on a generation of ROS

When cells uptake exogenous fatty acids, cascade, cellular responses and metabolic processes are triggered. Mcl-FA penetrates the cells by passive diffusion (108). Once inside, the FAs are activated by acyl-CoA synthetase to form fatty acyl-CoA, which is then transported to various cellular compartments, such as mitochondria and peroxisome, for metabolism. In peroxisome, fatty acyl-CoA will be degraded via *β*-oxidation, producing H_2O_2, which peroxisomal catalase converts into water and oxygen to protect the cell from oxidative damage caused by reactive oxygen species (ROS). According to previous research, the yeast response to exposure to C10 is considerably more complex and exhibits many similarities to oxidative stress (101). Additionally, it was reported that exposure of C10 in *Saccharomyces cerevisiae* could induce early and high accumulation of ROS (109). As exposure of 0.5 g/L of C10 at 0 h exhibited a more significant effect, we focused subsequent staining and gene expression analyses on cells exposed to this concentration to understand the cellular response to C10 exposure better. Expression levels were compared to those in control cells cultured without C10 under the same conditions, indicating an absence of stress in the control. To visualize the accumulation of ROS within the cells under a fluorescence microscope, we stained the cells with DCFH-DA dye at 96 h when the cells were in the exponential phase.

The preliminary attempts to detect ROS in pseudohyphal-forming cells yielded inconclusive results as upon staining the cells, a heterogeneous pattern of fluorescence intensity was observed, likely due to the short lifespan of ROS (Figure 20). The rapid degradation of ROS may have hindered our ability to capture a clear and consistent signal. As observed in Figure S4, some cells cultured in the presence of C10 exhibited a strong fluorescence signal, indicating high levels of ROS, and some others showed a

much weaker fluorescence signal. In contrast, most cells displayed no detectable fluorescence and appeared similar to the unstained control cells. In this study, ROS-sensitive dye provided only a limited and transient signal, consistent with the known rapid turnover of ROS, which complicates their detection and quantification in living cells. Despite the challenge of directly observing ROS, the detected signal suggests that oxidative stress might play a role in inducing pseudohyphal formation. This hypothesis is supported by previous studies in other yeast species, where oxidative stress has been linked to morphological changes and adaptive responses (89, 110).

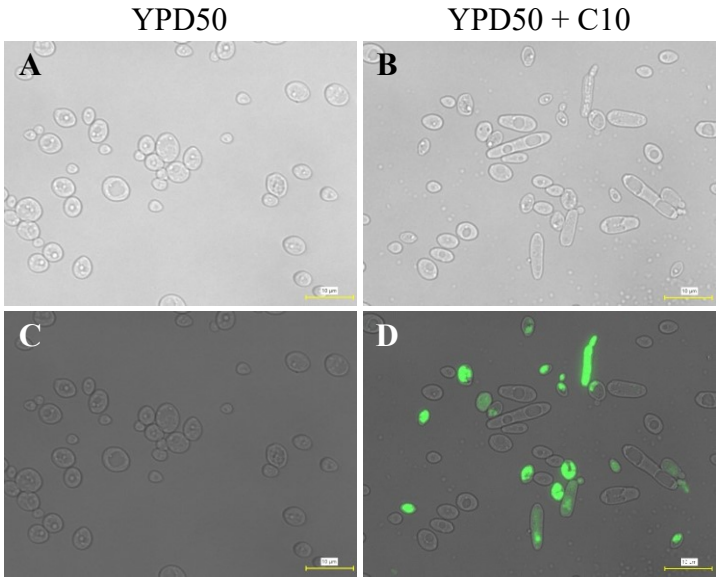

Figure 20 Reactive oxygen species (ROS) in the cells of *M. guilliermondii*. (A-B) The microscopic images of *M. guilliermondii* when culturing in YPD50 medium supplemented with 0.5 g/L of C10 (B). (C-D) The microscopic fluorescence images of *M. guilliermondii* stained with ROS Assay Kit-Highly Sensitive DCFH-DA- (Dojindo Laboratories). Bars: 10 µm.

To further investigate the cellular response to this stress, we analyzed the expression levels of key antioxidant genes involved in mitigating excess ROS at 48 h post-exposure, when the cells began to exhibit slowed growth. Specifically, we focused on the superoxide dismutase (SOD) family, including the cytosolic *SOD1*, mitochondrial *SOD2*, and the cell surface *SOD6*. While *SOD1* and *SOD2* are well-studied for their role in converting superoxide anions into H_2O_2 (111), *SOD6* is less characterized but was identified in the genome of *M. guilliermondii*. In *Candida albicans*, *SOD6* was predicted as a GPI-anchored cell wall protein, but its functions have not been thoroughly studied (112, 113). Notably, SOD1, SOD2, and SOD6 exhibited higher expression levels under C10 stress conditions compared to the control condition at 48 h post-exposure, with relative expression of 0.96, 2.34, and 0.71, respectively (Figure 21). However, at 72 h, the expression levels of these genes were lower than those observed at 48 h (Figure 21), suggesting an adaptive response to counteract oxidative stress induced by C10 at 48 h.

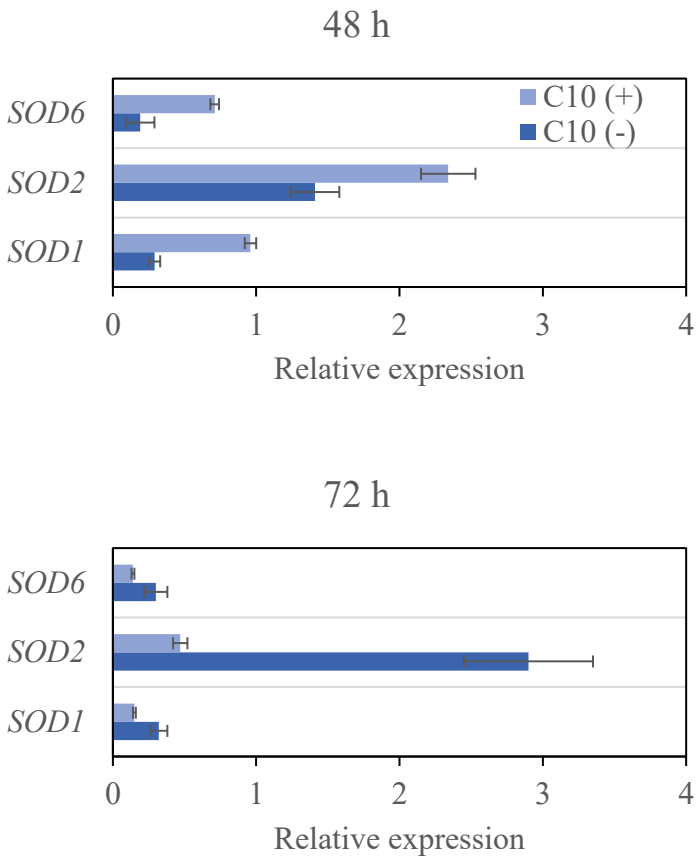

Figure 21 Expression level of genes related to antioxidant. C10 (-) refers to the control condition without the addition of C10, while C10 (+) refers to the addition of 0.5 g/L of C10 at 0 h.

3.3.5 Effect of decanoic acid on vacuole dynamics

ROS can be damaging at high levels, but at moderate levels, they serve as important signaling molecules (114). An imbalance between ROS production and the ability of the cells to detoxify them can trigger an oxidative stress response. This accumulation of ROS can lead to oxidative damage to proteins, DNA, and lipids. Exposure to C10 in the culture medium increases ROS production, thereby inducing cell oxidative stress. Oxidative stress triggers autophagy, a cellular process where cells degrade damaged components. Autophagy involves the encapsulation of cargo destined

for degradation within a double-membrane vesicle called an autophagosome, which then fuses with the vacuole, where the cargo is degraded (115). To further understand the response of *M. guilliermondii* to C10 exposure, we analyzed the expression levels of key autophagy-related genes (*ATG*) found in the genome of *M. guilliermondii* at 48 h and 72 h post-exposure (Figure 22).

Among the autophagy-related genes, ATG1 and ATG9 were significantly expressed at 48 h, with relative expressions of 13.36 and 17.72, respectively. The Atg1 complex, a central regulator of autophagy, is essential for initiation of autophagy (116). Atg9 is the only integral membrane protein and, along with its associated cycling system components, plays a crucial role in autophagosome formation by facilitating the expansion of the phagophore (117–119). In contrast, ATG8 exhibited high expression under non-stress control conditions at 48 and 72 h, but its relative expression was significantly lower under C10 stress. Conjugation of Atg8 is a crucial component of the core autophagy machinery necessary for phagophore expansion (71, 116). As Atg8 is primarily involved in the expansion and completion stages of autophagy, its expression may increase when yeast growth improves after 72 h, similar to the control condition. However, in this study, we did not assess ATG8 expression levels after growth recovery. The upregulation of ATG9 and ATG1 under C10 stress suggests the activation of the early stages of autophagy, potentially as a cellular response to manage ROS-induced damage and maintain cellular homeostasis. These findings indicate that C10 stress significantly affects ATG gene expression. Consistent with our observations, a previous study demonstrated that exposure to C10 induced autophagosome formation and modulated autophagic flux in *Dictyostelium discoideum*, a eukaryotic microorganism within the slime mold group, upon exposure to C10 (120).

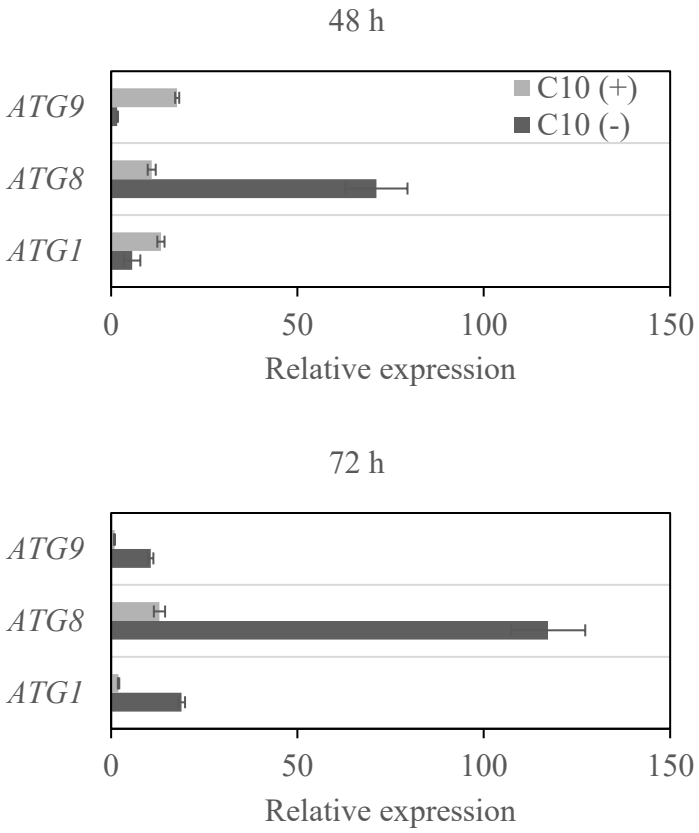

Figure 22 Expression level of genes related to autophagy. C10 (-) refers to the control condition without the addition of C10, while C10 (+) refers to the addition of 0.5 g/L of C10 at 0 h.

In yeast cells, the vacuole with abundant hydrolytic enzymes is essential for physiological processes and functions in autophagy, where it fuses with autophagosomes to degrade their cargo. Additionally, the morphology of the vacuole can change in response to various stimuli or stress (121, 122). Thus, the effect of C10 on the vacuole morphology of *M. guilliermondii* was also examined. Samples were taken on Day 3 and Day 5, stained with yeast vacuole membrane marker MDY-64, and visualized under a fluorescence microscope. Based on the microscopy images, notable differences in vacuole morphology were observed (Figure 23). Cells undergoing pseudohyphal formation under C10 stress exhibited elongated vacuoles compared with

the round vacuoles observed in cells cultured in the control medium and seed culture. The vacuoles of pseudohyphal-forming cells appeared significantly more prolonged and elongated, extending throughout the length of the cell. In a previous study, the increase in vacuole size observed in rapamycin-treated cells may be attributed to an increase in autophagy (123). Thus, the increase in vacuole size observed in cells exposed to C10 may also be due to the increased levels of autophagosome fusion to the vacuole, resulting from higher levels of autophagy. In addition, enlarged vacuoles can be an adaptive response to manage increased autophagy activity and maintain cellular homeostasis under stress conditions. Together with the upregulation of *ATG*, the observed elongation of vacuoles might further support the activation of autophagy under C10-induced stress in *M. guilliermondii*.

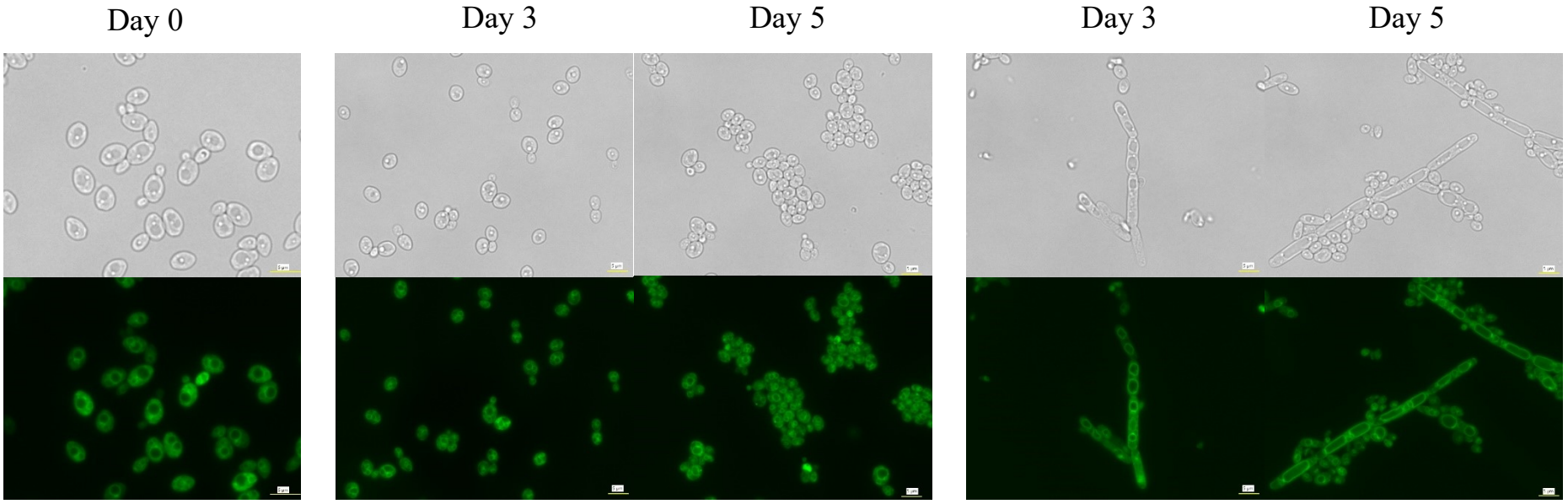

Figure 23 Effect of addition of C10 in YPD50 medium on vacuole of *M. guilliermondii*. The upper panel shows bright-field microscopy images and the lower panel shows fluorescence microscopy images of the same field of view stained with yeast vacuole membrane marker MDY-64. Bars: 10 µm.

3.3.6 Signaling pathways involved in dimorphic transition

The upregulation of *SOD* and *ATG* helps the cells manage oxidative stress by detoxifying ROS and recycling damaged parts. Research on yeast has identified major signaling pathways that control gene regulation in response to oxidative stress, including the mitogen-activated protein kinase (MAPK). The MAPK cascades are a conserved signaling system that eukaryotic cells use to respond to various environmental signals. A typical MAPK cascade consists of three protein kinases that are activated in sequence through phosphorylation after sensing a stimulus, and once active, MAPK can then phosphorylate targets like transcription factors and cytosolic proteins, enabling the cell to respond to the stimulus (15). In *Candida albicans* and *Saccharomyces cerevisiae*, the HOG MAPK pathway controls dimorphic transition and helps in adaptation to oxidative stress (89, 124, 125). The HOG pathway was initially discovered as a signaling mechanism in response to osmotic stress but was later found to play a role in oxidative stress as well (126). The HOG pathway relies on a two-component system formed by *SLN1*, *YPD1,* and *SSK1* (127, 128) (Figure 24). The Sln1 sensor kinase is a transmembrane protein whose activity decreases under osmotic and oxidative stress conditions, leading to the accumulation of Sln1 in its dephosphorylated form. The phosphate is transferred to the response regulator, Ssk1, through Ypd1, a histidine-containing phosphotransfer (HPt) protein. The signal is then transmitted form Sln1-Ypd1-Ssk1 by sequential phosphorylation of Ssk2, a MAPK kinase kinase (MAPKKK), and Pbs2, a MAPK kinase (MAPKK) to Hog1, a MAPK (129). Once activated, Hog1 translocated to the nucleus to regulate target gene expression (130).

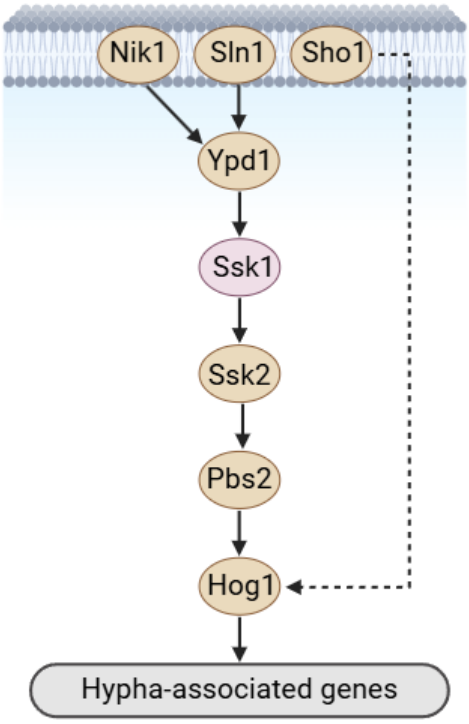

Figure 24 HOG MAPK pathway.

To further investigate whether *M. guilliermondii* mediates its response to oxidative stress induced by C10 exposure and the resulting dimorphic transition via the HOG MAPK cascade, we examined the expression levels of HOG MAPK cascade genes and their upstream regulators, as identified in the genome of *M. guilliermondii* at 48 h post-exposure. Among all the genes analyzed, only *YPD1* was significantly upregulated at relative expression of 68.0 at 48 h (Figure 25). This notable upregulation of YPD1, despite the lack of response from the other HOG-related genes, suggests that Ypd1 may have an alternative function beyond its typical involvement in the HOG pathway. Ypd1, typically involved in phosphorylating Ssk1 to activate the HOG pathway, may also phosphorylate Skn7, a transcription factor known to regulate oxidative stress response (131). In *S. cerevisiae*, Ypd1 functions as an HPt protein that facilitates all phosphorelay processes, transferring signals from Sln1 to the response regulators Ssk1 and Skn7 (132). Additionally, the loss of Ypd1 function is lethal to *S.*

cerevisiae (133), further highlighting its critical role in cellular signaling. Interestingly, while Ypd1 can also phosphorylate Skn7, it has been reported that the activation of oxidative stress-response genes by Skn7 occurs independently of Sln1-Ypd1 pathway (131). Moreover, the oxidative stress response mediated by Skn7 overlaps with that of Yap1 (134, 135).

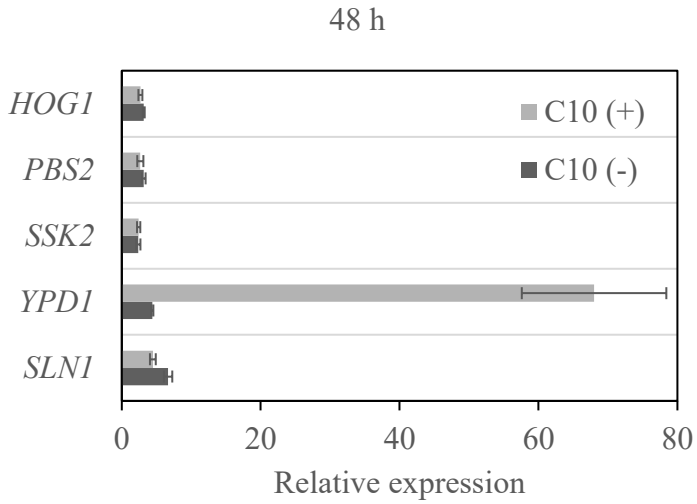

Figure 25 Expression level of genes related to MAPK. C10 (-) refers to the control condition without the addition of C10, while C10 (+) refers to the addition of 0.5 g/L of C10 at 0 h.

Unfortunately, we could not identify the gene encoding Skn7 and Yap1 in the *M. guilliermondii* genome, limiting our ability to evaluate the expression and role of these transcription factors under C10-induced stress. As a result, the precise role of Ypd1 in *M. guilliermondii* remains to be determined, as we could not definitively confirm direct interactions between Ypd1 and Skn7 or between Skn7 and Yap1 in response to oxidative stress. Notably, *YPD1* was significantly upregulated, raising the possibility that Ypd1 may have evolved unique roles in the response of *M. guilliermondii* to oxidative stress and dimorphism. A significant challenge in this study

was the incomplete annotation of the *M. guilliermondii* genome, which limited the identification of key regulators and constrained our ability to fully map the signaling pathways involved. Future works should focus on conducting functional studies to validate the involvement of Ypd1 in the oxidative stress response in *M. guilliermondii*.

3.4 Conclusion

In this study, we investigated the impact of C10 on the growth, morphology, lipid accumulation, and cellular physiology of the oleaginous yeast *M. guilliermondii*. Our findings reveal that C10 significantly induces a prolonged lag phase, accompanied by a morphological shift from yeast-like cells to pseudohyphal morphology. While forming pseudohyphae, the ability of *M. guilliermondii* to accumulate lipids or alter its fatty acid composition is not significantly affected. Despite the morphological transition, its oleaginous nature remains intact, with lipid biosynthesis proceeding similarly to control conditions. C10 induces oxidative stress, potentially triggering a morphological shift as an adaptive response. The upregulation of *SOD* and *ATG* genes suggests that both antioxidant activation and autophagy play important roles in the response to C10-induced stress. These findings demonstrate that *M. guilliermondii* is a highly versatile and resilient yeast strain that adapts to harsh environmental conditions while maintaining its oleaginous properties.

CHAPTER 4

Metabolic engineering of oleaginous yeast *Meyerozyma guilliermondii* for production of biodegradable polyhydroxyalkanoate (PHA)

4.1 Introduction

The growing concern about environmental effects of petroleum-based plastics and its difficulty in the disposal of has been increasing in public concern which increase attention to search for an alternative to conventional plastics. Bio-based plastics such as polyhydroxyalkanoates (PHA) can be the alternative as it is natural biopolymers that are synthesized and catabolized by various microorganisms. PHA is one of the biodegradable plastics that have close analogy to conventional plastics. PHA has desired features such as biocompatibility, biodegradability, and negligible cytotoxicity to the cells, thus it has a wide range of potential application. The building block of PHA consists of (*R*)-3-hydroxyalkanoic acid monomer unit which can be influence the thermoplastics and elastomeric properties of PHA (39). It can be divided into two groups depending on the number of carbon atoms in the monomeric units which is short-chain-length (scl) PHA consist of 3 to 5 carbon atoms and medium-chain-length (mcl) PHA have 6 to 14 carbon atoms (44). Many microorganisms either natural isolates or recombinants have been identified as PHA producers. Additionally, efforts have been directed towards engineering PHA biosynthesis in non-PHA producer including *Escherichia coli* , yeast and plant (41).

Yeast is a fast-growing unicellular eukaryote, serves as an excellent model system for studying metabolic pathways modifications to enable PHA synthesis in eukaryotic organisms. Although yeast does not naturally produce PHA due to the absence of *phaC*, several studies have successfully employed the peroxisomes of *Saccharomyces cerevisiae* (49, 51), *Pichia pastoris* (52) and *Yarrowia lipolytica* (53–55) in the

production of PHA. Yeast peroxisomes are involved in *β*-oxidation of fatty acids, generating (*R*)-3-hydroxyacyl-CoA intermediates of varying chain lengths that serves as substrates for mcl-PHA synthesis. In *Y. lipolytica*, an oleaginous yeast known for its high lipid accumulation, the expression of *phaC* from *Pseudomonas aeruginosa* targeted to the peroxisome enabled the production of both PHA homopolymers and copolymers when supplemented with exogenous fatty acids (53). PHA production was further enhanced by redirecting FA flux towards *β*-oxidation, achieved by deleting the TAG synthesis pathway and overexpressing the enoyl-CoA hydratase 2 domain, resulting in significant increase in PHA content (53). The mcl-PHA homopolymer (poly-3-hydroxydodecanoate) and the copolymer containing monomers of 3-hydroxyoctanoate, 3-hydroxydecanoate, 3-hydroxydodecanoate and 3-hydroxytetradecanoate monomers were synthesized in *Y. lipolytica* expressing *phaC* and cultured with FAs (55). These polymers exhibited distinct material properties, with the homopolymer demonstrating soft thermoplastic characteristics and the copolymer behaving like thermoplastic elastomer (55).

Another oleaginous yeast, *Meyerozyma guilliermondii* is a versatile yeast species widely studied for its biotechnological potential (3). Under optimal conditions, *M. guilliermondii* has been reported to accumulate lipids up to 60.6% (w/w) of its DCW (11) This yeast is recognized for its relatively fast growth rate and metabolic versatility, allowing it to adapt to diverse substrates and environmental conditions (3). Such robustness makes *M. guilliermondii* an attractive candidate for metabolic engineering, particularly for the production of alternative biopolymers and other value-added chemicals. However, a significant challenge in the metabolic engineering of *M. guilliermondii* is the lack of well-established and reliable method for targeted deletion of endogenous genes or chromosomal integration of exogenous genes at a specific locus.

This study addresses this limitation and represents the first attempt to engineer *M. guilliermondii* for PHA biosynthesis by redirecting metabolic flux from TAG synthesis to PHA production.

4.2 Materials and methods

4.2.1 Strains, media and growth condition

NEB® Stable Competent *E. coli* was utilized as the host for routine cloning. Cultures of *E. coli* and *Agrobacterium tumefaciens* were grown in Luria-Bertani (LB) medium [5 g/L of yeast extract, 10 g/L of tryptone and 10 g/L of NaCl] at 30 °C. The *M. guilliermondii* strains used in this study were listed in Table 14. Wild-type *M. guilliermondii* from our private collection (PK01) was used in this study Cultivation of *M. guilliermondii* strain was routinely performed on YPD agar (10 g/L of yeast extract, 20 g/L of peptone, 20 g/L of D-glucose and 15 g/L of agar) at 30 °C. Both YPD agar and YPD liquid media were supplemented with appropriate antibiotics for selection and maintenance. Seed cultures of *M. guilliermondii* were prepared by inoculating a single colony in 12 mL of YPD medium containing antibiotics in 100 mL Erlenmeyer flask and incubated overnight at 29 °C, 190 rpm in an orbital shaker incubator (BioShaker BR-43FH MR, Taitec Corp., Tokyo, Japan). The volume of seed culture was adjusted to an initial optical density (OD_{600}) of 14.0 – 16.0 before transferring to production medium with a working volume of 12 mL in 100 mL Erlenmeyer flask.

For lipid and PHA production, *M. guilliermondii* strains were cultured in nitrogen-limited mineral medium (-NMM) supplemented with 50 g/L of glucose. The -NMM contained nitrogen sources [1.5 g/L of yeast extract and 0.25 g/L of $(NH_4)_2SO_4$], 1.5 g/L of $MgSO_4 \cdot 7H_2O$, phosphate buffer [7 g/L of KH_2PO_4 and 5 g/L of $Na_2HPO_4 \cdot 7H_2O$], and trace element solution [0.08 g/L of $FeSO_4 \cdot 7H_2O$, 0.01 g/L of $ZnSO_4 \cdot 7H_2O$, 0.1 g/L of $CaCl_2 \cdot 7H_2O$, 0.1 g/L of $MnSO_4 \cdot 4H_2O$, 0.002 g/L of

$CuSO_4 \cdot 5H_2O$ and 0.002 g/L of $CoCl_2 \cdot 6H_2O$]. The initial pH of -NMM was adjusted to 5.5. Cultures were incubated at 29 °C, 190 rpm for 120 h in an orbital shaker incubator. After the incubation, the culture was harvested by centrifugation at 8000 rpm for 10 min, and washed twice with deionized water before further analyses.

Table 14 List of *M. guilliermondii* strains.

Strain	Description	Source
PK01	Wild-type	NBRC
PK01ΔLRO1	Δ*lro1*::AurR	This study
PK01ΔSCT1	Δ*sct1*::AurR	This study
PK01::phaABC	Δ*lro1*::*phaA*, *HygR*, *phaB*, *phaC*	This study

4.2.3 Vector and strains construction

Disruption of the *LRO1* and *SCT1* genes in *M. guilliermondii* was achieved by substituting portion of the coding regions with the *AurR* gene, which confers resistance to aureobasidin A and facilitates selection of transformations. To construct the disruption vectors, flanking sequences of approximately 1000 bp from the 5' (L) and 3' (R) regions adjacent to each target gene were PCR-amplified from the suspension of *M. guilliermondii* cells. These flanking regions were inserted into the pRI910 backbone vector at *PmeI* and *ApaI* restriction sites, to create the initial vectors, pRI-LRO1 and pRI-SCT1 (Figure 26). Subsequently, the *AurR* marker gene was PCR-amplified from the pAUR101 vector and cloned into pRI-LRO1 and pRI-SCT1 between the L and R ergions, yielding the final constructs, pRI-LRO101 and pRI-SCT101, respectively. Additionally, PHA-related genes which are *phaC*, *phaA* and *phaB* were synthesized by Invitrogen (Thermo Fisher Scientific). The *pha* genes cassette including a *HygR* gene

was introduced into pRI-LRO1 at *BamHI* restriction sites found on *LRO1* gene. The completed constructs were then transformed into E. coli NEB® Stable Competent cells for propagation and subsequent validation. The vector was extracted and introduced into Agrobacterium tumefaciens via electroporation using a Gene Pulser II, with pulse settings of 25 µF, 200 Ω and an applied voltage of 2 to 2.5 kV.

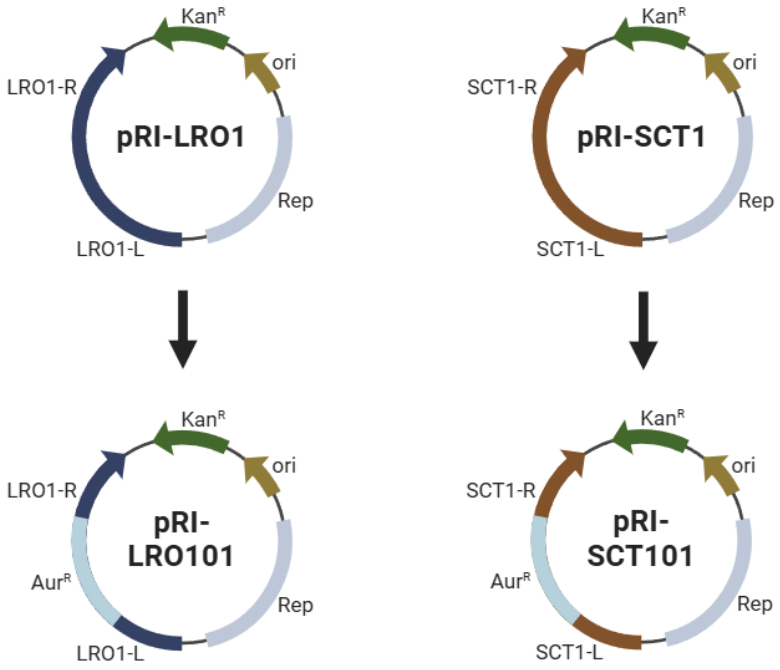

Figure 26 Vector construction.

4.2.4 Transformation of yeast cells

M. guilliermondii transformation was carried out using Agrobacterium-mediated transformation (AMT). Pre-cultured of *Agrobacterium tumefaciens* LBA4404 Electro-Cells harbouring the recombinant vector was mixed with the *M. guilliermondii* culture at a 1:1 ratio. The cell pellet was resuspended in 12 mL of YPD medium containing the appropriate selection antibiotics in 100 mL Erlenmeyer flask and co-cultured at 29 °C, 190 rpm for 24 h. Following incubation, the co-culture was plated on YPD agar containing the selective antibiotics and incubated at 30 °C for 3 to 5 days until colonies appeared. Emerging colonies were subcultured in YPD liquid medium

with the same antibiotic and incubated at 29 °C, 190 rpm for 2 days. This process repeated three times to ensure stability. Finally, the cultures were re-plated on YPD agar with selective antibiotics, incubated at 30 °C for an additional 3 to 5 days, and subjected to confirmation by PCR.

4.2.5 Determination of total lipid content by gravimetric analysis

Gravimetric analysis was used to measure lipid production based on the modified Folch method (72). Approximately, 15 mg of freeze-dried cell were added to a 2.0 mL polypropylene microvial containing 0.5 mm zirconia beads and 1.5 mL of Folch solvent [2:1 of chloroform: methanol (v/v)]. The cells were pulverized using a Shake Master Neo ver.1.0 (BMS-M10N21, BMS, Tokyo, Japan) at 1500 rpm, 15 min. After that, the cells were centrifuged at 14000 ×g for 5 min, the supernatant was discarded and the cell pellets were washed with 1.5 mL of deionized water. The cells were pulverized and centrifuged again, then the deionized water was discarded. The cell pellets were dried at 60 °C until a constant weight was obtained. The lipid content was determined by the difference in weight of the tube and expressed as a percent of dry cell weight.

4.2.6 Staining

BODIPY (Invitrogen) staining was employed to visualize the single cell oil production. The staining procedures were conducted according to the manufacturer's protocols. The stained cells were visualized using a digital inverted fluorescence microscope (Keyence Biorevo BZ-9000, Keyence, Osaka, Japan).

4.2.7 PHA analysis

PHA was quantified by gas chromatography (GC) following the method described previously with some modifications (136). Approximately, 30 mg of freeze-

dried cells were mixed with 2 mL of chloroform and 2 mL of methanolysis solution (85 vol% of methanol and 15 vol% concentrated sulphuric acid), and subsequently heated at 100 °C in a heating block for 2 h and 20 min. After heating, the samples were cooled to room temperature before adding with 1 mL of Milli-Q water and vortex vigorously. The layer at the bottom of the tube was transferred to a flat-bottomed test tube. Then, 0.1 mL of the solution was transferred to a GC vial and mixed with 0.1 mL of caprylic methyl ester (CME). CME was used as the internal standard at a 1:500 dilution in chloroform. The prepared samples were subjected to GC analysis using a SHIMADZU GC-2010 Plus (Shimadzu, Japan) equipped with an AOC-20i Auto Injector (Shimadzu, Japan), a DB-5 capillary column (Agilent J&W Scientific, Santa Clara, CA, USA) and a Flame Ionization Detector (FID).

4.3 Results and discussion

4.3.1 Effect of acyltransferase disruption in *M. guilliermondii*

Lipid accumulation in oleaginous yeast predominately occurs in the form of TAG via two key pathways which are the acyl-CoA synthesis pathway and the Kennedy pathway. Transcriptome analysis of oleaginous yeast under nitrogen-limited conditions revealed upregulation of genes involved in the synthesis of acyl-CoA from citate, as well as genes required for TAG synthesis via the Kennedy pathway (34, 137). This finding shows that these two pathways is important for TAG biosynthesis in oleaginous yeast. The rate-limiting step in TAG synthesis is the final reaction in the Kennedy pathway, where diacylglycerol (DAG) is acylated by either a DAG acyltransferase (DGA) or a phospholipid DAG acyltransferase (LRO1), resulting in TAG formation (138). In *Saccharomyces cerevisiae* strain Q4, the complete elimination of lipid accumulation has been achieved by deleting four acyltransferase-encoding genes which are *LRO1*, *DGA1*, *ARE1*, and *ARE2* (139), demonstrating the central role of these

enzymes in TAG biosynthesis. Thus, to enable PHA biosynthesis in *M. guilliermondii*, a metabolic engineering strategy was employed to redirect the fatty acid flux by disrupting the TAG synthesis pathway. This approach ensures the diversion of precursors toward PHA production, offering a promising route for bioplastic synthesis.

The genome of *M. guilliermondii* PK01 has been sequenced and annotated, revealing insights into its lipid biosynthesis pathways. Based on its full-length genome sequence, only *LRO1* was identified, while *DGA1* and *DGA2* could not be detected. In addition to *LRO1*, another acyltransferase, *SCT1*, which catalyzes the initial acylation step in the Kennedy pathway and is critical for initiating the sequential acylation reactions leading to TAG synthesis, was identified in *M. guilliermondii* PK01. Given their essential roles in TAG biosynthesis, *LRO1* and *SCT1* were targeted for disruption to evaluate their effects on TAG synthesis in this strain.

Following the disruption of LRO1, a significant reduction in lipid content was observed compared to the wild type strain (Figure 27). The lipid content of the ΔLRO1 mutant strain was at 14 wt% while the control was around 36 wt%. Almost 50% reduction was observed and the ΔLRO1 mutant loss its ability as oleaginous yeast as define as accumulation of lipid at least 20 wt % of its dry cell weight, indicating a significant impact on the LRO1 deletion on lipid biosynthesis. In contrast, the disruption of SCT1 did not reduce the lipid content as the lipid concentration and final DCW at 120 h was not much differ from the control, suggesting that SCT1 disruption did not substantially impair lipid accumulation. Residual biomass, calculated as DCW minus lipid concentration, showed a slight reduction in ΔSCT1 mutant relative to the control, while a more pronounced reduction was observed in the ΔLRO1 mutant, reflecting the altered cellular composition in these strains.

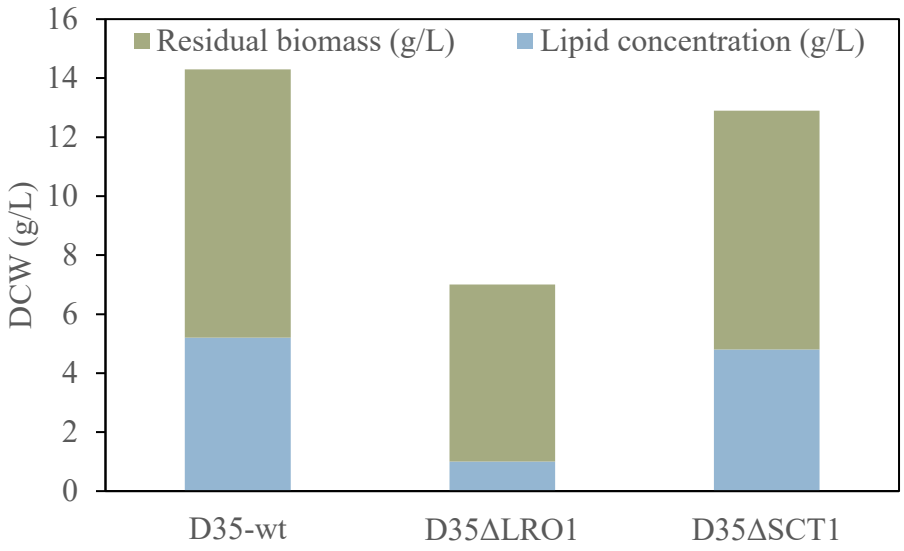

Figure 27 DCW of *M. guilliermondii* strains cultured in -NMM at 120 h.

The cells were stained with BODIPY to observe the accumulation of lipid and observed under a fluorescence microscope (Figure 28). BODIPY staining was used to assess the lipid body size and distribution in the control wild type and mutant strains of *M. guilliermondii*. It was revealed that LRO1 and SCT1 disruption did not noticeably affect cell morphology. In the control strain, lipid body appeared as large, round structures in green under fluorescence, consistent with their appearance under the bright-field. In the ΔLRO1 mutant strain, lipid bodies were significantly smaller, indicating a reduction in lipid accumulation. In contrast, in the ΔSCT1 mutant strain, large, round lipid bodies were observed under the bright-field similar like in the control. However, these structures did not fluoresce when stained with BODIPY, suggesting that they might not contain neutral lipids or that the composition of the lipids was altered, rendering them non-reactive to the dye.

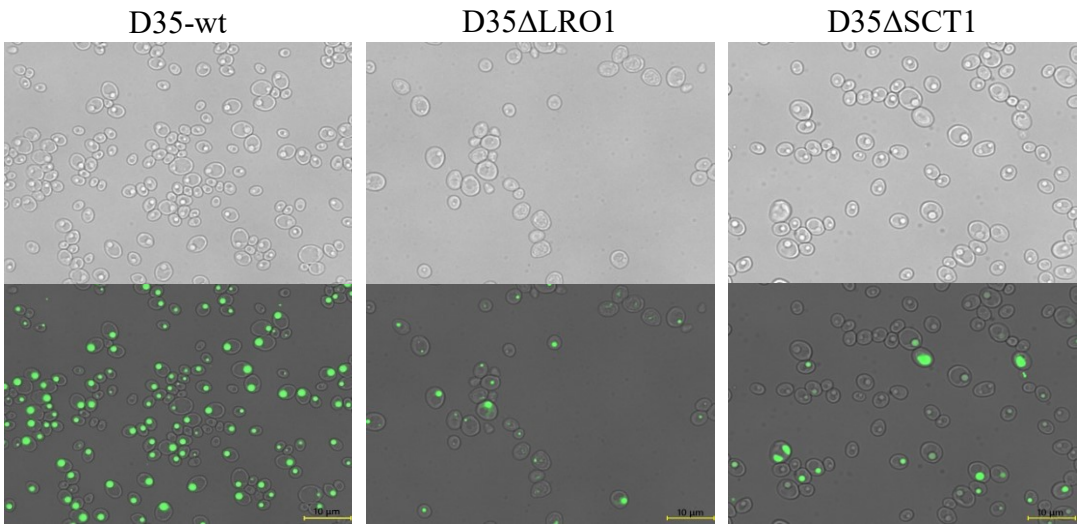

Figure 28 Lipid accumulated in the cells of *M. guilliermondii* strains at 120 h. (A-C) The microscopic images of *M. guilliermondii* when culturing in -NMM medium. (D-F) The microscopic fluorescence images of *M. guilliermondii* stained with BODIPY (493/505). Bars: 10 µm.

The observed decrease in lipid content in the ΔLRO1 mutant highlights the central role of LRO1 in the Kennedy pathway for TAG synthesis in *M. guilliermondii* as its disruption redirects fatty acid substrates away from storage lipid production. These results align with findings in *S. cerevisiae*, where *LRO1* deletion similarly led to reductions in TAG levels (139). While LRO1 is critical for TAG synthesis, the role of *SCT1* appears more nuanced, possibly contributing to phospholipid biosynthesis or compensatory pathways.

4.3.2 Expression of PHA-related genes

The disruption of the *LRO1* gene in *M. guilliermondii* resulted in a significant reduction in lipid content. This reduction could favor production of other metabolites, such as PHA. Following this, the genes *phaA*, *phaB*, and *phaC*, encoding *β*-ketothiolase, acetoacetyl-CoA reductase, and PHA synthase, respectively were integrated at the *LRO1* locus. These genes are essential for the synthesis of the PHA homopolymer poly(3-hydroxybutyrate) [P(3HB)], which consist of four-carbon monomer units. The *phaA* and *phaB* genes were synthesized based on their homologs in *Cupriavidus necator*, a model organism for PHA biosynthesis (47). Meanwhile, *phaC* was synthesized based on the *phaC1* STQK variant of *Pseudomonas sp. 61 – 3*, incorporating the double mutation S325T and Q481K (141). The synthesis of PHA is dependent on PhaC, a key enzyme responsible for polymerizing (*R*)-3-hydroxyacyl-CoA monomers into high molecular weight polyester granules. PhaC also influences the properties of the PHA produced, including its monomer composition and molecular weight. PhaC has been classified into four different classes based on subunit composition, substrate specificity and primary structure (56). As the central enzyme in PHA biosynthesis, PhaC is a main target for genetic engineering aimed at enhancing its activity and broadening its substrate specificity. While *Pseudomonas phaC1* is classified as a Class II PHA synthase with substrate specificity for mcl-PHA, the STQK variant was choose in this study due to its broadens substrate specificity to include scl-PHA monomers like 2-hydroxyalkanoic acids, while maintaining activity toward conventional monomers.

A plasmid vector was constructed to facilitate the expression of PHA biosynthetic genes (Figure 29). The vector was designed to harbour the genes required for PHA production, each driven by its own promoter and terminator to ensure efficient

and independent expression. The *phaA*, *hygR*, *phaB* and *phaC* were expressed under the control of the TDH3, TEF, ICL1, and ACS1 promoters and terminators, respectively. This study represents the first attempt to integrate the PHA biosynthetic genes into the *M. guilliermondii* genome using the AMT method and the pRI-910 background vector. The resulting transformants were subsequently evaluated for their ability to synthesize PHA.

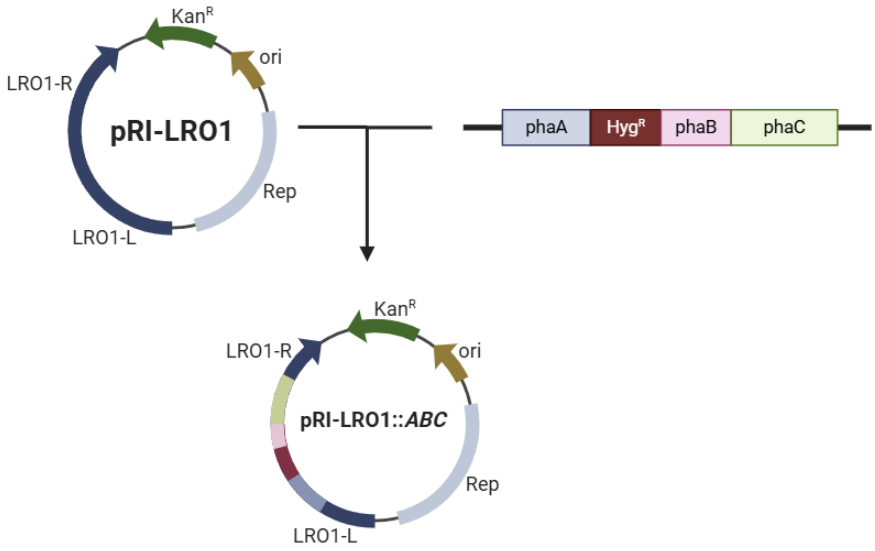

Figure 29 Construction of vector harbouring PHA genes.

4.3.3 PHA biosynthesis in the recombinant *M. guilliermondii* strain

The *M. guilliermondii* strain engineered with *phaA*, *phaB* and *phaC* integrated at the *LRO1* locus was subjected to PHA biosynthesis and analyzed using GC. The GC chromatogram revealed a significant reduction in the peaks corresponding to palmitic acid (C16:0) and oleic acid (C18:1) in *M. guilliermondii* PK01::phaABC compared to the control strain D35-wt (Figure 30). C16:0 and C18:1 are the major fatty acid composition produced by *M. guilliermondii* strain.

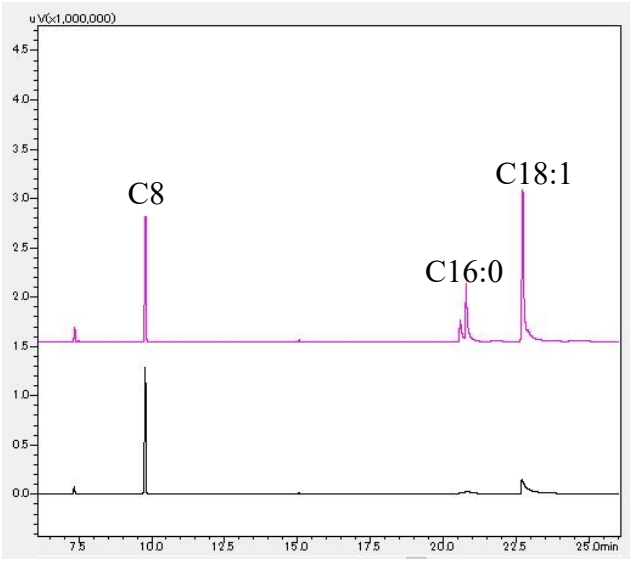

Figure 30 GC chromatogram of PK01-wt (pink) and PK01::phaABC (black). C8 was used as internal standard in all the sample.

When compared to the standard 3HB peaks in the chromatogram, a small peak corresponding to 3HB was detected in the engineered strain D35::phaABC (Figure 31), suggesting that the introduced PHA biosynthesis pathway was functional and capable of producing low levels of 3HB. However, the yield of 3HB appeared to be minimal under the conditions tested.

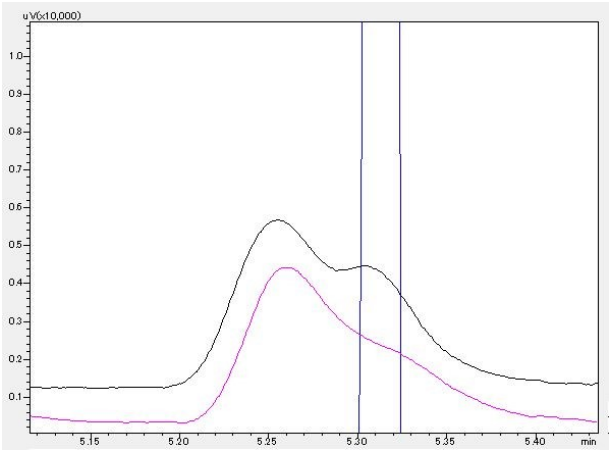

Figure 31 GC chromatogram of PK01-wt (pink), PK01::phaABC (black) and 3HB standard (blue).

The low level of PHA accumulation may be attributed to the limited availability of PHA monomer. To enhance monomer supply, utilizing the *β*-oxidation pathway could be a promising approach. Incorporation of *phaJ* encoding enoyl-CoA hydratase, which converts enoyl-CoA intermediates into PHA precursors, is expected to further increase PHA accumulation, particularly mcl-PHA. This strategy has been demonstrated in *Y. lipolytica* where the expression of *phaJ* in the lipid-deficient Q4 strain increased PHA production to 7% of its DCW (53). However, the addition of another gene to the PHA expression cassette (Figure 29) may increase the vector size, potentially reducing the efficiency of the AMT method. To address this limitation, the use of p2A self-cleaving peptide linker might be useful to simplify the vector construction (142).

4.4 Conclusion

This study elucidates the critical role of LRO1 in TAG biosynthesis demonstrating that its disruption significantly reduces lipid accumulation. The integration of PHA biosynthesis genes at the *LRO1* locus represents an innovative approach to redirect fatty acid flux toward PHA production. Although the yield of PHA was minimal, these results provide a proof of concept for engineering *M. guilliermondii* as a platform for bioplastic production. Future studies could explore additional genetic modifications to enhance PHA synthesis in the ΔLRO1 mutant background, such as downregulating alternative lipid biosynthesis. These approaches may further optimize *M. guilliermondii* for sustainable biopolymer production.

CHAPTER 5

General conclusion and future direction

This work emphasizes the versatility of *M. guilliermondii* in accumulating microbial lipids from waste oils, demonstrating its potential to broaden industrial application. The utilization of PAO and other byproducts from the palm oil industry as feedstock presents a promising strategy for waste valorization while simultaneously enhancing the economic and environmental sustainability of the palm oil sector. The remarkable resilience of *M. guilliermondii*, showed by its ability to undergo morphological adaptation under fatty acid stress, makes it an attractive candidate for sustainable bioprocess. Moreover, this study highlights the potential of *M. guilliermondii* as a robust platform for production of PHA. However, the challenges associated with genetic modification of *M. guilliermondii* remain a significant bottleneck, particularly in achieving efficient expression of PHA biosynthesis genes.

Future research should prioritize the expansion of palm oil byproducts, such as PAO, as sustainable feedstocks, coupled with process optimization to maximize substrate conversion efficiency and align with global sustainability goals. The observed pseudohyphal transition induced by specific fatty acids calls for further detailed investigation to elucidate its regulatory mechanisms and potential implications for industrial application, such as improved substrate uptake or stress tolerance. Addressing the challenges of genetic engineering in *M. guilliermondii* is essential, with a focus on developing more efficient transformation systems, advance genome-editing tools, and stable expression vectors tailored for this yeast.

Furthermore, comprehensive studies on the metabolic pathways involved in fatty acid utilization and their integration with PHA biosynthesis pathways are needed.

Engineering *M. guilliermondii* to efficiently direct fatty acid carbon flux toward PHA synthesis has the potential to significantly improve production yields. Finally, exploring the dual utility of *M. guilliermondii* for microbial lipid and PHA production could pave the way for innovative biorefinery approaches that exploit its ability to efficiently metabolize waste oils for high-value biproducts.

REFERENCES

1. **Beopoulos, A., Chardot, T., and Nicaud, J. M.:** *Yarrowia lipolytica*: A model and a tool to understand the mechanisms implicated in lipid accumulation, Biochimie., **91**, 692–696 (2009).

2. **Poontawee, R., Lorliam, W., Polburee, P., and Limtong, S.:** Oleaginous yeasts: Biodiversity and cultivation, Fungal Biol. Rev., **44**, 100295 (2023).

3. **Yan, W., Gao, H., Qian, X., Jiang, Y., Zhou, J., Dong, W., Xin, F., Zhang, W., and Jiang, M.:** Biotechnological applications of the non-conventional yeast *Meyerozyma guilliermondii*, Biotechnol. Adv., **46**, 107674 (2021).

4. **Kuenz, A., Tölle, M., and Bromann, S.:** Investigations on riboflavin production by wild-type yeast strain for supplementation of organic feed, Org. Agric., **13**, 399–410 (2023).

5. **Yu, X., Guo, N., Chi, Z., Gong, F., Sheng, J., and Chi, Z.:** Inulinase overproduction by a mutant of the marine yeast *Pichia guilliermondii* using surface response methodology and inulin hydrolysis, Biochem. Eng. J., **43**, 266–271 (2009).

6. **da Silva, R. R., Zaiter, M. A., Boscolo, M., da Silva, R., and Gomes, E.:** Xylose consumption and ethanol production by *Pichia guilliermondii* and *Candida oleophila* in the presence of furans, phenolic compounds, and organic acids commonly produced during the pre-treatment of plant biomass, Brazilian J. Microbiol., **54**, 753–759 (2023).

7. **da Silva, R. R., da Conceição, P. J. P., de Menezes, C. L. A., de Oliveira Nascimento, C. E., Machado Bertelli, M., Pessoa Júnior, A., de Souza, G.**

M., da Silva, R., and Gomes, E.: Biochemical characteristics and potential application of a novel ethanol and glucose-tolerant *β*-glucosidase secreted by *Pichia guilliermondii* G1.2, J. Biotechnol., **294**, 73–80 (2019).

8. **Boretsky, Y. R., Pynyaha, Y. V., Boretsky, V. Y., Fedorovych, D. V., Fayura, L. R., Protchenko, O., Philpott, C. C., and Sibirny, A. A.:** Identification of the genes affecting the regulation of riboflavin synthesis in the flavinogenic yeast *Pichia guilliermondii* using insertion mutagenesis, FEMS Yeast Res., **11**, 307–314 (2011).

9. **Ganapathy, B., Yahya, A., and Ibrahim, N.:** Bioremediation of palm oil mill effluent (POME) using indigenous *Meyerozyma guilliermondii*, Environ. Sci. Pollut. Res., **26**, 11113–11125 (2019).

10. **Zhang, W., Sun, C., and Wang, W.:** Bioremediation of Aflatoxin B 1 by *Meyerozyma guilliermondii*, Toxins (Basel)., **16**, 305 (2024).

11. **Wang, G. Y., Chi, Z., Song, B., Wang, Z. P., and Chi, Z. M.:** High level lipid production by a novel inulinase-producing yeast *Pichia guilliermondii* Pcla22, Bioresour. Technol., **124**, 77–82 (2012).

12. **Pereira, R. S., Mussatto, S. I., and Roberto, I. C.:** Inhibitory action of toxic compounds present in lignocellulosic hydrolysates on xylose to xylitol bioconversion by *Candida guilliermondii*, J. Ind. Microbiol. Biotechnol., **38**, 71–78 (2011).

13. **Ling, L., Li, Z., Jiao, Z., Zhang, X., Ma, W., Feng, J., Zhang, J., and Lu, L.:** Identification of novel endophytic yeast strains from tangerine peel, Curr. Microbiol., **76**, 1066–1072 (2019).

14. **Carneiro, C. V. G. C., E Silva, F. C. de P., and Almeida, J. R. M.:** Xylitol production: Identification and comparison of new producing yeasts, Microorganisms., **7**, 1–15 (2019).

15. **Marshall, C. J.:** Map kinase kinase kinase, MAP kinase kinase and MAP kinase, Curr. Opin. Genet. Dev., **4**, 82–89 (1994).

16. **Atzmüller, D., Ullmann, N., and Zwirzitz, A.:** Identification of genes involved in xylose metabolism of *Meyerozyma guilliermondii* and their genetic engineering for increased xylitol production, AMB Express., **10**, 78 (2020).

17. **Ramírez-Castrillón, M., Jaramillo-Garcia, V. P., Rosa, P. D., Landell, M. F., Vu, D., Fabricio, M. F., Ayub, M. A. Z., Robert, V., Henriques, J. A. P., and Valente, P.:** The oleaginous yeast *Meyerozyma guilliermondii* BI281A as a new potential biodiesel feedstock: Selection and lipid production optimization, Front. Microbiol., **8**, 1176 (2017).

18. **Da Cunha, M. A. A., Converti, A., Santos, J. C., Ferreira, S. T. S., and Da Silva, S. S.:** PVA-hydrogel entrapped *candida guilliermondii* for xylitol production from sugarcane hemicellulose hydrolysate, Appl. Biochem. Biotechnol., **157**, 527–537 (2009).

19. **Hernández-Pérez, A. F., Costa, I. A. L., Silva, D. D. V., Dussán, K. J., Villela, T. R., Canettieri, E. V., Carvalho, J. A., Soares Neto, T. G., and Felipe, M. G. A.:** Biochemical conversion of sugarcane straw hemicellulosic hydrolyzate supplemented with co-substrates for xylitol production, Bioresour. Technol., **200**, 1085–1088 (2016).

20. **Silva, C. J. S. M., and Roberto, I. C.:** Optimization of xylitol production by *Candida guilliermondii* FTI 20037 using response surface methodology, Process

Biochem., **36**, 1119–1124 (2001).

21. **Papanikolaou, S., and Aggelis, G.:** Lipids of oleaginous yeasts. Part I: Biochemistry of single cell oil production, Eur. J. Lipid Sci. Technol., **113**, 1031–1051 (2011).

22. **Aggelis, G., Papadiotis, G., and Komaitis, M.:** Microbial Fatty Acid Specificity, Folia Microbiol. (Praha)., **42**, 117–120 (1997).

23. **Papanikolaou, S., Chevalot, I., Komaitis, M., Marc, I., and Aggelis, G.:** Single cell oil production by *Yarrowia lipolytica* growing on an industrial derivative of animal fat in batch cultures, Appl. Microbiol. Biotechnol., **58**, 308–312 (2002).

24. **Chia, W. Y., Chong, Y. Y., Chew, K. W., Vimali, E., Jayaram, M., Selvarajoo, A., Muthuvelu, K. S., Varalakshmi, P., Show, P. L., and Arumugasamy, S. K.:** Outlook on biorefinery potential of palm oil mill effluent for resource recovery, (2020)

25. **A Aziz, M. M., Kassim, K. A., ElSergany, M., Anuar, S., Jorat, M. E., Yaacob, H., Ahsan, A., Imteaz, M. A., and Arifuzzaman:** Recent advances on palm oil mill effluent (POME) pretreatment and anaerobic reactor for sustainable biogas production, Renew. Sustain. Energy Rev., **119**, 109603 (2020).

26. **Setiadi, T., Trianto, A., Aznury, M., and Pancoro, A.:** Production of polyhydroxyalkanoate (PHA) by *Ralstonia eutropha* JMP 134 with volatile fatty acids from palm oil mill effluent as precursors, Water Sci. Technol., **72**, 1889–1895 (2015).

27. **Kuntom, A., Siew, W. L., and Tan, Y. A.:** Characterization of palm acid oil, J.

Am. Oil Chem. Soc., **71**, 525–528 (1994).

28. **Noge, H., Ueno, Y., Kadir, H. A., and Yahya, W. J.:** Utilization of palm acid oil for a diffusion combustion burner as fuel and nitrogen oxides reduction by the thermally decomposed hydrocarbons, Energy., **224**, 120173 (2021).

29. **Amalina, I. F., Haziq, J. M., Syukor, A. R. A., Ridwan, A. F. A., and Rashid, A. H. M.:** Study of palm acid oil (PAO) from sludge palm oil mill effluent (POME) as goat's feed, Mater. Today Proc., **41**, 96–101 (2020).

30. **Putri Primandari, S. R., Yaakob, Z., Mohammad, M., and Mohamad, A. B.:** Characteristics of residual oil extracted from palm oil mill effluent (POME), World Appl. Sci. J., **27**, 1482–1484 (2013).

31. **Gupta, R., Banerjee, S., Pandit, S., Gupta, P. K., Mathriya, A. S., Kumar, S., Lahiri, D., Nag, M., Ray, R. R., and Joshi, S.:** A comprehensive review on enhanced production of microbial lipids for high-value applications, Biomass Convers. Biorefinery., **13**, 15357–15380 (2023).

32. **Shields-Menard, S. A., Amirsadeghi, M., French, W. T., and Boopathy, R.:** A review on microbial lipids as a potential biofuel, Bioresour. Technol., **259**, 451–460 (2018).

33. **Jovanovic, S., Dietrich, D., Becker, J., Kohlstedt, M., and Wittmann, C.:** Microbial production of polyunsaturated fatty acids — high-value ingredients for aquafeed, superfoods, and pharmaceuticals, Curr. Opin. Biotechnol., **69**, 199–211 (2021).

34. **Takaku, H., Matsuzawa, T., Yaoi, K., and Yamazaki, H.:** Lipid metabolism of the oleaginous yeast *Lipomyces starkeyi*, Appl. Microbiol. Biotechnol., **104**,

6141–6148 (2020).

35. **Valdés, G., Mendonça, R. T., Parra, C., and Aggelis, G.:** Patterns of lignocellulosic sugar assimilation and lipid Production by newly isolated yeast strains from Chilean Valdivian Forest, Appl. Biochem. Biotechnol., **192**, 1124–1146 (2020).

36. **Chee, J. Y., Tan, Y., Samian, M. R., and Sudesh, K.:** Isolation and characterization of a *Burkholderia* sp. USM (JCM15050) capable of producing polyhydroxyalkanoate (PHA) from triglycerides, fatty acids and glycerols, J. Polym. Environ., **18**, 584–592 (2010).

37. **Kostik, V., Memeti, S., and Bauer, B.:** Fatty acid composition of edible oils and fats, J. Hyg. Eng. Des., **4**, 112–116 (2013).

38. **Suriyamongkol, P., Weselake, R., Narine, S., Moloney, M., and Shah, S.:** Biotechnological approaches for the production of polyhydroxyalkanoates in microorganisms and plants — A review, Biotechnol. Adv., **25**, 148–175 (2007).

39. **Lee, S. Y.:** Plastic bacteria? Progress and prospects for polyhydroxyalkanoate production in bacteria, Trends Biotechnol., **14**, 431–438 (1996).

40. **Guérin, P., Renard, E., and Langlois, V.:** Degradation of natural and artificial poly[(*R*)-3-hydroxyalkanoate]s: from biodegradation to hydrolysis, Plast. from Bact. Nat. Funct. Appl., **14**, 283–321 (2010).

41. **Reddy, C. S. K., Ghai, R., and Kalia, V. C.:** Polyhydroxyalkanoates : an overview, Bioresour. Technol., **87**, 137–146 (2003).

42. **Tsuge, T.:** Metabolic improvements and use of inexpensive carbon sources in microbial production of polyhydroxyalkanoates, J. Biosci. Bioeng., **94**, 579–584

(2002).

43. **Schubert, P., Steinbüchel, A., and Schlegel, H. G.:** Cloning of the *Alcaligenes eutrophus* genes for synthesis of poly-beta-hydroxybutyric acid (PHB) and synthesis of PHB in *Escherichia coli*, J. Bacteriol., **170**, 5837–5847 (1988).

44. **Madison, L. L., and Huisman, G. W.:** Metabolic engineering of poly(3-hydroxyalkanoates): from DNA to plastic, Microbiol. Mol. Biol., **63**, 21–53 (1999).

45. **Anderson, A. J., and Dawes, E. A.:** Occurrence, metabolism, metabolic role, and industrial uses of bacterial polyhydroxyalkanoates, Microbiol. Rev., **54**, 450–472 (1990).

46. **Fukui, T., and Shiomi, N.:** Expression and characterization of (R)-specific enoyl coenzyme A hydratase involved in polyhydroxyalkanoate biosynthesis by *Aeromonas caviae*, J. Bacteriol., **180**, 667–673 (1998).

47. **Pohlmann, A., Fricke, W. F., Reinecke, F., Kusian, B., Liesegang, H., Cramm, R., Eitinger, T., Ewering, C., Pötter, M., Schwartz, E., Strittmatter, A., Voß, I., Gottschalk, G., Steinbüchel, A., Friedrich, B., and Bowien, B.:** Genome sequence of the bioplastic-producing "Knallgas" bacterium Ralstonia eutropha H16, Nat. Biotechnol., **24**, 1257–1262 (2006).

48. **Reinecke, F., and Steinbüchel, A.:** *Ralstonia eutropha* strain H16 as model organism for PHA metabolism and for biotechnological production of technically interesting biopolymers, J. Mol. Microbiol. Biotechnol., **16**, 91–108 (2008).

49. **Zhang, B., Carlson, R., and Srienc, F.:** Engineering the monomer composition

of polyhydroxyalkanoates synthesized in *Saccharomyces cerevisiae*, Appl. Environ. Microbiol., **72**, 536–543 (2006).

50. **Leaf, T. A., Peterson, M. S., Stoup, S. K., Somers, D., and Srienc, F.:** *Saccharornyces cerevisiae* expressing bacterial polyhydroxybutyrate synthase produces poly-3- hydroxybutyrate, Microbiology., **142**, 1169–1180 (1996).

51. **Poirier, Y., Erard, N., and Petétot, J. M. C.:** Synthesis of polyhydroxyalkanoate in the peroxisome of *Saccharomyces cerevisiae* by using intermediates of fatty acid *β*-oxidation, Appl. Environ. Microbiol., **67**, 5254–5260 (2001).

52. **Poirier, Y., Erard, N., and Petétot, J. M. C.:** Synthesis of polyhydroxyalkanoate in the peroxisome of *Pichia pastoris*, FEMS Microbiol. Lett., **207**, 97–102 (2002).

53. **Haddouche, R., Poirier, Y., Delessert, S., Sabirova, J., Pagot, Y., Neuvéglise, C., and Nicaud, J. M.:** Engineering polyhydroxyalkanoate content and monomer composition in the oleaginous yeast *Yarrowia lipolytica* by modifying the -oxidation multifunctional protein, Appl. Microbiol. Biotechnol., **91**, 1327–1340 (2011).

54. **Gao, C., Qi, Q., Madzak, C., and Lin, C. S. K.:** Exploring medium-chain-length polyhydroxyalkanoates production in the engineered yeast *Yarrowia lipolytica*, J. Ind. Microbiol. Biotechnol., **42**, 1255–1262 (2015).

55. **Rigouin, C., Lajus, S., Ocando, C., Borsenberger, V., Nicaud, J. M., Marty, A., Avérous, L., and Bordes, F.:** Production and characterization of two medium-chain-length polydroxyalkanoates by engineered strains of *Yarrowia lipolytica*, Microb. Cell Fact., **18**, 1–9 (2019).

56. **Rehm, B. H. a:** Polyester synthases: natural catalysts for plastics, Biochem. J., **376**, 15–33 (2003).

57. **Sun, H., Cai, X., Yan, B., Bai, H., Meng, D., Mo, X., He, S., Su, G., and Jiang, C.:** Multi-Omics Analysis of Lipid Metabolism for a Marine Probiotic *Meyerozyma guilliermondii* GXDK6 Under High NaCl Stress, Front. Genet., **12**, 1–12 (2022).

58. **Annamalai, N., Sivakumar, N., and Oleskowicz-Popiel, P.:** Enhanced production of microbial lipids from waste office paper by the oleaginous yeast *Cryptococcus curvatus*, Fuel., **217**, 420–426 (2018).

59. **Ahmad, F. B., Zhang, Z., Doherty, W. O. S., Te'o, V. S. J., and O'Hara, I. M.:** Improved microbial oil production from oil palm empty fruit bunch by *Mucor plumbeus*, Fuel., **194**, 180–187 (2017).

60. **Fei, Q., Chang, H. N., Shang, L., Choi, J. dal rae, Kim, N. J., and Kang, J. W.:** The effect of volatile fatty acids as a sole carbon source on lipid accumulation by *Cryptococcus albidus* for biodiesel production, Bioresour. Technol., **102**, 2695–2701 (2011).

61. **Ma, X., Zheng, H., Addy, M., Anderson, E., Liu, Y., Chen, P., and Ruan, R.:** Cultivation of *Chlorella vulgaris* in wastewater with waste glycerol: Strategies for improving nutrients removal and enhancing lipid production, Bioresour. Technol., **207**, 252–261 (2016).

62. **Ganeshkumar, V., Subashchandrabose, S. R., Dharmarajan, R., Venkateswarlu, K., Naidu, R., and Megharaj, M.:** Use of mixed wastewaters from piggery and winery for nutrient removal and lipid production by *Chlorella* sp. MM3, Bioresour. Technol., **256**, 254–258 (2018).

63. **Zhu, L. D., Li, Z. H., Guo, D. B., Huang, F., Nugroho, Y., and Xia, K.:** Cultivation of *Chlorella* sp. with livestock waste compost for lipid production, Bioresour. Technol., **223**, 296–300 (2017).

64. **Ma, X., Gao, Z., Gao, M., Ma, Y., Ma, H., Zhang, M., Liu, Y., and Wang, Q.:** Microbial lipid production from food waste saccharified liquid and the effects of compositions, Energy Convers. Manag., **172**, 306–315 (2018).

65. **Chi, Z., Zheng, Y., Jiang, A., and Chen, S.:** Lipid production by culturing oleaginous yeast and algae with food waste and municipal wastewater in an integrated process, Appl. Biochem. Biotechnol., **165**, 442–453 (2011).

66. **Gao, R., Li, Z., Zhou, X., Cheng, S., and Zheng, L.:** Oleaginous yeast *Yarrowia lipolytica* culture with synthetic and food waste-derived volatile fatty acids for lipid production, Biotechnol. Biofuels., **10**, 1–15 (2017).

67. **Gao, Z., Ma, Y., Liu, Y., and Wang, Q.:** Waste cooking oil used as carbon source for microbial lipid production: Promoter or inhibitor, Environ. Res., **203**, 111881 (2022).

68. **Bahadi, M., Yusoff, M. F. M., Salimon, J., Jumaah, M. A., and Derawi, D.:** Physicochemical characteristics of Malaysian crude palm kernel oil, Malaysian J. Chem., **21**, 17–27 (2019).

69. **Amri Ibrahim, N.:** Characteristics of Malaysian palm kernel and its products, J. Oil Palm Res., **25**, 245–252 (2013).

70. **Patel, A., and Matsakas, L.:** A comparative study on *de novo* and *ex novo* lipid fermentation by oleaginous yeast using glucose and sonicated waste cooking oil, Ultrason. Sonochem., **52**, 364–374 (2019).

71. **Geng, J., and Klionsky, D. J.:** The Atg8 and Atg12 ubiquitin-like conjugation systems in macroautophagy., EMBO Rep., **9**, 859–864 (2008).

72. **Folch, J., Lees, M., and Sloane Stanley, G. H.:** A simple method for the isolation and purification of total lipids from animal tissues, J. Biol. Chem., **226**, 497–509 (1957).

73. **Tsuzuki, W., Kitamura, Y., Suzuki, T., and Mase, T.:** Effects of glucose on lipase activity, Biosci. Biotechnol. Biochem., **63**, 1467–1470 (1999).

74. **Yousuf, A., Sannino, F., Addorisio, V., and Pirozzi, D.:** Microbial conversion of olive oil mill wastewaters into lipids suitable for biodiesel production, J. Agric. Food Chem., **58**, 8630–8635 (2010).

75. **Souza, J. L. S., Da Silva, A. F., Carvalho, P. H. A., Pacheco, B. S., Pereira, C. M. P., and Lund, R. G.:** Aliphatic fatty acids and esters: Inhibition of growth and exoenzyme production of *Candida*, and their cytotoxicity in vitro: Anti-*Candida* effect and cytotoxicity of fatty acids and esters, Arch. Oral Biol., **59**, 880–886 (2014).

76. **Offeman, R. D., Franqui-Espiet, D., Cline, J. L., Robertson, G. H., and Orts, W. J.:** Extraction of ethanol with higher carboxylic acid solvents and their toxicity to yeast, Sep. Purif. Technol., **72**, 180–185 (2010).

77. **Thinagaran, L., and Sudesh, K.:** Evaluation of sludge palm oil as feedstock and development of efficient method for its utilization to produce polyhydroxyalkanoate, Waste and Biomass Valorization., **10**, 709–720 (2019).

78. **Riedel, S. L., Jahns, S., Koenig, S., Bock, M. C. E., Brigham, C. J., Bader, J., and Stahl, U.:** Polyhydroxyalkanoates production with *Ralstonia eutropha*

from low quality waste animal fats, J. Biotechnol., **214**, 119–127 (2015).

79. **Huang, C., Luo, M. T., Chen, X. F., Qi, G. X., Xiong, L., Lin, X. Q., Wang, C., Li, H. L., and Chen, X. De:** Combined "*de novo*" and "*ex novo*" lipid fermentation in a mix-medium of corncob acid hydrolysate and soybean oil by *Trichosporon dermatis*, Biotechnol. Biofuels., **10**, 1–11 (2017).

80. **Ratledge, C., and Wynn, J. P.:** The biochemistry and molecular biology of lipid accumulation in oleaginous microorganisms, Adv. Appl. Microbiol., **51**, 1–51 (2002).

81. **Sutanto, S., Zullaikah, S., Tran-Nguyen, P. L., Ismadji, S., and Ju, Y. H.:** *Lipomyces starkeyi*: Its current status as a potential oil producer, Fuel Process. Technol., **177**, 39–55 (2018).

82. **Papanikolaou, S., Chevalot, I., Galiotou-Panayotou, M., Komaitis, M., Marc, I., and Aggelis, G.:** Industrial derivative of tallow: A promising renewable substrate for microbial lipid, single-cell protein and lipase production by *Yarrowia lipolytica*, Electron. J. Biotechnol., **10**, 425–435 (2007).

83. **Kahar, P., Rachmadona, N., Pangestu, R., Palar, R., Triyono Nugroho Adi, D., Betha Juanssilfero, A., Yopi, Manurung, I., Hama, S., and Ogino, C.:** An integrated biorefinery strategy for the utilization of palm-oil wastes, Bioresour. Technol., **344**, 126266 (2022).

84. **Sitepu, I. R., Garay, L. A., Sestric, R., Levin, D., Block, D. E., German, J. B., and Boundy-Mills, K. L.:** Oleaginous yeasts for biodiesel: Current and future trends in biology and production, Biotechnol. Adv., **32**, 1336–1360 (2014).

85. **Papadaki, A., Fernandes, K. V., Chatzifragkou, A., Aguieiras, E. C. G., da**

Silva, J. A. C., Fernandez-Lafuente, R., Papanikolaou, S., Koutinas, A., and Freire, D. M. G.: Bioprocess development for biolubricant production using microbial oil derived via fermentation from confectionery industry wastes, Bioresour. Technol., **267**, 311–318 (2018).

86. **Patel, A., Mu, L., Shi, Y., Rova, U., Christakopoulos, P., and Matsakas, L.:** Single-cell oils from oleaginous microorganisms as green bio-lubricants: Studies on their tribological performance, Energies., **14**, 6685 (2021).

87. **Fei, Q., Fu, R., Shang, L., Brigham, C. J., and Chang, H. N.:** Lipid production by microalgae *Chlorella protothecoides* with volatile fatty acids (VFAs) as carbon sources in heterotrophic cultivation and its economic assessment, Bioprocess Biosyst. Eng., **38**, 691–700 (2015).

88. **Huang, X. F., Liu, J. N., Lu, L. J., Peng, K. M., Yang, G. X., and Liu, J.:** Culture strategies for lipid production using acetic acid as sole carbon source by *Rhodosporidium toruloides*, Bioresour. Technol., **206**, 141–149 (2016).

89. **Chen, H., Zhou, X., Ren, B., and Cheng, L.:** The regulation of hyphae growth in *Candida albicans*, Virulence., **11**, 337–348 (2020).

90. **Uwamahoro, N., Verma-Gaur, J., Shen, H. H., Qu, Y., Lewis, R., Lu, J., Bambery, K., Masters, S. L., Vince, J. E., Naderer, T., and Traven, A.:** The pathogen *Candida albicans* hijacks pyroptosis for escape from macrophages, MBio., **5**, 10–1128 (2014).

91. **Noble, S. M., Gianetti, B. A., and Witchley, J. N.:** *Candida albicans* cell-type switching and functional plasticity in the mammalian host, Nat. Rev. Microbiol., **15**, 96–108 (2017).

92. **Gancedo, J. M.:** Control of pseudohyphae formation in *Saccharomyces cerevisiae*, FEMS Microbiol. Rev., **25**, 107–123 (2001).

93. **Kumar, A.:** The Complex Genetic Basis and Multilayered Regulatory Control of Yeast Pseudohyphal Growth, Annu. Rev. Genet., **55**, 1–21 (2021).

94. **Lo, W., and Dranginis, A. M.:** The cell surface flocculin Flo11 is required for pseudohyphae formation and invasion by *Saccharomyces cerevisiae*, Mol. Biol. Cell., **9**, 161–171 (1998).

95. **Magdouli, S., Brar, S. K., and Blais, J. F.:** Morphology and rheological behaviour of *Yarrowia lipolytica*: Impact of dissolved oxygen level on cell growth and lipid composition, Process Biochem., **65**, 1–10 (2018).

96. **Kurtzman, C., Fell, J. W., and Boekhout, T.:** The yeasts: a taxonomic study. Elsevier (2011)

97. **Livak, K. J., and Schmittgen, T. D.:** Analysis of relative gene expression data using real-time quantitative PCR and the 2-ΔΔCT method, Methods., **25**, 402–408 (2001).

98. **Guo, Z. P., Khoomrung, S., Nielsen, J., and Olsson, L.:** Changes in lipid metabolism convey acid tolerance in *Saccharomyces cerevisiae*, Biotechnol. Biofuels., **11**, 297 (2018).

99. **Alexandre, H., Mathieu, B., and Charpentier, C.:** Alteration in membrane fluidity and lipid composition, and modulation of H+-ATPase activity in *Saccharomyces cerevisiae* caused by decanoic acid, Microbiology., **142**, 469–475 (1996).

100. **Osman, Y. A., and Ingram, L. O.:** Mechanism of ethanol inhibition of

fermentation in *Zymomonas mobilis* CP4, J. Bacteriol., **164**, 173–180 (1985).

101. **Legras, J. L., Erny, C., Le Jeune, C., Lollier, M., Adolphe, Y., Demuyter, C., Delobel, P., Blondin, B., and Karst, F.:** Activation of two different resistance mechanisms in *Saccharomyces cerevisiae* upon exposure to octanoic and decanoic acids, Appl. Environ. Microbiol., **76**, 7526–7535 (2010).

102. **Sudbery, P. E.:** The germ tubes of *Candida albicans* hyphae and pseudohyphae show different patterns of septin ring localization, Mol. Microbiol., **41**, 19–31 (2001).

103. **Lastauskienė, E., Čeputytė, J., Girkontaitė, I., and Zinkevičienė, A.:** Phenotypic switching of *Candida guilliermondii* is associated with pseudohyphae formation and antifungal resistance, Mycopathologia., **179**, 205–211 (2015).

104. **Sachivkina, N., Podoprigora, I., and Bokov, D.:** Morphological characteristics of *Candida albicans*, *Candida krusei*, *Candida guilliermondii*, and *Candida glabrata* biofilms, and response to farnesol, Vet. World., **14**, 1608–1614 (2021).

105. **Ferreira, T. C., De Moraes, L. M. P., and Campos, É. G.:** Cell density-dependent linoleic acid toxicity to *Saccharomyces cerevisiae*, FEMS Yeast Res., **11**, 408–417 (2011).

106. **Wang, Y., Yan, R., Tang, L., Zhu, L., Zhu, D., and Bai, F.:** Dimorphism of Trichosporon cutaneum and impact on its lipid production, Biotechnol. Biofuels., **12**, 203 (2019).

107. **Yang, X., Jin, G., Wang, Y., Shen, H., and Zhao, Z. K.:** Lipid production on free fatty acids by oleaginous yeasts under non-growth conditions, Bioresour.

Technol., **193**, 557–562 (2015).

108. **Kamp, F., Guo, W., Souto, R., Pilch, P. F., Corkey, B. E., and Hamilton, J. A.:** Rapid flip-flop of oleic acid across the plasma membrane of adipocytes, J. Biol. Chem., **278**, 7988–7995 (2003).

109. **Borrull, A., López-Martínez, G., Poblet, M., Cordero-Otero, R., and Rozès, N.:** New insights into the toxicity mechanism of octanoic and decanoic acids on *Saccharomyces cerevisiae*, Yeast., **32**, 451– 460 (2015).

110. **Román, E., Correia, I., Prieto, D., Alonso, R., and Pla, J.:** The HOG MAPK pathway in *Candida albicans*: more than an osmosensing pathway, Int. Microbiol., **23**, 23–29 (2020).

111. **Fridovich, I.:** Oxygen toxicity: A radical explanation, J. Exp. Biol., **201**, 1203–1209 (1998).

112. **Richard, M. L., and Plaine, A.:** Comprehensive analysis of glycosylphosphatidylinositol-anchored proteins in *Candida albicans*, Eukaryot. Cell., **6**, 119–133 (2007).

113. **Frohner, I. E., Bourgeois, C., Yatsyk, K., Majer, O., and Kuchler, K.:** *Candida albicans* cell surface superoxide dismutases degrade host-derived reactive oxygen species to escape innate immune surveillance, Mol. Microbiol., **71**, 240–252 (2009).

114. **D'Autréaux, B., and Toledano, M. B.:** ROS as signalling molecules: Mechanisms that generate specificity in ROS homeostasis, Nat. Rev. Mol. Cell Biol., **8**, 813–824 (2007).

115. **Klionsky, D. J., Cuervo, A. M., and Seglen, P. O.:** Methods for monitoring

autophagy from yeast to human, Autophagy., **3**, 181–206 (2007).

116. **Wen, X., and Klionsky, D. J.:** An overview of macroautophagy in yeast, J. Mol. Biol., **428**, 1681–1699 (2016).

117. **Mari, M., and Reggiori, F.:** Atg9 trafficking in the yeast *Saccharomyces cerevisiae*, Autophagy., **3**, 145–148 (2007).

118. **Noda, T., Kim, J., Huang, W. P., Baba, M., Tokunaga, C., Ohsumi, Y., and Klionsky, D. J.:** Apg9p/Cvt7p is an integral membrane protein required for transport vesicle formation in the Cvt and autophagy pathways, J. Cell Biol., **148**, 465–479 (2000).

119. **Yamamoto, H., Kakuta, S., Watanabe, T. M., Kitamura, A., Sekito, T., Kondo-Kakuta, C., Ichikawa, R., Kinjo, M., and Ohsumi, Y.:** Atg9 vesicles are an important membrane source during early steps of autophagosome formation, J. Cell Biol., **198**, 219–233 (2012).

120. **Warren, E. C., Kramár, P., Lloyd-Jones, K., and Williams, R. S. B.:** Decanoic acid stimulates autophagy in *D. discoideum*, Cells., **10**, 2946 (2021).

121. **Ishii, A., Kawai, M., Noda, H., Kato, H., Takeda, K., Asakawa, K., Ichikawa, Y., Sasanami, T., Tanaka, K., and Kimura, Y.:** Accelerated invagination of vacuoles as a stress response in chronically heat-stressed yeasts, Sci. Rep., **8**, 2644 (2018).

122. **Meaden, P. G., Arneborg, N., Guldfeldt, L. U., Siegumfeldt, H., and Jakobsen, M.:** Endocytosis and vacuolar morphology in *Saccharomyces cerevisiae* are altered in response to ethanol stress or heat shock, Yeast., **15**, 1211–1222 (1999).

123. **Dubouloz, F., Deloche, O., Wanke, V., Cameroni, E., and De Virgilio, C.:** The TOR and EGO protein complexes orchestrate microautophagy in yeast, Mol. Cell., **19**, 15–26 (2005).

124. **Ikner, A., and Shiozaki, K.:** Yeast signaling pathways in the oxidative stress response, Mutat. Res. - Fundam. Mol. Mech. Mutagen., **569**, 13–27 (2005).

125. **Yin, Z., Stead, D., Walker, J., Selway, L., Smith, D. A., Brown, A. J. P., and Quinn, J.:** A proteomic analysis of the salt, cadmium and peroxide stress responses in *Candida albicans* and the role of the Hog1 stress-activated MAPK in regulating the stress-induced proteome, Proteomics., **9**, 4686–4703 (2009).

126. **Alonso-Monge, R., Navarro-García, F., Román, E., Negredo, A. I., Eisman, B., Nombela, C., and Pla, J.:** The Hog1 mitogen-activated protein kinase is essential in the oxidative stress response and chlamydospore formation in *Candida albicans*, Eukaryot. Cell., **2**, 351–361 (2003).

127. **Singh, K. K.:** The *Saccharomyces cerevisiae* Sln1p-Ssk1p two-component system mediates response to oxidative stress and in an oxidant-specific fashion, Free Radic. Biol. Med., **29**, 1043–1050 (2000).

128. **Posas, F., Wurgler-Murphy, S. M., Maeda, T., Witten, E. A., Thai, T. C., and Saito, H.:** Yeast HOG1 MAP kinase cascade is regulated by a multistep phosphorelay mechanism in the SLN1-YPD1-SSK1 "two-component" osmosensor, Cell., **86**, 865–875 (1996).

129. **Posas, F., and Saito, H.:** Activation of the yeast SSK2 MAP kinase kinase kinase by the SSK1 two-component response regulator, EMBO J., **17**, 1385–1394 (1998).

130. **Proft, M., Pascual-Ahuir, A., De Nadal, E., Arïo, J., Serrano, R., and Posas, F.:** Regulation of the Sko1 transcriptional repressor by the Hog1 MAP kinase in response to osmotic stress, EMBO J., **20**, 1123–1133 (2001).

131. **Li, S., Ault, A., Malone, C. L., Raitt, D., Dean, S., Johnston, L. H., Deschenes, R. J., and Fassler, J. S.:** The yeast histidine protein kinase, Sln1p, mediates phosphotransfer to two response regulators, Ssk1p and Skn7p, EMBO J., **17**, 6952–6962 (1998).

132. **Lu, J. M. Y., Deschenes, R. J., and Fassler, J. S.:** *Saccharomyces cerevisiae* Histidine Phosphotransferase Ypd1p Shuttles between the Nucleus and Cytoplasm for *SLN1*-Dependent Phosphorylation of Ssk1p and Skn7p, Eukaryot. Cell., **2**, 1304–1314 (2003).

133. **Maeda, T., Wurgler-Murphy, S. M., and Saito, H.:** A two-component system that regulates an osmosensing MAP kinase cascade in yeast, Nature., **369**, 242–245 (1994).

134. **He, X. J., and Fassler, J. S.:** Identification of novel Yap1p and Skn7p binding sites involved in the oxidative stress response of *Saccharomyces cerevisiae*, Mol. Microbiol., **58**, 1454–1467 (2005).

135. **Lee, J., Godon, C., Lagniel, G., Spector, D., Garin, J., Labarre, J., and Toledano, M. B.:** Yap1 and Skn7 control two specialized oxidative stress response regulons in yeast, J. Biol. Chem., **274**, 16040–16046 (1999).

136. **Braunegg, G., Sonnleitner, B. Y., and Lafferty, R. M.:** A rapid gas chromatographic method for the determination of poly-*β*-hydroxybutyric acid in microbial biomass, Eur. J. Appl. Microbiol. Biotechnol., **6**, 29–37 (1978).

137. **Pomraning, K. R., Collett, J. R., Kim, J., Panisko, E. A., Culley, D. E., Dai, Z., Deng, S., Hofstad, B. A., Butcher, M. G., and Magnuson, J. K.:** Transcriptomic analysis of the oleaginous yeast *Lipomyces starkeyi* during lipid accumulation on enzymatically treated corn stover hydrolysate, Biotechnol. Biofuels., **12**, 162 (2019).

138. **Czabany, T., Athenstaedt, K., and Daum, G.:** Synthesis, storage and degradation of neutral lipids in yeast, Biochim. Biophys. Acta - Mol. Cell Biol. Lipids., **1771**, 299–309 (2007).

139. **Sandager, L., Gustavsson, M. H., Ståhl, U., Dahlqvist, A., Wiberg, E., Banas, A., Lenman, M., Ronne, H., and Stymne, S.:** Storage lipid synthesis is non-essential in yeast, J. Biol. Chem., **277**, 6478–6482 (2002).

140. **Friedlander, J., Tsakraklides, V., Kamineni, A., Greenhagen, E. H., Consiglio, A. L., MacEwen, K., Crabtree, D. V., Afshar, J., Nugent, R. L., Hamilton, M. A., Shaw, A. J., South, C. R., Stephanopoulos, G., and Brevnova, E. E.:** Engineering of a high lipid producing *Yarrowia lipolytica* strain, Biotechnol. Biofuels., **9**, 1–12 (2016).

141. **Taguchi, S., Yamada, M., Matsumoto, K., Tajima, K., Satoh, Y., Munekata, M., Ohno, K., Kohda, K., Shimamura, T., Kambe, H., and Obata, S.:** A microbial factory for lactate-based polyesters using a lactate-polymerizing enzyme, Proc. Natl. Acad. Sci. U. S. A., **105**, 17323–17327 (2008).

142. **Kim, J. H., Lee, S. R., Li, L. H., Park, H. J., Park, J. H., Lee, K. Y., Kim, M. K., Shin, B. A., and Choi, S. Y.:** High cleavage efficiency of a 2A peptide derived from porcine teschovirus-1 in human cell lines, zebrafish and mice, PLoS One., **6**, e18556 (2011).

LIST OF PUBLICATIONS

Zain, N. A. A., Kahar, P., Sudesh, K., Ogino, C., & Kondo, A. (2024). Production of single cell oil by *Lipomyces starkeyi* from waste plant oil generated by the palm oil mill industry. Journal of Bioscience and Bioengineering. 138 (2) 153-162. (Published).

Zain, N. A. A., Tan, K. L., Kahar, P., & Ogino, C. Lipid production from palm acid oil (PAO) as a sole carbon source by *Meyerozyma guilliermondii*. (Submitted revised manuscript to Processes).

Zain, N. A. A., Kahar, P., Kondo, A., & Ogino, C. Dimorphism of oleaginous yeast *Meyerozyma guilliermondii* during production of single-cell oil under decanoic acid stress. (Submitted revised manuscript to Journal of Bioscience and Bioengineering).

Zain, N. A. A., Kahar, P., Kondo, A., & Ogino, C. Metabolic engineering of oleaginous yeast *Meyerozyma guilliermondii* for production of biodegradable polyhydroxyalkanoate (PHA). (Under preparation).

Co-authored Publication

Kahar, P., **Zain, N. A. A**., Pangestu, R., & Ogino, C. Important key points regarding the circular bioeconomy in the palm oil industry, The Palm Oil Export Market. (Book chapter).